

Ingrid Røstad Brøndbo

Seasonal storage for excess solar energy on farms in Norway

A case study of Skjetlein High School

Master's thesis in Energy and Environmental Engineering

Supervisor: Steve Vøller

June 2023

Ingrid Røstad Brøndbo

Seasonal storage for excess solar energy on farms in Norway

A case study of Skjetlein High School

Master's thesis in Energy and Environmental Engineering
Supervisor: Steve Völler
June 2023

Norwegian University of Science and Technology
Faculty of Information Technology and Electrical Engineering
Department of Electric Power Engineering



Norwegian University of
Science and Technology

Abstract

The number of solar energy installations in Norway has grown rapidly in recent years. While households account for most of these installations, many businesses and schools are also investing in solar photovoltaics (PV). Farmers have the option to install PV on their agricultural land. This concept, known as agrivoltaics (APV), involves the dual use of energy production and agriculture on the same land area. The number of APV installations globally has grown over the past years, but it is still a relatively new concept in Norway. Such systems predominantly generate power during summer, while Norwegian electricity consumers use the most electricity during winter. Additionally, these winter months are the period when the electricity spot prices reach their highest peaks. For farmers with APV, utilizing seasonal storage can be a solution to this challenge. Seasonal storage can charge during periods of excess power production and discharge when the prices are high. This can contribute to more efficient use of the produced solar power and may benefit the farmer financially.

This thesis will investigate the implementation of APV and seasonal storage at Skjetlein High School. Additionally, the cost-effectiveness of seasonal storage will be discussed. Possible APV scenarios will be simulated and used in a storage model. An optimization model is constructed to find a suitable storage size (capacity and power rating) according to one of two control strategies. The first control strategy aims to minimize the total electricity bill, while the other strategy aims to minimize the electricity bill and storage investment costs. The results show that the integration of seasonal storage can reduce electricity bill costs from 62-78%. However, the thesis suggests that seasonal storage systems are less economically feasible than smaller storage systems with a duration from weeks to a couple of months.

Sammendrag

Antall solcelleanlegg i Norge har opplevd en kraftig vekst de siste årene. Majoriteten av disse anleggene har blitt installert på boligtak, men en økende mengde bedrifter og skoler anskaffer også solceller. Bønder har muligheten til å installere solcelleanlegg på dyrket mark, også kjent som agrivoltaics (APV). Globalt sett har antallet APV installasjoner vokst de siste årene, men APV er fortsatt et relativt nytt konsept i Norge. APV anlegg genererer i hovedsak kraft om sommeren, mens norske strømforbrukere konsumerer mest strøm i løpet av vinteren. For bønder med APV anlegg, kan sesonglagring være en mulig løsning på denne utfordringen. Sesonglagringsenheten kan lades i perioder med overflødig kraftproduksjon og utlades når prisene er høye. Dette kan bidra til en mer effektiv bruk av solenergien som genereres, og kan også ha økonomiske fordeler for bonden.

Denne oppgaven vil undersøke implementeringen av APV og sesongbasert lagring ved Skjetlein videregående skole. I tillegg vil kostnadseffektiviteten til sesongbasert lagring bli diskutert. Mulige APV-scenarier vil bli simulert og brukes sammen med to lagringsmodeller. En optimeringsmodell er konstruert for å finne en passende lagringsstørrelse (kapasitet og effekt) i henhold til en av to kontrollstrategier. Den første kontrollstrategien har som mål å minimere den totale strømregningen, mens den andre strategien har som mål å minimere strømregningen og lagringsinvesteringskostnadene. Resultatene viser at integrering av sesonglagring kan redusere strømregningen med 62-78%. Arbeidet antyder imidlertid at sesongbaserte lagringssystemer er mindre økonomisk gjennomførbare enn mindre lagringssystemer med en varighet fra uker til et par måneder.

Preface

This Master's Thesis concludes the final semester of the integrated master's program in Energy and Environmental Engineering (Energi og Miljø) at the Norwegian University of Science and Technology (NTNU).

I would like to thank my supervisor, Steve Völler at NTNU, for guidance throughout the semester. Additionally, I would like to thank Skjetlein High School for giving me valuable information and access to data sets. Finally, I would like to express my gratitude to family, friends and my boyfriend for being supportive throughout this semester.

Table of Contents

Abstract	i
Sammendrag	i
Preface	ii
List of Figures	v
List of Tables	viii
Acronyms	x
1 Introduction	1
1.1 Motivation	1
1.2 Objective	2
1.3 Approach	3
1.4 Structure of the Report	3
2 Solar PV	4
2.1 Agrivoltaics	4
2.2 Bifacial PV	5
2.3 Local Climate and Solar Irradiance	6
2.4 Slope and Azimuth	8
2.5 Solar PV Parameters	9
2.6 Solar Cell Physics	10
3 Energy Storage Systems	12
3.1 Energy Storage Systems	12
3.1.1 Main Parameters of an ESS	13
3.2 Vanadium Redox Flow Batteries	15
3.3 Hydrogen Storage Systems	16
4 Method	18
4.1 Skjetlein High School	18
4.1.1 Electricity Demand	18
4.1.2 PV systems	19
4.1.3 Cost of Electricity	21
4.1.4 Revenue from Sold Power	23
4.2 PVSyst	24
4.2.1 Meteorological Data	25
4.2.2 APV Scenario Design	25
4.2.3 Component Selection	26

4.2.4	Detailed Losses	27
4.2.5	Near Shadings	29
4.3	Optimization and Linear Programming	31
4.3.1	Assumptions	32
4.3.2	Sets	32
4.3.3	Parameters	33
4.3.4	Economic Parameters	33
4.3.5	Decision Variables	33
4.3.6	Power and Energy Balance	34
4.3.7	Storage Modelling	34
4.3.8	Grid Modelling	36
4.3.9	Objective Functions	36
4.3.10	Overview of Input Data	37
5	Results	39
5.1	PVSyst Simulations	39
5.1.1	Excisting Rooftop PV	39
5.1.2	AgriPV Scenarios	41
5.2	VRFB Storage Optimization	44
5.2.1	Maximum Storage Capacity and Rated Power	44
5.2.2	Control Strategy 1 - Minimize Total Electricity Costs . . .	45
5.2.3	Control Strategy 2 - Minimize Total Electricity Costs and Investment Costs	51
5.3	Hydrogen Storage Optimization	57
5.3.1	Control Strategy 1 - Minimize Total Electricity Costs . . .	57
5.3.2	Control Strategy 2 - Minimize Total Electricity Costs and Investment Costs	61
6	Discussion	65
6.1	PV System Modelling	65
6.1.1	Rooftop PV	65
6.1.2	Agrivoltaics	66
6.1.3	Storage Control Strategy 1	66
6.1.4	Storage Control Strategy 2	67
6.2	Spot Prices	67
6.3	General Reflections	68
6.4	Comment on Cost Calculation Error	68
6.5	Suggestions for Future Work	69
7	Conclusions	70
	References	71
	Appendices:	79
	A - Python Script for Data Aggregation	79
	B - PVSyst Simulation Recommendations by Next2Sun	80
	C - GitHub Repository	84
	D - PVSyst Reports from Base Case Scenario	85

List of Figures

1	Aerial photography of Skjetlein High School showing the areas of existing rooftop PV installations marked in blue.	2
2	APV example designs (vertically mounted bifacial, dynamic shades, and solar grazing with sheep). Photographies extracted from [9]–[11].	5
3	Over Easy Solar vertical bifacial pilot installation in Oslo, Norway [19].	6
4	The location of Skjetlein High School in Trondheim according to the Köppen-Geiger climate classification system. Modified from [23].	7
5	The components of solar radiation, based on [25].	8
6	PV slope and azimuth illustrated, from [27].	9
7	Solar PV cell during electron movement caused by high-energy photons [35].	11
8	Illustration of the solar cell, module, and array [37].	11
9	Classification of energy storage technologies, extracted from [38].	12
10	Main components of the vanadium redox flow battery. Taken from [26].	16
11	Schematic of hydrogen storage system, extracted from [26]. The components are not drawn to scale.	17
12	Electricity demand curve at Skjetlein High School in hourly resolution from the year 2021 to 2022.	19
13	All existing rooftop PV installations at Skjetlein.	20
14	Nord Pool spot prices in NO3, Trondheim (hourly resolution) from the year 2021 to 2022 [60].	22
15	PVSyst simulation flowchart, inspired by [67].	25
16	Chosen areas for APV at Skjetlein.	26
17	APV scenario North-E/W.	30
18	APV scenario North-S/N.	30
19	APV scenario South-E/W.	31
20	Simulated monthly production compared to real production [kWh] for STO building PV system (41.2 kWp).	40
21	Simulated monthly production compared to real production [kWh] for TIP building PV system (84 kWp).	40
22	Simulated monthly production compared to real production [kWh] for the main building PV system (110 kWp).	41
23	Total rooftop PV production [kWh] (base case scenario).	41

24	North E/W scenario including base case.	42
25	North S/N scenario including base case.	43
26	South E/W scenario including base case.	44
27	South E/W scenario - control strategy 1 - plots 1/2.	47
28	South E/W scenario - control strategy 1 - plots 2/2.	47
29	North E/W scenario - control strategy 1 - plots 1/2.	48
30	North E/W scenario - control strategy 1 - plots 2/2.	49
31	South E/W scenario - control strategy 1 - plots 1/2.	50
32	South E/W scenario - control strategy 1 - plots 2/2.	50
33	South E/W scenario - control strategy 2 - plots 1/2.	53
34	South E/W scenario - control strategy 2 - plots 2/2.	53
35	North E/W scenario - control strategy 2 - plots 1/2.	54
36	North E/W scenario - control strategy 2 - plots 2/2.	55
37	North S/N scenario - control strategy 2 - plots 1/2.	56
38	North S/N scenario - control strategy 2 - plots 2/2.	56
39	South E/W Scenario - control strategy 1 - plots 1/2.	58
40	South E/W Scenario - control strategy 1 - plots 2/2.	58
41	North E/W Scenario - control strategy 1 - plots 1/2.	59
42	North E/W Scenario - control strategy 1 - plots 2/2.	59
43	North S/N Scenario - control strategy 1 - plots 1/2.	60
44	North S/N Scenario - control strategy 1 - plots 2/2.	60
45	South E/W Scenario - control strategy 2 - plots 1/2.	62
46	South E/W Scenario - control strategy 2 - plots 2/2.	62
47	North E/W Scenario - control strategy 2 - plots 1/1.	63
48	North S/N Scenario - control strategy 2 - plots 1/2.	64
49	North S/N Scenario - control strategy 2 - plots 2/2.	64
C.1	PVSyst simulation recommendations from Next2Sun [67].	80
C.2	Bifacial PV panel data sheet page 1/2.	81
C.3	Bifacial PV panel data sheet page 2/2.	82
C.4	Inverter data sheet page 1/1.	83
E.1	PVSyst report STO building page 1/9.	85
E.2	PVSyst report STO building page 2/9.	86
E.3	PVSyst report STO building page 3/9.	87
E.4	PVSyst report STO building page 4/9.	88
E.5	PVSyst report STO building page 5/9.	89
E.6	PVSyst report STO building page 6/9.	90
E.7	PVSyst report STO building page 7/9.	91
E.8	PVSyst report STO building page 8/9.	92
E.9	PVSyst report STO building page 9/9.	93
E.10	PVSyst report TIP building page 1/9.	94
E.11	PVSyst report TIP building page 2/9.	95
E.12	PVSyst report TIP building page 3/9.	96
E.13	PVSyst report TIP building page 4/9.	97
E.14	PVSyst report TIP building page 5/9.	98
E.15	PVSyst report TIP building page 6/9.	99
E.16	PVSyst report TIP building page 7/9.	100
E.17	PVSyst report TIP building page 8/9.	101
E.18	PVSyst report TIP building page 9/9.	102
E.19	PVSyst report main building page 1/9.	103
E.20	PVSyst report main building page 2/9.	104

E.21 PVSyst report main building page 3/9.	105
E.22 PVSyst report main building page 4/9.	106
E.23 PVSyst report main building page 5/9.	107
E.24 PVSyst report main building page 6/9.	108
E.25 PVSyst report main building page 7/9.	109
E.26 PVSyst report main building page 8/9.	110
E.27 PVSyst report main building page 9/9.	111
F.1 PVSyst report APV North E/W page 1/10.	112
F.2 PVSyst report APV North E/W page 2/10.	113
F.3 PVSyst report APV North E/W page 3/10.	114
F.4 PVSyst report APV North E/W page 4/10.	115
F.5 PVSyst report APV North E/W page 5/10.	116
F.6 PVSyst report APV North E/W page 6/10.	117
F.7 PVSyst report APV North E/W page 7/10.	118
F.8 PVSyst report APV North E/W page 8/10.	119
F.9 PVSyst report APV North E/W page 9/10.	120
F.10 PVSyst report APV North E/W page 10/10.	121
F.11 PVSyst report APV North S/N page 1/10.	122
F.12 PVSyst report APV North S/N page 2/10.	123
F.13 PVSyst report APV North S/N page 3/10.	124
F.14 PVSyst report APV North S/N page 4/10.	125
F.15 PVSyst report APV North S/N page 5/10.	126
F.16 PVSyst report APV North S/N page 6/10.	127
F.17 PVSyst report APV North S/N page 7/10.	128
F.18 PVSyst report APV North S/N page 8/10.	129
F.19 PVSyst report APV North S/N page 9/10.	130
F.20 PVSyst report APV North S/N page 10/10.	131
F.21 PVSyst report APV South E/W page 1/10.	132
F.22 PVSyst report APV South E/W page 2/10.	133
F.23 PVSyst report APV South E/W page 3/10.	134
F.24 PVSyst report APV South E/W page 4/10.	135
F.25 PVSyst report APV South E/W page 5/10.	136
F.26 PVSyst report APV South E/W page 6/10.	137
F.27 PVSyst report APV South E/W page 7/10.	138
F.28 PVSyst report APV South E/W page 8/10.	139
F.29 PVSyst report APV South E/W page 9/10.	140
F.30 PVSyst report APV South E/W page 10/10.	141

List of Tables

2.5.1 Albedo values for different surfaces, extracted from [33].	10
3.1.1 Battery terms, based on [43].	14
3.1.2 Battery characteristics, extracted from [44].	14
4.1.1 Components used in existing rooftop PV systems at Skjetlein. . .	20
4.1.2 Installed peak power, orientation, and tilt of existing PV systems at Skjetlein.	20
4.1.3 Grid tariff charges from Tensio during 2022 and 2021 under the category "NMT Low voltage power - all low voltage products" [63], [64].	23
4.1.4 Power charges from Tensio during 2021 and 2022 under the cat- egory "NMT Low voltage power - all low voltage products" [63], [64].	23
4.2.1 Components used in rooftop PV simulations.	27
4.2.2 Soiling values chosen for all simulations (in percentage).	28
4.2.3 All APV scenarios.	31
4.3.1 Storage inputs for the optimization models.	38
4.3.2 Economic Parameters for the optimization models.	38
5.1.1 Specific yields for different APV scenarios and their performance ratios.	44
5.2.1 Maximum storage capacity and rated power for each APV scenario from minimizing curtailment.	45
5.2.2 APV scenario results using control strategy 1.	46
5.2.3 APV scenario results using control strategy 2.	51
5.3.1 APV scenario results using control strategy 1.	57
5.3.2 APV Scenario results using control strategy 2.	61
6.1.1 Summary of results for control strategy 1.	66
6.1.2 Summary of APV Scenario Results using Control Strategy 2. . .	67

Acronyms

APV agrivoltaics	LER land equivalent ratio
BG bifacial gain	LIB lithium-ion battery
BIF bifacial irradiance factor	LIBs lithium-ion batteries
CAES compressed air energy storage	LMT Landbruksmeteorologisk tjeneste
DoD Depth of Discharge	LP Linear Programming
DSO distribution system operator	MILP Mixed Integer Linear Programming
DSOs distribution system operators	MW megawatt
E/P energy to power ratio	MWh megawatt hour
ESS energy storage system	MWp megawatt-peak
ESSs energy storage systems	NVE the Norwegian Directorate of Water Resources and Energy
GHI Global horizontal irradiance	OM operation and maintenance
ha hectare	PCU power conversion unit
IFE Institute for Energy Technology	PHES pumped hydroelectric energy storage
IEA International Energy Agency	PR performance ratio
IPCC Intergovernmental Panel on Climate Change	PV photovoltaics
ITRPV International Technology Roadmap for Photovoltaic	SoC State of Charge
kW kilowatt	STC Standard Test Conditions
kWp kilowatt-peak	TMY typical meteorological year
LDES long-duration energy storage	

VRFB vanadium redox flow battery ies

VRFBs vanadium redox flow batter- **W_p** watt-peak

1 | Introduction

1.1 Motivation

Norway is one of the world's leading countries in renewable energy production because over 90% of power production comes from hydropower [1]. As a result, the use of other renewable energy sources, such as solar, has been limited. Solar photovoltaics (PV) production currently accounts for only 0.1% of the total power production in Norway, or 0.225 TWh [2]. Despite low solar power production, the number of installations has increased rapidly over the past few years and continues to grow [3]. Data from the Norwegian Directorate of Water Resources and Energy (NVE) reveals that the installed solar PV capacity tripled from 2021 to 2022. The majority of these PV systems were installed on small household roof surfaces with a power output below 20 kilowatt (kW) [4]. Large roof areas are often preferred for schools and companies, leading to higher power output. Farmers can also utilize large roof areas, but they have an additional option to install solar PV on their agricultural land. This concept is known as agrivoltaics (APV) [5].

The aim of APV is to minimize the negative impact on food production and to compensate by providing extra income from the generated solar power [6]. As land-based PV installations continue to grow in Norway, APV can be a possible way to increase land-use efficiency while providing farmers with an extra income. APV systems are often large and can cause high peak power generation during the summer months, which may not be able to be fed directly into the local grid due to policy restrictions and/or capacity limitations. By implementing seasonal storage, the APV system owner can increase their self-sufficiency and, at the same time, gain more control over electricity import and export [7]. Seasonal storage is defined as storage that charges during one season and discharges in another.

The main motivation for writing this thesis is the growth of land-based solar PV installations in Norway and how implementing seasonal storage in such systems can be beneficial for the owner. Skjetlein High School, located in Trondheim, Norway (N63°20' E10°18'), will be the research case for this thesis. The school owns livestock stables and conducts farming on grain and grass in various fields. The school is the ideal case for researching APV with seasonal storage because it follows a seasonal electricity consumption curve and currently has several rooftop PV installations in operation as illustrated in Figure 1.



Figure 1: Aerial photography of Skjetlein High School showing the areas of existing rooftop PV installations marked in blue.

1.2 Objective

This thesis aims to analyze the utilization of seasonal storage in combination with APV at Skjetlein High School. This is done by designing various possible APV system scenarios at the school. Then, two storage control strategies will be implemented using optimization to achieve a seasonal charge/discharge pattern. The first control strategy aims to minimize the electricity bill, while the other strategy aims to minimize investment costs in storage and the electricity bill. The optimization model will dimension a suitable storage size to fit the school's needs while satisfying the control strategy. The model will use historic hourly electricity consumption data from the school in addition to hourly spot prices from Nord Pool. To limit the scope of the thesis, hydrogen storage and vanadium redox flow batteries (VRFBs) will be considered as possible storage solutions. For the sake of simplicity, this thesis can be summarized into the following points:

- Presenting an overview of relevant literature and system theory with an emphasis on APV and seasonal storage.
- Simulating already existing rooftop solar installations and APV scenarios at Skjetlein. Historic power production data from the existing rooftop installations will be compared to the simulated production data.
- Create optimization models for hydrogen storage and VRFBs.

1.3 Approach

To simulate existing PV systems and possible APV scenarios, PVSyst will be utilized. The output will provide an hourly production profile for each PV system. The total simulated production from the existing rooftop PV systems will be aggregated and combined with one of the APV scenarios. This will give an overview of the total solar PV production containing each of the APV scenarios. The results from each of the PV simulations will be inserted into two storage optimization models, one for VRFBs and hydrogen storage. The optimization models will consist of mathematical constraints based on the storage characteristics. The models will be made with Pyomo, a Python-based optimization modelling language. Some of the results from the optimization model include storage size (capacity and power rating) and the operational pattern of the storage, which will be plotted in Python.

1.4 Structure of the Report

- **Chapter 1, Introduction**, presents the motivation and objectives of the thesis.
- **Chapter 2, Solar PV**, presents relevant literature and theoretical concepts regarding solar PV systems, with an emphasis on APV.
- **Chapter 3, Energy Storage Systems**, gives a brief overview of the literature and theoretical concepts related to energy storage systems, with an emphasis on technologies suited for seasonal storage.
- **Chapter 4, Method**, provides a detailed description of the methodology used in this thesis. This involves collecting data, simulating PV systems and creating an optimization model.
- **Chapter 5, Results**, presents the results from the thesis. This includes PV simulations and storage optimization results.
- **Chapter 6, Discussion**, provides a discussion of the main analyses and findings in this thesis. Additionally, suggestions for further work are presented.
- **Chapter 7, Conclusions**, concludes and summarizes the thesis findings and discussions.

2 | Solar PV

This section will explain the relevant literature and theoretical background regarding solar PV systems, with an emphasis on APV. PV systems encompass a variety of topics and theories, ranging from semiconductor physics and material science to system design considerations. However, it is important to clarify that even though APV scenario simulations are a crucial part of the thesis, they do not represent the entire study. Therefore, this chapter will not delve too deeply into the specific theories, but the aim is to give the reader a holistic overview of the theories and literature relevant to the PV simulations that will be conducted in the thesis.

2.1 Agrivoltaics

To mitigate the effects of global warming, renewable energy production must increase globally, which requires large areas of land. At the same time, food security is threatened by the effects of climate change and a growing global population. According to the Intergovernmental Panel on Climate Change (IPCC), cropland is expected to decrease globally by between 50 million hectare (ha) and 650 million ha (twice the size of India) by the year 2100 [8]. This will lead to increased competition for limited land resources. In this context, using agricultural land to produce crops and generate solar power simultaneously (known as APV) is an opportunity to increase land use efficiency.

APV was first introduced in the 1980s by Adolf Goetzberger and Armin Zastrow and refers to various methods of combining crops with solar PV installations. Different APV system designs range from greenhouses made of semi-transparent PV panels to vertically mounted solar panels on crops. Figure 2 illustrates some APV designs.



Figure 2: APV example designs (vertically mounted bifacial, dynamic shades, and solar grazing with sheep). Photographies extracted from [9]–[11].

The land equivalent ratio (LER) is often used as a performance index for land use efficiency when using APV systems. The LER is equal to the crop yield in an APV system ($Y_{crop-APV}$) divided by the crop yield in an agricultural system without PV ($Y_{crop-mono}$) in addition to the electricity generation in an APV system ($Y_{elec-APV}$) divided by the electricity generation from a conventional PV system ($Y_{elec-mono}$). This formula is illustrated in Equation 2.1.

$$LER = \frac{Y_{crop-APV}}{Y_{crop-mono}} + \frac{Y_{elec-APV}}{Y_{elec-mono}} \quad (2.1)$$

A LER value greater than one suggests that by combining solar PV generation and crop cultivation, the APV system can increase the overall productivity on the same land area [12]. In a Swedish study, an optimization model for vertically mounted APV was created and resulted in a LER estimation of 1.2 [13]. Similarly, a recent study at Skjetlein High School simulated a LER value of 1.79, corresponding to a 79% improvement in land-use efficiency through the use of APV [14]. These findings demonstrate the potential to increase the productivity of an area by using APV. In light of this, it is important to consider how future advancements in PV technology may enhance the use of APV.

2.2 Bifacial PV

One such advancement is the bifacial PV panels which have the ability to generate electricity from both the front and the rear surface. According to the International Technology Roadmap for Photovoltaic (ITRPV), bifacial PV cells accounted for around 20% of the world's PV cell market in 2020. This share is expected to reach 70% by 2030 [15]. In the context of APV systems, bifacial panels are suitable for an elevated design, harvesting solar irradiance from both the front and rear side of the panel [16].

The advantages of bifacial panels in APV systems, particularly in elevated, vertically mounted systems, is a current field of study for researchers all over the world. According to [17], vertically mounted bifacial PV panels are able to capture a higher quantity of irradiation compared to monofacial PV panels, especially in high-latitude regions. This finding is further explored in an ongoing research project conducted by Over Easy Solar, Fraunhofer ISE, and Institute for Energy

Technology (IFE) which aims to gather data from a variety of vertically mounted PV systems at various latitudes and climate conditions [18]. Preliminary results from a pilot installation in Oslo are already promising, achieving an annual specific yield (kWh/kWp) up to 30% higher than that of a conventional flat roof solution [19]. This installation is shown in Figure 3.



Figure 3: Over Easy Solar vertical bifacial pilot installation in Oslo, Norway [19].

2.3 Local Climate and Solar Irradiance

The power output from an APV system is highly dependent on the local climate and solar irradiance. To identify the climate of Trondheim, the Köppen-Geiger classification system can be utilized [20]. According to the system, Trondheim is classified as a subarctic climate (Dfc), see Figure 4. This means that the area is characterized by long, cold winters and short, warm-to-cool summers. Generally, the power output of a solar PV panel increases with lower temperatures [21]. This relationship stems from high temperatures increasing the solar cells' internal energy leakage due to the electrons being more active in warm conditions [22]. Consequently, Trondheim's climate positively affects the PV power production potential. Solar cell physics will be further explained in Section 2.6.

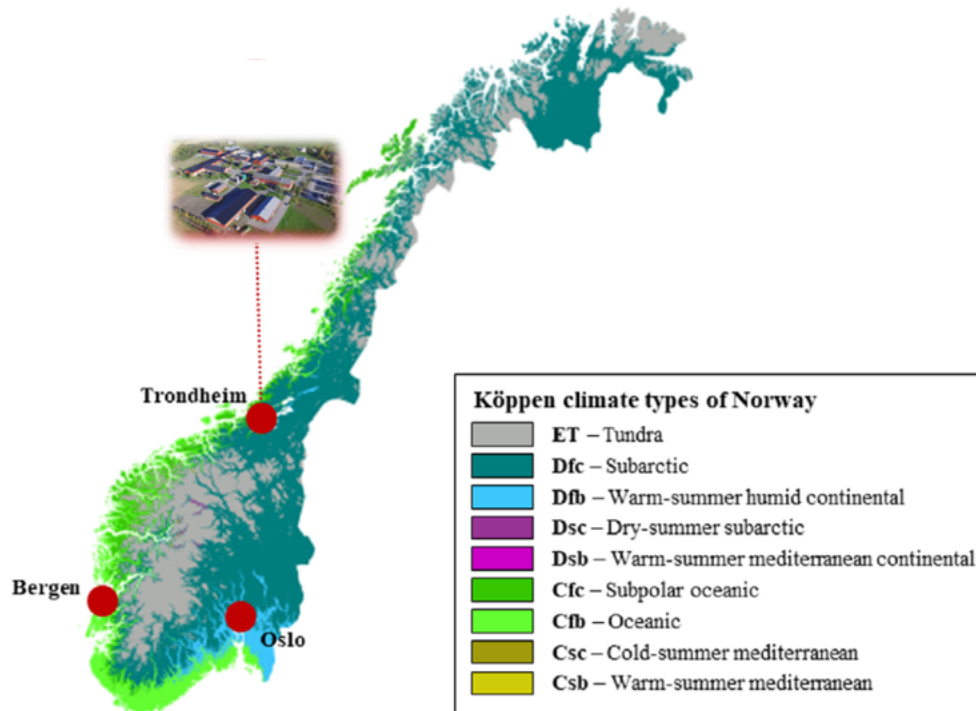


Figure 4: The location of Skjetlein High School in Trondheim according to the Köppen-Geiger climate classification system. Modified from [23].

Although lower temperatures can lead to a higher power output, solar irradiance is essential for PV panels to generate electricity. Solar irradiance is defined as the amount of electromagnetic radiation received from the sun per unit area, usually measured in W/m^2 [24]. Globally, the majority of PV panels are monofacial, which means that they only absorb irradiance from the front side. The total irradiance hitting the surface of a monofacial PV panel is the sum of the direct, diffuse, and reflected irradiance, also known as the Global horizontal irradiance (GHI). These components are shown in Figure 5. Direct irradiance is the radiation that directly hits the PV panel. Not all the sun's radiation directly reaches the PV panel, some are scattered in the atmosphere and become diffuse irradiance. Some of the radiation also hits the ground and is reflected from the ground to the panel (albedo) [23]. High-quality irradiance data are needed to simulate an APV system accurately.

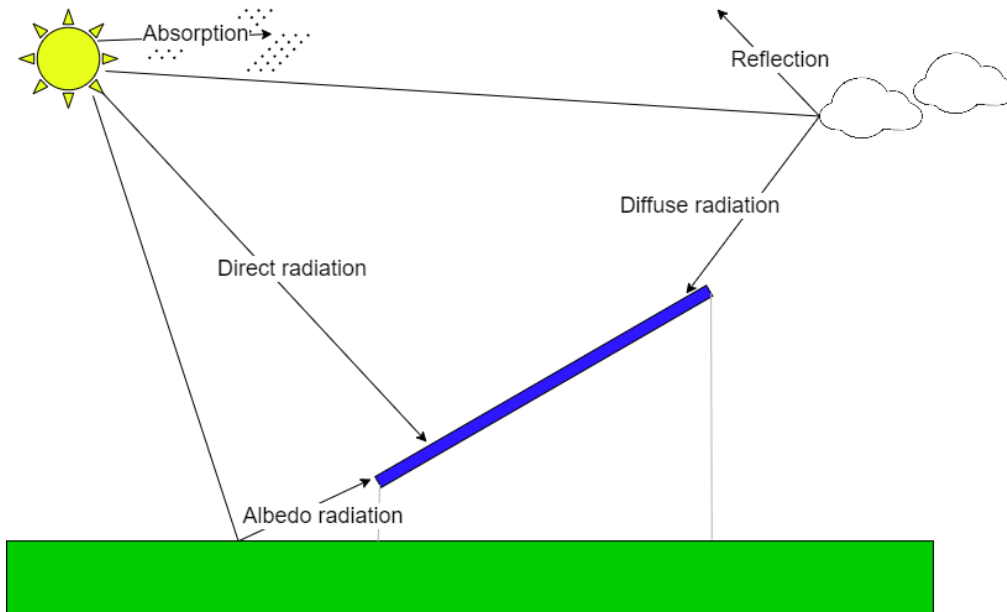


Figure 5: The components of solar radiation, based on [25].

2.4 Slope and Azimuth

The following two paragraphs are extracted from page 20 of the specialization project conducted by the author during the autumn semester of 2022 [26]:

In order to utilize solar irradiation to the greatest possible extent, it is important to choose the appropriate slope and azimuth of the panels. The slope (also called tilt angle) is the angle of the PV panel from the horizontal plane [27]. The azimuth, also called orientation angle, is the angle of the PV panel relative to the south as illustrated in Figure 6. South orientation is often defined as 0° while east and west are often defined as -90° and 90° , respectively. In Norway, an azimuth of zero degrees (panels facing south) will maximize power production, but it is also common to use an east-west configuration.

Solar PV installations with panels facing south produce the most power during mid-day, while systems with an east-west configuration produce the most during the morning and evening. The slope of a panel that maximizes power production (optimal slope) depends on the latitude of the location. If the location is far north (high latitude), the sun will stay at a lower point in the sky. This means that the optimal slope becomes larger because the panels must be perpendicular to the sun's rays to maximize power production. At low latitudes (closer to the equator), the sunlight will shine more directly on the panels and thus increase the efficiency [27]. In the south of Norway, at latitude 38, a slope of 38° will maximize power production. North in Norway, in Tromsø at the 69th latitude, a slope of approx. 47° will maximize power production [28]. The average optimal slope for panels in Norway is 40° , but due to relatively low power production during the winter months, it may be appropriate to use a lower slope.

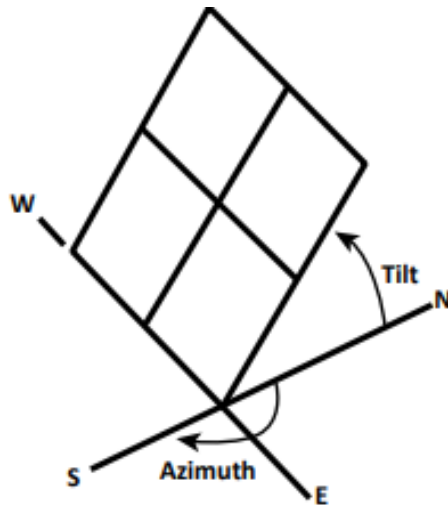


Figure 6: PV slope and azimuth illustrated, from [27].

2.5 Solar PV Parameters

As mentioned earlier, power production from a solar panel depends on a number of factors, such as temperature and solar irradiance. Because of this, the electrical performance of PV panels is measured under Standard Test Conditions (STC), which is an industry-wide standard. These test conditions are defined as 1000 W/m^2 irradiance, 25°C cell temperature, 1.5 AM^1 , and zero wind speed [29]. The maximum electric output power for a solar panel under STC is measured as watt-peak (Wp) or kilowatt-peak (kWp).

The performance ratio (PR) is a measure of how efficiently a PV system produces energy compared to its maximum potential. For monofacial panels, the PR is equal to the actual energy output from the system divided by the energy output in STC conditions (theoretical output) as shown in Equation 2.2 [30]. For bifacial panels, the PR must include a bifacial irradiance factor (BIF) to include irradiance on the rear side [31]. The PR can be affected by various factors, such as shading losses, operating temperature, inverter efficiency, wiring losses and maintenance.

$$PR = \frac{kWh_{AC}}{kWh_{DC,STC}} \quad (2.2)$$

Another known parameter for PV systems is the specific yield, which is equal to the energy generated (kWh) divided by the installed capacity (kWp) over a fixed period of time (often a year). The specific yield normalizes the energy production of a PV system according to its installed capacity. Therefore, this parameter simplifies the process of comparing the production of different PV systems with each other. In Norway, PV systems typically have a specific yield ranging from $700\text{-}1000 \text{ kWh/kWp/year}$ [32].

Since APV systems are located in open landscapes and among plants, the albedo

¹AM = Air mass, the thickness of the atmosphere [26].

will significantly impact the system's performance. The albedo value (α) ranges from 0 to 1, indicating how well a ground surface reflects solar radiation. Some common albedo values are shown in Table 2.5.1. Keep in mind that the value is not constant and depends on the time of day, season, latitude, and whether it is cloudy or sunny [33]. The formula for the albedo coefficient is given in Equation 2.3 where G_{refl} is the total solar radiation reflected by the ground surface, and G_{in} is the total solar radiation reaching the ground surface [34]. Both values have the unit W/m^2 .

Table 2.5.1: Albedo values for different surfaces, extracted from [33].

Surface	Albedo
Grass	0.15 - 0.26
Snow	0.55 - 0.98
Black soil	0.08 - 0.13
Clay soil	0.16 - 0.23
Sand	0.21 - 0.60

$$\alpha = \frac{G_{refl}}{G_{in}} \tag{2.3}$$

2.6 Solar Cell Physics

After explaining concepts related to performance and solar irradiance, moving on to how solar cells use solar energy to produce electricity is natural. A solar cell simply harnesses the energy from sunlight to produce electricity. Two layers of semiconductor material, often silicon, make up a solar cell. These layers undergo a process called "doping," where electrons are either added or subtracted within the material. One layer is n-doped, which has an excess of electrons (negatively charged), while the other layer is p-doped, which has a deficiency of electrons (positively charged). A depletion area develops when these layers are in close proximity to one another, generating an electric field. When high-energy photons (sunlight) hit the materials, electrons near the depletion area move from the p-doped layer to the n-doped layer, as illustrated in Figure 7. This process creates a potential difference, or voltage, which enables the current to be utilized by a connected load [35].

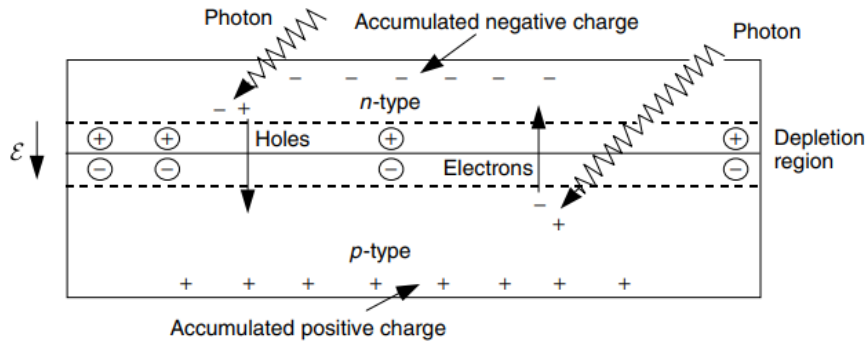


Figure 7: Solar PV cell during electron movement caused by high-energy photons [35].

A single PV cell generates roughly half a voltage. Therefore, it is uncommon for installations to consist of only one single cell. Several solar cells are connected in series to form PV panels, also called modules, to increase the voltage. Solar PV arrays consist of modules connected in series and parallel to increase both current and voltage [36]. The different PV configurations are illustrated in Figure 8.

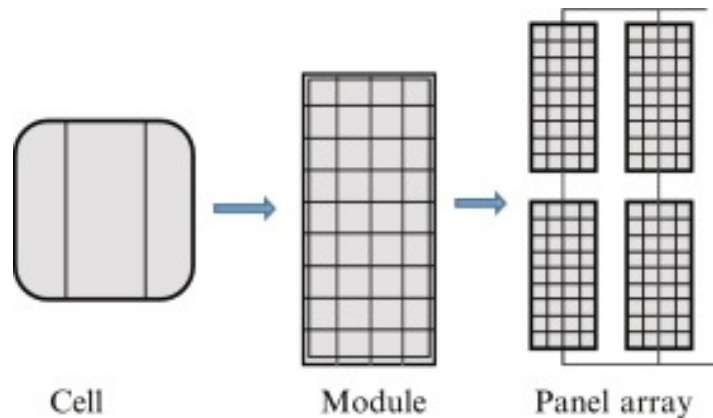


Figure 8: Illustration of the solar cell, module, and array [37].

3 | Energy Storage Systems

This section will cover literature and theoretical background related to energy storage systems (ESSs), emphasising systems suited for seasonal storage.

3.1 Energy Storage Systems

As mentioned earlier, ESSs are an important factor in the ongoing energy transition, and a wide range of storage technologies exist on the market. These technologies have various differences, including how they store energy, how long the energy can be stored, the costs involved, and the amount of energy that is possible to store. Other factors, such as how quickly stored energy can be used and which applications the technology is suitable for, are also important. Energy storage is usually grouped into categories based on the form of storage. The five main categories are mechanical, electrochemical (e.g., batteries), electrical, chemical, and thermal storage. Common energy storage technologies are shown in Figure 9.

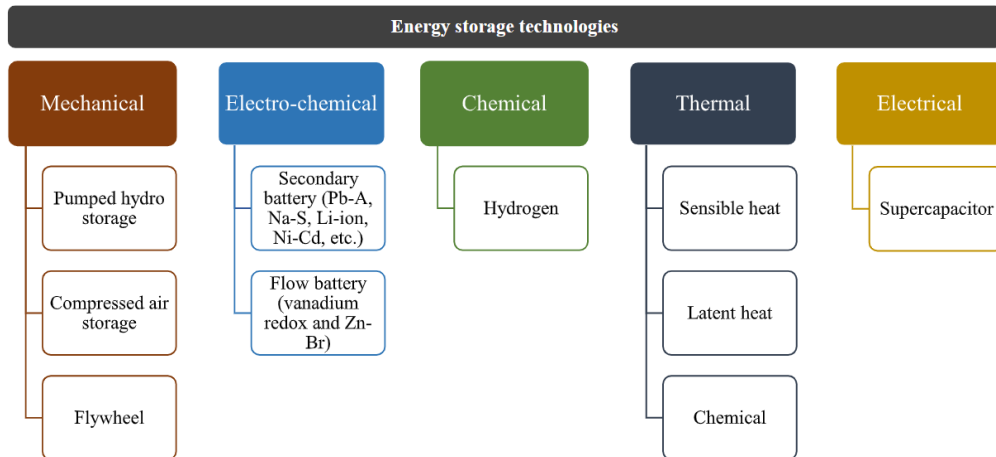


Figure 9: Classification of energy storage technologies, extracted from [38].

Hydropower has traditionally been the primary source of energy for most long-term storage systems, either by storing and releasing water behind dams when power is needed or by using pumped hydroelectric energy storage (PHES). Another common technology for long-duration energy storage is compressed air energy storage (CAES), where air is pumped into an underground reservoir during excess power production. Both PHES and CAES suffer from geographic

limitations and can not be applied everywhere. The flywheel is another mechanical storage technology typically used to supply high power over short periods, similar to how electrical energy storage technologies such as supercapacitors operate [39]. The mechanical, electrical, and thermal energy storage technologies are unsuitable for the specific case of this thesis and are therefore not studied further.

3.1.1 Main Parameters of an ESS

Different energy storage system (ESS) devices may vary greatly in their characteristics. Thus, it is important to classify some of the most important storage parameters, as illustrated in Table 3.1.1. Additionally, Table 3.1.2 shows some of the characteristics of various electrochemical storage devices (batteries). A commonly utilized battery is the lithium-ion battery (LIB). As seen in Table 3.1.2, this battery has high specific energy, making it suitable for light-weight applications such as consumer electronics and cars [40].

For stationary systems, lithium-ion batteries (LIBs) are well-suited for services that require high power and short to medium duration (2-4 hours per day) [41]. However, large-scale LIB systems in the megawatt (MW) range are becoming common in recent years. An example of this is the Tesla Megapack, which has been deployed at 33 projects globally [42]. Nevertheless, there are still challenges associated with LIBs, such as fire risks and toxicity, and especially the dependence on raw materials such as nickel and cobalt [41]. LIBs also have a relatively short cycle life, which can be as low as 500 full equivalent cycles¹ depending on the chemistry within the cell [7].

¹A full equivalent cycle is the sum of every charge/discharge action, adding up to one full charge and one full discharge of a battery.

Table 3.1.1: Battery terms, based on [43].

Battery specification	Unit	Description
SoC	<i>%, Ah or Wh</i>	The present battery capacity as a percentage of maximum capacity.
DoD	<i>%, Ah or Wh</i>	The battery capacity that has been discharged as a percentage of maximum capacity.
Self-discharge	<i>%, Wh/d or Wh/year</i>	Energy capacity loss within the battery which occurs due to internal reactions.
Specific energy	<i>Wh/kg</i>	Energy stored per unit of weight. Also referred to as the gravimetric energy density.
Energy density	<i>Wh/L</i>	Energy stored per unit of volume. Also referred to as the volumetric energy density.
Calendar life	<i>years</i>	The duration where the storage is expected to be operational before losing considerable performance.
Cycle life	<i>cycles</i>	The number of cycles (with 100% DoD) the battery can perform before losing considerable performance.
Response time	<i>ms, s or min</i>	The time it takes for the storage to go from a non-discharging state to a full discharge.

Table 3.1.2: Battery characteristics, extracted from [44].

Battery type	Specific energy [Wh/kg]	Round-trip efficiency [%]	Daily self-discharge [%]	Calendar Life [years]
Li-ion	75-250	85-95	0.1-0.3	5-15
Pb-Acid	30-50	70-80	0.1-0.3	5-15
Ni-Cd	50-75	70	0.03-0.6	10-20
Flow ^a	10-35	65-85	0	15

^a These characteristics belong to the vanadium redox flow battery (VRFB).

One promising alternative to the LIB for long-term storage is the redox flow battery, which offers several advantages, including decoupled energy and power, high efficiency, quick response time, and long cycle life. Among redox flow batteries, the vanadium redox flow battery (VRFB) is particularly promising as it uses vanadium as both the anode and cathode, eliminating the cross-contamination problem commonly found in other flow batteries [45].

Storing energy in the form of hydrogen gas is another promising long-term storage solution due to its high energy density. Hydrogen can be produced with surplus renewable energy through the electrolysis of water. The gas can be converted back into electricity through fuel cells. Both VRFB and hydrogen storage systems will be further explained in Section 3.2 and Section 3.3.

3.2 Vanadium Redox Flow Batteries

A vanadium redox flow battery consists of two external tanks filled with electrolytes (anode and cathode) that are circulated using pumps as illustrated in Figure 10 [46]. When discharging the battery, the anode (negative electrode) undergoes oxidation (electron loss) which causes reduction (electron gain) in the cathode (positive electrode). The electrochemical reaction is reversed when the battery charges, as illustrated in Reaction 1 and Reaction 2.

VRFBs are unique in the sense that they make the energy storage capacity (electrolyte) and battery power (stacks) decoupled, which allows for customization of energy capacity (kWh) at given power (kW). The storage capacity of the flow battery is determined by the volume of the electrolyte tanks and the concentration of reactants, while the power is determined by the number and configuration of cell stacks and choice of components [47]. Additionally, since the VRFB do not use solid electrodes, it greatly reduces the issue of battery degradation. A VRFB can function at total capacity and 100% DoD without experiencing any degradation. The largest VRFB in the world has an energy capacity of 800 megawatt hour (MWh) and a power rating of 200 MW [48].

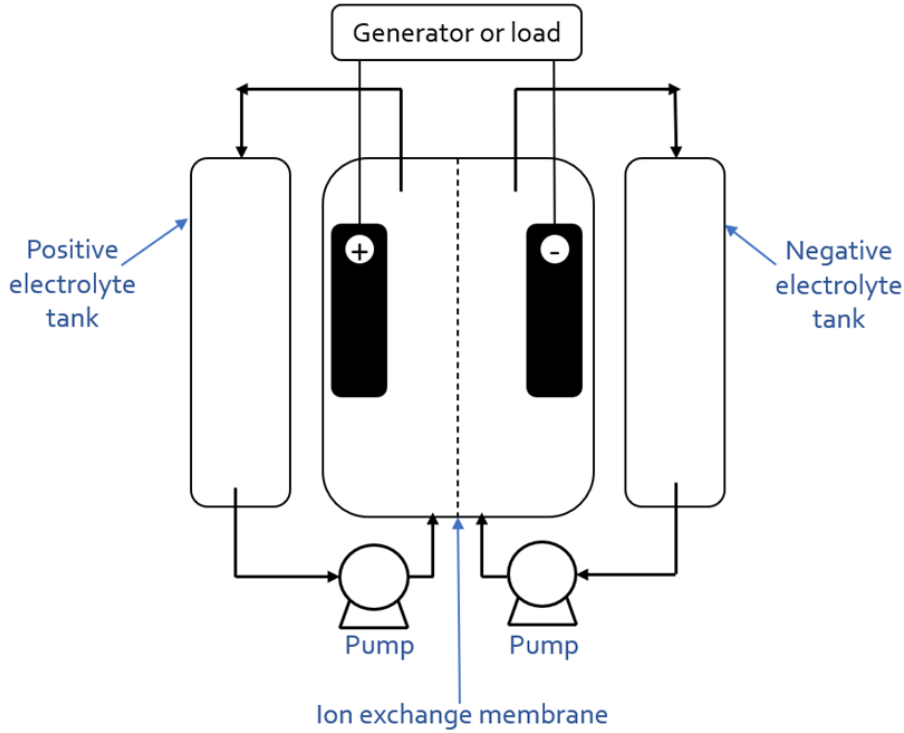
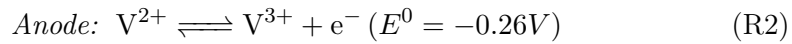
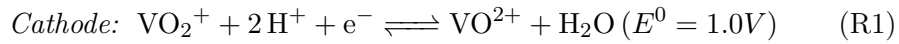


Figure 10: Main components of the vanadium redox flow battery. Taken from [26].



3.3 Hydrogen Storage Systems

In 2021, the global hydrogen demand reached 94 million tonnes. The majority of this demand was met by hydrogen produced from fossil fuels such as coal and natural gas [49]. However, hydrogen is gaining increasing recognition as a potential energy carrier for renewable energy. The process of producing hydrogen through electricity is known as water electrolysis. This process involves splitting water molecules by using energy as shown in Reaction 3 [50]. Hydrogen can then be stored as a compressed gas in liquid or solid form. The most common and developed storage method for hydrogen is compressed gas. The main drawback of this method is low volumetric and gravimetric energy density (measured in MJ/L and MJ/kg , respectively). However, this is not necessarily a problem for stationary storage where there may not be a strict space constraint. Compressed hydrogen is usually inserted into high-pressure (typically at 350-700 bar), thick-walled, cylindrically-shaped tanks, similar to how natural gas is stored [50]. Figure 11 shows a simple compressed hydrogen storage system schematic.

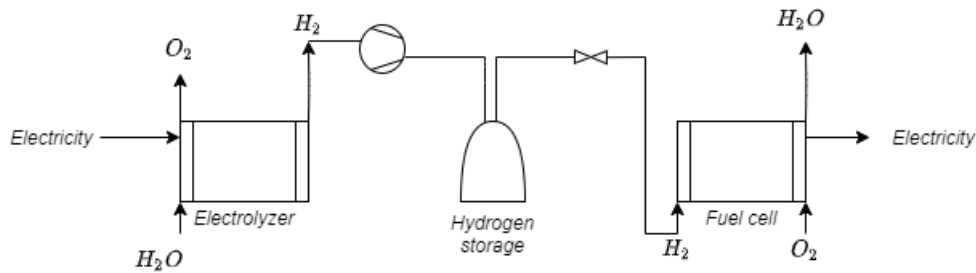
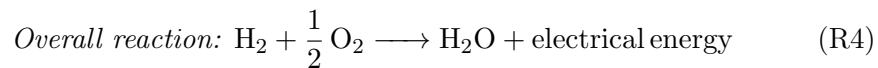


Figure 11: Schematic of hydrogen storage system, extracted from [26]. The components are not drawn to scale.

The hydrogen can be sent through a fuel cell when electricity is needed. A fuel cell generates direct current through an electrochemical reaction using externally supplied chemicals such as hydrogen, alcohols, or hydrocarbons [50]. The process of producing electricity through hydrogen is shown in Reaction 4. The fuel cell consists of two electrodes (anode and cathode), which are separated by an electrolyte that transports electrically charged particles between the electrodes [51]. Some of the advantages of fuel cells include silent operation, few moving parts, fuel flexibility, and a rapid load following response. Additionally, fuel cells have a higher efficiency than internal combustion engines [50].



The following paragraph is extracted from page 23 of the specialization project conducted by the author during the autumn semester of 2022 [26]:

Two of the most common electrolyzer types are Alkaline Water and Polymer Electrolyte Membrane (PEM) Water Electrolyzers (AWEs and PEMWEs). As for fuel cells, some common technologies for hydrogen storage systems are Polymer Electrolyte Membrane Fuel Cells (PEMFCs) and Solid Oxide Fuel Cells (SOFCs) [52].

4 | Method

This chapter explains the methodology used in this thesis. This involves the process of collecting data, simulating PV systems, and creating a storage optimization model. The chapter is divided into three parts. The first section presents information regarding data collection from Skjetlein High School and how the electricity bill was calculated. The second part explains the inner workings of creating APV scenarios and PVSyst simulations. Lastly, the storage optimization model will be explained in detail.

4.1 Skjetlein High School

As mentioned in Section 1.1, Skjetlein High School (N63°20' E10°18') is the research case of this thesis due to their knowledge of farming and experience with solar PV installations. This year, Skjetlein installed Norway's first APV system, which will yield approximately 50 kW of solar PV capacity. In addition, a VRFB for daily dispatching will be installed in June of 2023. The purpose of the system is to research solar power production as well as the consequences of APV on crop production in the Norwegian climate. This section will go through the process of collecting data and calculating the electricity bill at Skjetlein High School.

4.1.1 Electricity Demand

A number of factors, such as social behaviour, time, and economy, influence a consumer's electricity demand. Energy consumption in Norway is naturally higher during the winter than in the summer due to the cold climate. This trend can also be seen in the yearly hourly electricity demand profile for Skjetlein High School as illustrated in Figure 12.

In order to reflect the current electricity consumption at Skjetlein, it was decided to utilize hourly electricity consumption data from the years 2021 and 2022 in this thesis. The data was extracted as excel-files using the Optima Energy website [53] with access from the school. However, the extracted data set did not account for the hourly solar photovoltaic (PV) power consumed by the school. To fix this, Equation 4.1, Equation 4.2, and Equation 4.3 were utilized where P_{load} represents the actual electricity demand of Skjetlein, which is derived by considering the consumed solar PV power ($P_{pvconsumed}$) and the electricity bought from the grid (P_{grid}). The consumed solar PV power was assumed to be equal to the difference between the electricity produced from two of the three PV in-

installations at Skjetlein (STO and TIP building, see Table 4.1.1) and the sold PV power to the grid.

$$P_{load} = P_{grid} + P_{pv_{consumed}} \quad (4.1)$$

$$P_{pv_{consumed}} = P_{pv_{tot}} - P_{pv_{sold}} \quad (4.2)$$

$$P_{pv_{tot}} = P_{pv_{STO}} + P_{pv_{TIP}} \quad (4.3)$$

The third PV installation (main building) was not taken into account as it was installed in October of 2022. The PV monitoring platforms for the two other installations (STO and TIP building) contained power production in fifteen-minute intervals. To aggregate this data into hourly data, a Python script was constructed, which is shown in Appendix A. The resulting electricity demand curve for the years 2021 and 2022 is shown in Figure 12.

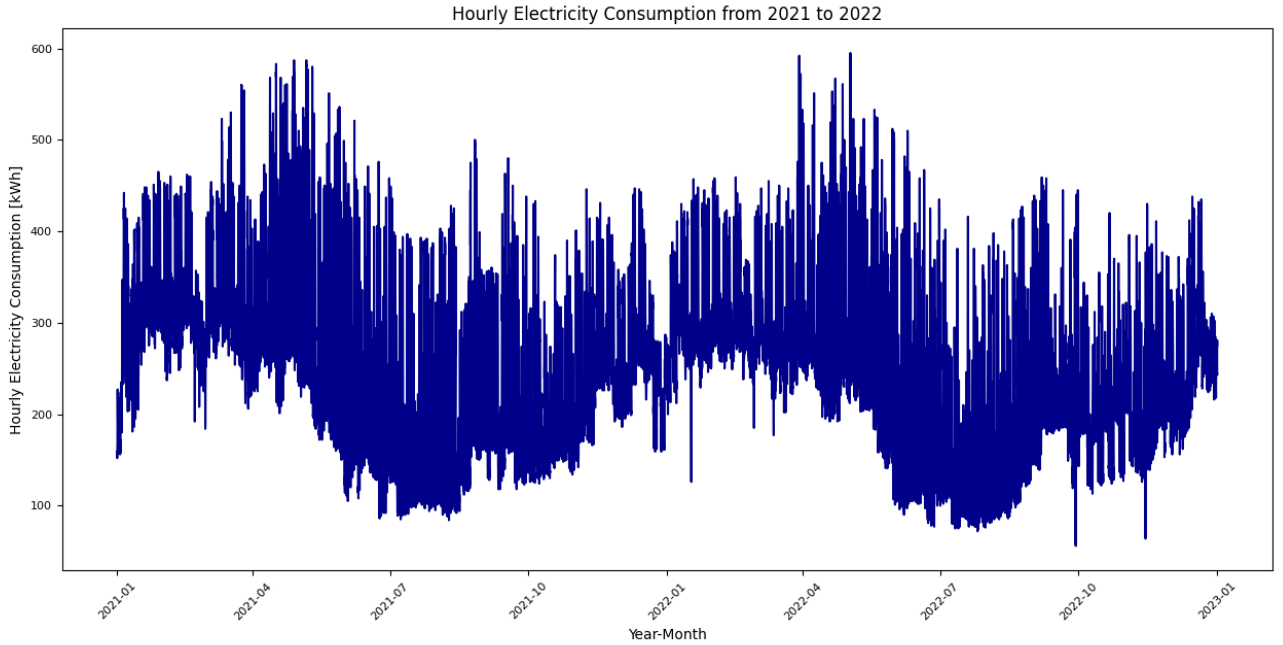


Figure 12: Electricity demand curve at Skjetlein High School in hourly resolution from the year 2021 to 2022.

4.1.2 PV systems

Skjetlein High School currently has three rooftop solar PV installations, as illustrated in Figure 13. Component information regarding the installations is shown in Table 4.1.1. The school provided additional information, such as the panels' orientation and tilt, which is shown in Table 4.1.2. This information was used to model the existing PV systems at Skjetlein, which will be explained further in detail in Section 4.2.



Figure 13: All existing rooftop PV installations at Skjetlein.

Table 4.1.1: Components used in existing rooftop PV systems at Skjetlein.

Building	Panels	Inverter(s)
STO building	Luxor Solar Secure Line 60	SolarEdge SE27.6K-RW000NNP2
TIP building	Luxor Solar 300M/156-60+ Line Full Black	LX-Eco SolarEdge SE82.8K-RW0P0BNU4
Main building	JA Solar JAM72S20-455/MR	Growatt Max 50KTL3-XL

Table 4.1.2: Installed peak power, orientation, and tilt of existing PV systems at Skjetlein.

Building	Peak Power [kWp]	Orientation	Tilt
STO building	41.2	186°	26°
TIP building	84	203°	24°
Main building	110.1	294° and 115°	13°

4.1.3 Cost of Electricity

Anyone who purchases electricity for their own use is an end-user [54]. End-users purchase power from a power supplier (wholesale retailer), which can offer various contracts. These contracts include a fixed monthly price, a surcharge, and mainly either the spot price or a fixed price for electricity [55]. This thesis assumes that Skjetlein High School has a contract based on the spot price. Large consumers may have other types of contracts, but in this work, we choose to simulate using a spot price contract. Using this contract, end-users purchase electricity at the same price that power suppliers pay at the Nord Pool power exchange [54].

On Nord Pool's website, historical spot price data are publicly available. This thesis will utilize hourly spot prices from 2021 and 2022 because the data corresponds to our historical electricity demand from Skjetlein. Figure 14 shows how the electricity spot price varies throughout the years 2021 and 2022. The prices show that there is a significant seasonal price variation for the two years. In Norway, the prices are usually higher in the winter than in the summer due to heating demands. Additionally, unregulated hydropower helps to drive the costs down during summer [56].

The electricity spot prices in 2021 and 2022 were generally high compared to previous years, such as 2020. One of the reasons for the high prices in 2021 was abnormally low reservoir levels in the fall, causing the prices to increase [57]. In 2022, Russia invaded Ukraine, causing gas prices to rise across Europe, which influenced Norwegian electricity prices. The reservoir levels were also low during the summer and spring of 2022, contributing to higher electricity prices [58].

Regarding future electricity prices, the long-term power market analysis from NVE indicates that Norway's average annual electricity price will continue to increase until 2030 [59]. The analysis is based on weather modelling, CO₂ and fuel prices. It is important to note that the report was published in October 2021 and that the world has changed since then.

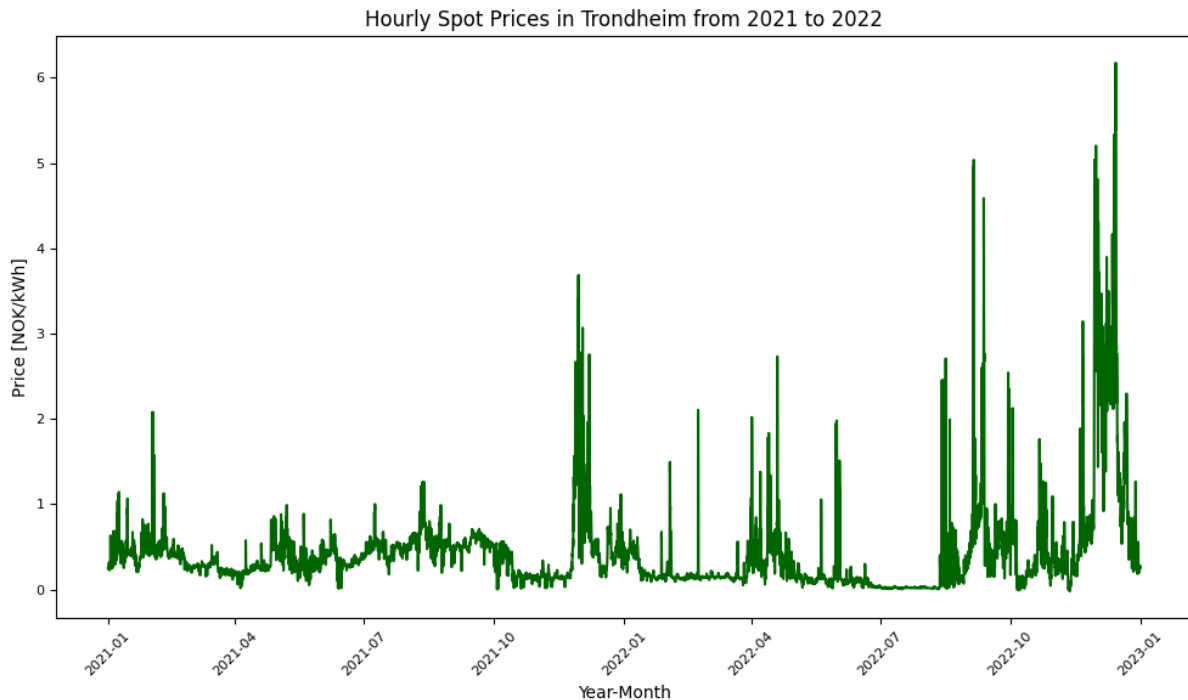


Figure 14: Nord Pool spot prices in NO3, Trondheim (hourly resolution) from the year 2021 to 2022 [60].

In addition to the price of electricity, the end-user also pays for grid access and usage (grid tariff). The pricing is set to cover the expenses of the distribution system operator (DSO) such as maintenance, losses in the grid, fees, and some margin to account for price variability [61]. As the distribution system operators (DSOs) are monopolists, they are regulated by NVE. The grid tariff usually consists of the following three parts:

- A fixed charge [NOK/year] - fixed cost (C_{fixed}), which covers the costs associated with the operation of the power grid [62].
- An energy charge [NOK/kWh] - variable cost (C_{ec}) for electricity consumption every month [62].
- A power charge [NOK/kW/month] - variable cost for peak consumption (C_{peak}) every month. This cost is calculated differently depending on the yearly electricity consumption [62].
- Taxes (for example, consumption tax (C_{ct}) and value-added tax¹).

These charges vary among the DSOs in Norway. In the area of Skjetlein, Tensio is the DSO. Table 4.1.3 shows the fixed charges, energy charges and consumption tax from 2021 and 2022 under the "NMT Low-voltage power - all low voltage products" category. Skjetlein High School has a yearly electricity consumption above 100 000 kWh/year, which means that the power charge is settled according to the highest hourly electricity consumption every month [62]. The power

¹Value added tax is the tax paid for goods and services.

rate throughout the years 2021 and 2022 were the same during the winter and summer months as illustrated in Table 4.1.4. To illustrate how the power charge is calculated, an example is provided in Equation 4.4. This equation shows the calculation of the power charge for a peak consumption of 501 kW in December 2021.

Table 4.1.3: Grid tariff charges from Tensio during 2022 and 2021 under the category "NMT Low voltage power - all low voltage products" [63], [64].

	2021	2022
Fixed charge [NOK/year]	8800	4800
Energy charge [NOK/kWh]	0.05	0.05
Consumption tax [NOK/kWh]	0.167	0.089 or 0.15 ^a

^a The consumption tax was set to 0.089 from January to March and 0.15 from March to December [64].

Table 4.1.4: Power charges from Tensio during 2021 and 2022 under the category "NMT Low voltage power - all low voltage products" [63], [64].

	Winter charge (November - April)	Summer charge (May - October)
0-99 kW [NOK/kW/month]	59	39
100-400 kW [NOK/kW/month]	49	33
400 + kW [NOK/kW/month]	39	27

$$C_{peak} = 99 \cdot 59 + 400 \cdot 49 + 2 \cdot 39 \quad (4.4)$$

In addition to the grid tariff costs, the end-user also has to pay a fee for the Energy Fund (Enova) and payment for electricity certificates² [54]. The costs related to the Enova fee and electricity certificates are neglected in this thesis. The main costs of the yearly electricity bill for Skjetlein High School are summarized in Equation 4.5, where $E[m]$ is the monthly energy consumption in kWh and $P_{peak}[m]$ is the monthly peak power in kW .

$$E_{costs} = C_{fixed} + (C_{ec} + C_{ct} + C_{spot}) \cdot E[m] + C_{peak} \cdot P_{peak}[m] \quad (4.5)$$

4.1.4 Revenue from Sold Power

Skjetlein High School currently supplies excess solar PV production through the Norwegian "Plus Customer" scheme. Through the scheme, prosumers³ can reduce their electricity import from the grid and thus save electricity costs. There is no limit on how much electricity the PV installation can produce, but the

²Electricity certificates are an economic support scheme intended to accelerate the development of new renewable power production [65].

³According to NVE, a prosumer is defined as a consumer with both production and consumption of electricity behind the grid connection point [66].

scheme only applies if the prosumer never delivers more than 100 kW per hour of solar power to the distribution grid [66]. This restriction is not a problem for small solar PV systems, but it can be a challenge for larger systems.

Surplus electricity can be injected into the grid when the production exceeds consumption. The power supplier will pay the prosumer for selling the power, and the DSO will charge the prosumer through a marginal loss rate (MLR) for possible extra losses in the system due to export. How much the prosumer gets paid is dependent on the agreement with the power supplier. In this context, we assume that the excess power production from Skjetlein is sold at the spot price.

The marginal loss rate depends on the local DSO and the season of the year. Since Tensio is the DSO in the area of Skjetlein, the marginal loss rate is set to 6% during winter and 4% during summer, assuming marginal loss rates from 2022 [62]. The total yearly revenue from the PV system is summarized in Equation 4.6. The total yearly costs are shown in Equation 4.7 and involve both Equation 4.6 and Equation 4.5.

$$E_{revenues} = (C_{spot} - C_{spot} \cdot MLR) \cdot E_{surplus} \quad (4.6)$$

$$\begin{aligned} E_{total-costs} &= E_{costs} - E_{revenues} \\ &= C_{fixed} + (C_{ec} + C_{ct} + C_{spot}) \cdot E[m] \\ &\quad + C_{peak} \cdot P_{peak}[m] \\ &\quad - (C_{spot} - C_{spot} \cdot MLR) \cdot E_{surplus} \end{aligned} \quad (4.7)$$

4.2 PVSyst

Various computer programs exist to simulate PV systems, such as PV*SOL, Helios, PVSyst, and PVGIS. PVSyst version 7.3 was chosen for this thesis as the author had undergone training on the software. PVSyst is one of the most utilized programs to design PV installations and to simulate power generation. Therefore, it was deemed a good fit for this project. As seen in Figure 15, PVSyst uses a wide range of parameters to generate the most realistic results possible.

This section will go through the process of choosing input parameters and designing APV and existing rooftop installations at Skjetlein High School using PVSyst. Existing PV installations were simulated to calculate the combined simulated power output (rooftop PV and APV). The power output from the existing systems will be compared with the real data obtained from Skjetlein.

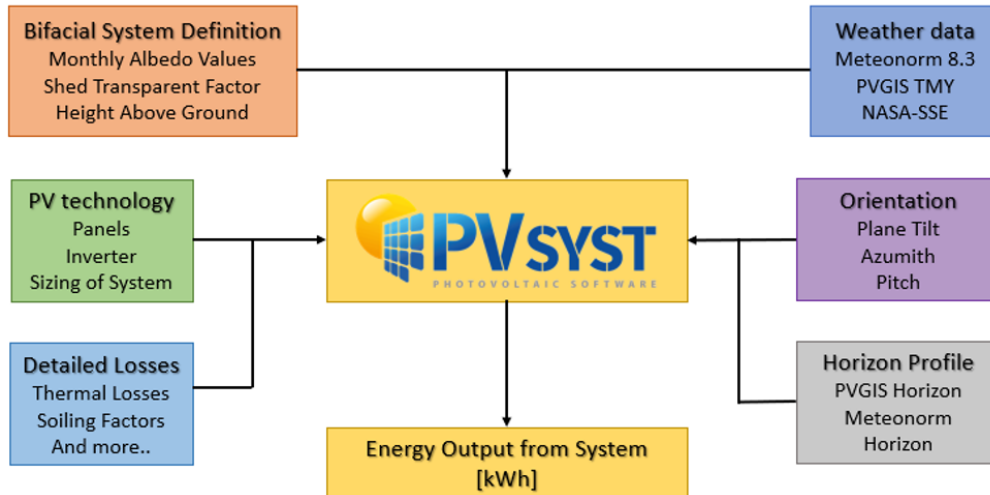


Figure 15: PVSystem simulation flowchart, inspired by [67].

4.2.1 Meteorological Data

The first data that is chosen in PVSystem is the geographical location of Skjetlein High School. Then, meteorological data can be inserted manually or chosen from one of the available data sources (Meteonorm 8.1, Nasa SSE, or PVGIS). As mentioned in Section 2.3, power generation from a PV system is heavily dependent on solar radiation and temperature, and it is therefore important to use meteorological data of good quality.

Meteorological data from Skjetlein can be extracted from Landbruksmeteorologisk tjeneste (LMT) which contains historical measurements from 84 different farm locations in Norway, including Skjetlein High School [68]. This data was downloaded and inserted into PVSystem, but the irradiance data from Skjetlein was very high relative to clear sky conditions in January, which created an error in PVSystem. A previous study at Skjetlein has also detected this problem [67]. According to the developers of PVSystem, the software can sometimes have problems with measured meteorological data from high latitudes [69]. Therefore, instead of inserting local weather measurements, data from Meteonorm 8.1 was used as it is considered the most reliable meteorological data source. Meteonorm uses a mix of ground and satellite measurements to provide hourly climate data [70]. Even though Meteonorm is considered the most reliable data source, its largest uncertainty is the irradiance data [71].

4.2.2 APV Scenario Design

Before simulating anything in PVSystem, the choice of APV location and system designs was made. The choice of location was based on work carried out in autumn 2022 in the specialization project [26]. The chosen APV locations were chosen to be one area north of the school and one area south of the school as illustrated in Figure 16. The northern area has a steep hill, so having two scenarios to test different APV orientations would be interesting. The southern area is flat. Thus, only one simulation scenario was chosen for this area. Three APV simulation scenarios were carried out in total.

The orientation and tilt of the panels were decided based on a previous APV study, where an East/West (-90° , 90°) vertical bifacial approach on a flat ground resulted in a higher power production compared to a south-oriented system simulated at Skjetlein [67]. An East/West orientation produces power mainly in the morning, afternoon, or early evening. According to [72], PV systems with East/West orientation can improve the mismatch between the local electricity production and consumption for a household. Even though Skjetlein High School is not a typical household, the concept can still be applied to them.

In the United Kingdom, several dairy farmers have had experiences with vertically mounted East/West APV systems. According to the farmers, the PV production peaks fit well with the daily morning and evening milking times [73]. Since dairy farming is also a part of the activities at Skjetlein, an East/West vertical approach was implemented in two of the three scenarios to match the daily electricity consumption. One East/West scenario was placed in the northern area of the school, while the other scenario was placed in the southern area. The last scenario was decided to be a South/North facing APV system in the northern area, which would be compared to the East/West system.



Figure 16: Chosen areas for APV at Skjetlein.

4.2.3 Component Selection

The components used in the existing rooftop PV systems are shown in Table 4.1.1. However, a few of these components did not exist in the PVSyst database for the student version of the software. Therefore, the components shown in Table 4.2.1 were used in the PVSyst simulation.

Table 4.2.1: Components used in rooftop PV simulations.

Building	Peak Power [kWp]	Panels	Inverter(s)
STO building	41.2	Luxor Solar LX-280M/156-60+ GG	Huawei SUN2000-28KTL
TIP building	84	Luxor Solar LX-300M/156-60+ GG Full Black	SolarEdge SE55K/SE82.8K
Main building	110.1	JA Solar JAM72S20-455/MR	Growatt Max 50KTL3-XL

For the APV systems, the inverter was chosen to be the Huawei SUN2000 KTL according to the Next2Sun key facts for simulation parameters as seen in Figure C.1. The inverter data sheet from PVSyst can be found in Figure C.4. The panel for the APV systems was chosen to be the AKCOME Hi-Chaser 465 Wp due to its high bifaciality factor⁴ of 0.9. The data sheet for this panel is shown in Appendix B.

4.2.4 Detailed Losses

Depending on the simulation, changes have been made to a few parameters in the "Detailed Losses" section in PVSyst. The detailed losses that have been changed from the default values are the soiling loss factor and the thermal losses.

The soiling loss factor represents the monthly solar radiation losses from panels covered by snow, dirt, dust, etc. The factors were set based on indicative table values from SN-NSPEK 3031 [75] and through email correspondence with Norconsult [76]. The soiling values for APV scenarios were set to 2 or 3 per cent to take into account dust and other particles that cannot be washed off the vertical panels. As spring is a season where dust levels tend to increase, the soiling factor increased by one per cent compared to the rest of the year [77].

⁴This factor is a measure of how much energy the rear side of the panel will produce compared to the front side of the panel [74].

Table 4.2.2: Soiling values chosen for all simulations (in percentage).

Months	APV Scenarios ^a	STO ^b	TIP ^c	Main Building ^d
January	2	20	40	60
February	3	25	50	75
March	3	15	30	45
April	3	3	5	8
May	3	2	2	2
June	2	2	2	2
July	2	2	2	2
August	2	2	2	2
September	2	2	2	2
October	2	2	2	2
November	2	5	10	15
December	2	18	35	53

^a Values based on [76].

^b Extracted from Table P.3 in [75].

^c Extracted from Table P.2 in [75].

^d Extracted from Table P.1 in [75].

In PVSyst, thermal losses refer to the losses expected when the temperature is not equal to the STC temperature. The thermal loss factor is described by Equation 4.8 where U_c is the constant loss factor and U_v is a factor proportional to the wind velocity v [30].

$$U = U_c + U_v \cdot v \quad (4.8)$$

These factors depend on how the PV system is mounted and how much air is circulating around the modules. There exist default thermal loss factors in PVSyst based on measurements in several locations. These default values are shown in the list below. For all APV scenarios, the values in point number 1 were chosen. For the rooftop PV systema on the STO and TIP building, the values from point number 3 were chosen. Lastly, for the PV system on the main building, the values in point number 2 were chosen.

1. "Free" mounted modules with air circulation:

$$U_c = 29.0 \text{ W/m}^2 \cdot \text{K}$$

$$U_v = 0 \text{ W/m}^2 \cdot \text{K} \cdot \text{m/s}$$

2. Domes:

$$U_c = 27.0 \text{ W/m}^2 \cdot \text{K}$$

$$U_v = 0 \text{ W/m}^2 \cdot \text{K} \cdot \text{m/s}$$

3. Semi-integrated with air duct behind:

$$U_c = 20.0 \text{ W/m}^2 \cdot \text{K}$$

$$U_v = 0 \text{ W/m}^2 \cdot \text{K} \cdot \text{m/s}$$

4. Integration with fully insulated back:

$$U_c = 15.0 \text{ W/m}^2 \cdot \text{K}$$

$$U_v = 0 \text{ W/m}^2 \cdot \text{K} \cdot \text{m/s}$$

4.2.5 Near Shadings

A near-shading scene for the scenarios was created in PVSyst to visualize the installations and to simulate shadows from nearby objects. Trondheim Municipality was contacted and helped create the topographical 3D map shown in Figure 17. The vertically mounted PV panels were positioned to follow the terrain, which has been utilized in other APV projects on hills [78]. Furthermore, a portion of the hill that was not too steep was chosen to be the APV site. This was done to avoid shadows from nearby trees and to ensure that a tractor could safely drive between the panels without driving into them. The peak power installation for the northern scenarios was limited to 711 kWp due to the shading from nearby panels and terrain. The scenarios north of the school are illustrated in Figure 17 and Figure 18.

The installed peak power for the southern scenario was chosen to be 1.6 megawatt-peak (MWp) as a "best-case" scenario and is illustrated in Figure 19. This site was chosen due to the lack of nearby shadow sources. According to the local DSO, Skjetlein can choose to install up to 3 MWp of solar PV if sufficient reactive power compensation is delivered to the grid [67]. Choosing a maximum system size of 1.6 MWp keeps Skjetlein way below the maximum value. For all the scenarios, the PV arrays were set with a height above ground of 0.8 meters to account for the mounting structure, and the pitch⁵ was set to 13 meters to make sure that a tractor with a width of 10 meters can drive safely between the panels [67]. To summarize, all the scenarios with the peak installation are listed in Table 4.2.3.

⁵The pitch is simply the distance from one PV row to the nearest other.

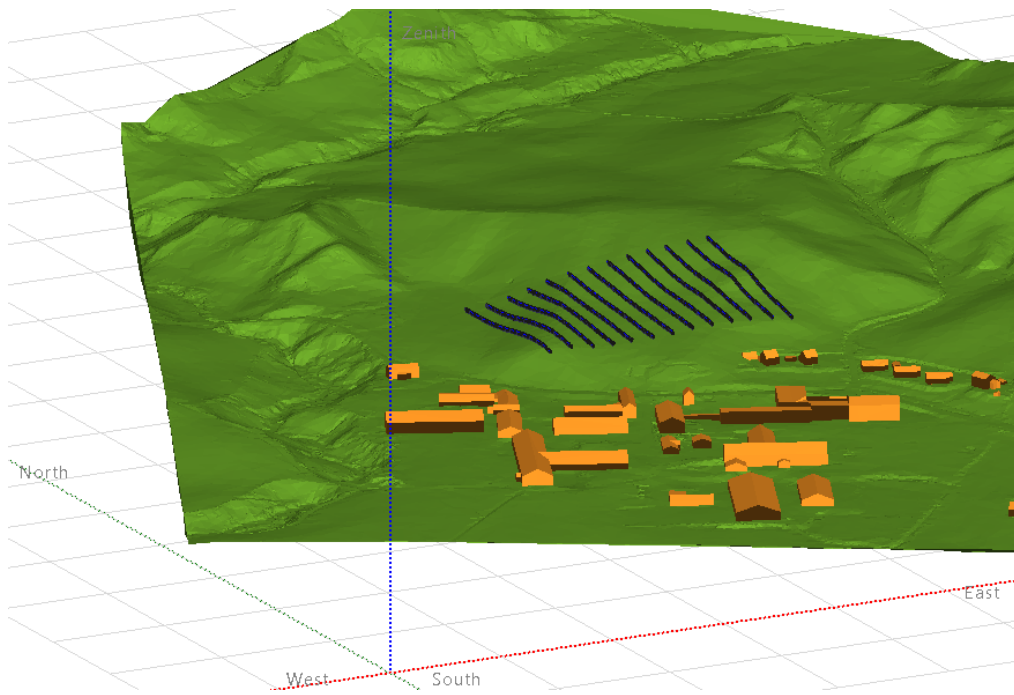


Figure 17: APV scenario North-E/W.

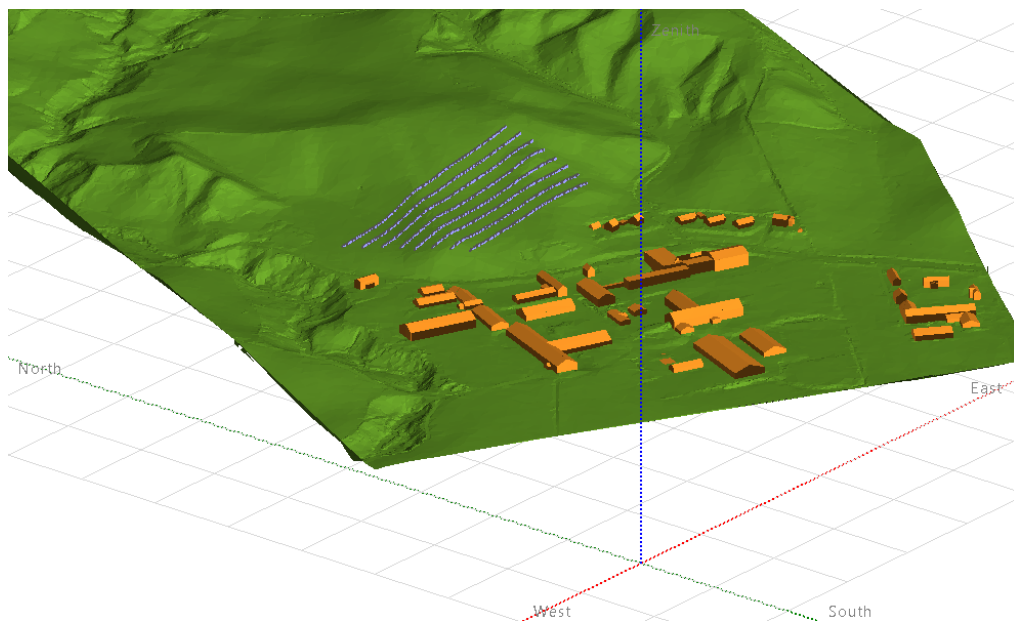


Figure 18: APV scenario North-S/N.

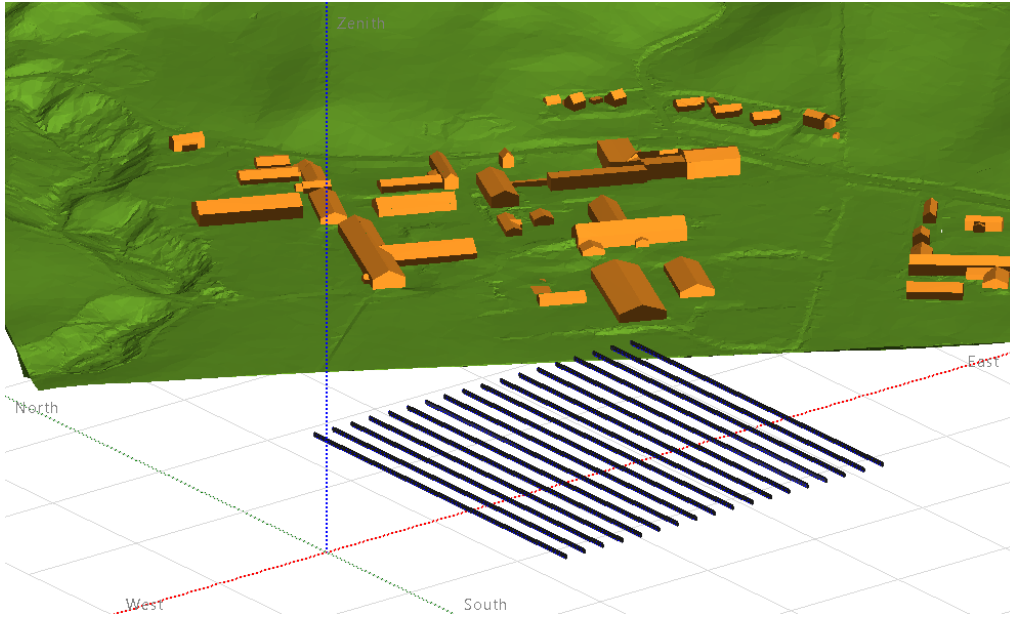


Figure 19: APV scenario South-E/W.

Table 4.2.3: All APV scenarios.

APV Scenario	Tilt	Installed Peak Power [kWp]
North E/W (-90°, 90°)	90°	711
North S/N (0°, 180°)	90°	711
South E/W (-90°, 90°)	90°	1600

4.3 Optimization and Linear Programming

Optimization, also known as mathematical programming, is a method to determine optimal values for a set of variables based on a given objective function. The objective function is either maximized or minimized. Often, variables are subject to certain conditions which must be fulfilled. In Linear Programming (LP), these constraints are linear and have the following format:

$$\begin{aligned} & \text{minimize} && C(x) \\ & \text{subject to} && f(x) \end{aligned}$$

Where $C(x)$ is the objective function and $f(x)$ is one or more constraints. In this thesis, Mixed Integer Linear Programming (MILP) is utilized, which is a form of LP which incorporates binary decision variables [79]. Several different optimization modelling tools exist, and Pyomo has been chosen for this thesis. Pyomo is an open-source software package for optimization modelling in Python and includes tools for formulating, solving, and analyzing optimization models [80]. This section will go through the storage optimization models created in this thesis for either VRFB or hydrogen storage. The section will first introduce the

model assumptions. The link to the source code of the optimization models can be found in Appendix C.

4.3.1 Assumptions

Eleven modelling assumptions were made while creating the optimization models. The following list shows the assumptions.

- The time step is set to one hour (t) due to computational time.
- The simulation duration is two years (T), which yields 17520 time steps.
- The electricity demand is assumed to be known and equal to the demand from 2021 and 2022.
- The Nord Pool spot prices are assumed to be known and equal to the prices from 2021 and 2022.
- Financial support from the Norwegian government ("strømstøtte") is ignored.
- The efficiency of the power conversion unit (inverter) is assumed to be 100%.
- Skjetlein High School is assumed to be one aggregated load.
- The load is assumed to be purely active (reactive power is neglected).
- Grid constraints are ignored.
- Battery degradation is ignored.
- Self-discharge is neglected.

4.3.2 Sets

In an optimization model, sets contain elements that the model uses to index variables, parameters and constraints. In the two optimization models, seven sets were created:

- $T \rightarrow$ Simulation time horizon (1 to 17520) [h].
- $P_{\text{load}}(t) \rightarrow$ Electrical load at hour t [kWh].
- $P_{\text{PV}}(t) \rightarrow$ Power generated by PV system at hour t [kW].
- $C_{\text{spot}}(t) \rightarrow$ Nord Pool spot price at hour t [NOK/kWh].
- $C_{\text{ec}}(t) \rightarrow$ Energy charge at hour t , see Section 4.1.3 [NOK/kWh].
- $C_{\text{pc}}(t) \rightarrow$ Power charge at hour t , see Section 4.1.3. Originally in monthly values, but expanded to hourly resolution [NOK/kW].
- $C_{\text{ct}}(t) \rightarrow$ Consumption tax at hour t , see Section 4.1.3.

4.3.3 Parameters

Parameters are known values which are not optimized during the solution process. In the two optimization models, twelve parameters were created:

- $\Delta t \rightarrow$ Time step, set to one hour in optimization model [h].
- $\eta_{\text{ch}} \rightarrow$ Charging efficiency of storage system [%].
- $\eta_{\text{dch}} \rightarrow$ Discharging efficiency of storage system [%].
- $\eta_{\text{RTE}} \rightarrow$ Round-trip efficiency of storage system [%].
- $E_{\text{DoD}} \rightarrow$ Depth of Discharge (DoD) of storage system [%].
- $E_{\text{soc}_{\text{max}}} \rightarrow$ Maximum state of charge (SoC) of storage system [%].
- $E_{\text{soc}_{\text{min}}} \rightarrow$ Minimum state of charge (SoC) of storage system [%].
- $E_{\text{life}} \rightarrow$ Calendar life of storage system [years]
- $E_{\text{cap}_{\text{max}}} \rightarrow$ Maximum capacity of storage system [kWh].
- $P_{\text{rated}_{\text{max}}} \rightarrow$ Maximum rated power of storage system [kW].
- $P_{\text{g_in_max}}(t) \rightarrow$ Maximum grid import at hour t [kW].
- $P_{\text{g_out_max}}(t) \rightarrow$ Maximum grid export at hour t [kW].

4.3.4 Economic Parameters

In addition to the parameters explained above, the model also includes six economic parameters:

- $E_{\text{fixed}} \rightarrow$ Fixed yearly energy charge, see Section 4.1.4 [NOK].
- $MLR \rightarrow$ Marginal loss rate, see Section 4.1.3 [%].
- $r \rightarrow$ Discount rate [%].
- $\epsilon \rightarrow$ Annuity factor [-].
- $E_{\text{ec}} \rightarrow$ Capacity components costs [NOK/kWh].
- $E_{\text{pc}} \rightarrow$ Power components costs [NOK/kWh].

4.3.5 Decision Variables

In an optimization model, the decision variables are the unknowns of the model which we want to determine based on the objective function and the constraints. All of these variables are set to be non-negative. There are nine decision variables in total:

- $P_{\text{g_in}}(t) \rightarrow$ Power imported from the grid at hour t [kW].

- $P_{g_out}(t)$ → Power exported to the grid at hour t [kW].
- $P_{ch}(t)$ → Power used for charging the storage system at hour t [kW].
- $P_{dch}(t)$ → Power used for discharging the storage system at hour t [kW].
- $P_d(t)$ → Power curtailed at hour t [kW].
- $E(t)$ → Energy stored in the battery at time t [kWh].
- $P_{dch-bin}(t)$ → Binary decision variable that indicates whether the storage system is discharging at hour t [-].
- E_{cap} → Energy capacity of the storage system [kWh].
- P_{rated} → Rated power of the storage system [kW].

4.3.6 Power and Energy Balance

A crucial aspect of the optimization model is ensuring that the load at Skjetlein is always satisfied. The power balance is shown in Equation 4.9. The stored energy in the battery (*kWh*) at time t is equal to the stored energy from the last time step in addition to charging and discharging power adjusted for efficiency as illustrated in Equation 4.10 [81]. VRFB and hydrogen storage systems are known to have very low self-discharge. This value is therefore neglected for both storage systems [44].

$$\begin{aligned}
 P_{load}(t) &= P_{g_in}(t) - P_{g_out}(t) \\
 &+ P_{PV}(t) - P_{ch}(t) \\
 &+ P_{dch}(t) - P_d(t), \\
 &\text{for } t = 1, \dots, T
 \end{aligned} \tag{4.9}$$

$$\begin{aligned}
 E(t) &= E(t-1) \\
 &+ \left(\eta_{ch} \cdot P_{ch}(t-1) - \frac{1}{\eta_{dch}} \cdot P_{dch}(t-1) \right) \cdot \Delta t, \\
 &\text{for } t = 2, \dots, T
 \end{aligned} \tag{4.10}$$

In reality, the charging and discharging efficiencies (η_{ch} and η_{dch}) depend on the current through the storage. To reduce model complexity, the charging and discharging efficiencies were assumed to be constant for both VRFB and hydrogen storage. The charging and discharging efficiencies were assumed to be equal and based on the round-trip efficiency as shown in Equation 4.11 [7]. This is a common assumption in storage optimization.

$$\eta_{dch} = \eta_{ch} = \sqrt{\eta_{RTE}} \tag{4.11}$$

4.3.7 Storage Modelling

It is well-known that storage systems cannot charge and discharge simultaneously. To implement this in the model, the binary decision variable $P_{dch-bin}(t)$

is introduced. This variable is 1 when the storage system discharges and 0 when it charges, as shown in Equation 4.12 and Equation 4.13. To make sure that the storage does not discharge more energy than what is available, Equation 4.14 was implemented.

$$P_{\text{dch}}(t) \leq P_{\text{dch-bin}}(t) \cdot (P_{\text{load}}(t) - P_{\text{PV}}(t)) \quad \text{for } t = 1, \dots, T \quad (4.12)$$

$$P_{\text{ch}}(t) \leq (1 - P_{\text{dch-bin}}(t)) \cdot (P_{\text{PV}}(t) - P_{\text{load}}(t)) \quad \text{for } t = 1, \dots, T \quad (4.13)$$

$$P_{\text{dch}}(t) = \begin{cases} 0 & \text{if } t = 1 \\ E(t-1) \cdot \frac{1}{\Delta t} & t = 2, \dots, T \end{cases} \quad (4.14)$$

In this thesis, the role of the storage is to store excess solar PV production and not store electricity from the grid. Thus, Equation 4.15 was implemented to the model such that the storage cannot charge and import from the grid at the same time. Additionally, the system cannot import electricity from the grid and at the same time export to the grid as shown in Equation 4.16.

$$P_{\text{ch}}(t) \cdot P_{\text{g_in}}(t) = 0 \quad \text{for } t = 1, \dots, T \quad (4.15)$$

$$P_{\text{g_in}}(t) \cdot P_{\text{g_out}}(t) = 0 \quad \text{for } t = 1, \dots, T \quad (4.16)$$

Equation 4.17 ensures that the storage system does not discharge beyond its rated DoD, which is important for maintaining the lifespan of the storage. To avoid extreme operating conditions, the maximum and minimum storage state of charge was implemented through Equation 4.18 and Equation 4.19 [79]. Furthermore, the charged and discharged power is restricted by the rated power as illustrated in Equation 4.20 and Equation 4.21. Lastly, a maximum limit on capacity and rating was set by Equation 4.22 and Equation 4.23.

$$E(t) \leq E_{\text{cap}} \cdot E_{\text{DoD}} \quad \text{for } t = 1, \dots, T \quad (4.17)$$

$$E(t) \leq E_{\text{cap}} \cdot E_{\text{soc}_{\text{max}}} \quad \text{for } t = 1, \dots, T \quad (4.18)$$

$$E(t) \geq E_{\text{cap}} \cdot E_{\text{soc}_{\text{min}}} \quad \text{for } t = 1, \dots, T \quad (4.19)$$

$$P_{\text{ch}}(t) \leq P_{\text{rated}} \quad \text{for } t = 1, \dots, T \quad (4.20)$$

$$P_{\text{dch}}(t) \leq P_{\text{rated}} \quad \text{for } t = 1, \dots, T \quad (4.21)$$

$$E_{\text{cap}} \leq E_{\text{cap}_{\text{max}}} \quad \text{for } t = 1, \dots, T \quad (4.22)$$

$$P_{\text{rated}} \leq P_{\text{rated}_{\text{max}}} \quad \text{for } t = 1, \dots, T \quad (4.23)$$

4.3.8 Grid Modelling

The power imported from the grid cannot be more than the maximum limit as shown in Equation 4.24. In this thesis, the maximum limit is equal to the highest hourly load observed for the years 2021 and 2022 at Skjetlein. The power export limit is set by the "Plus Customer" scheme and is implemented through Equation 4.25. Due to the power charge mentioned in Section 4.1.3, the peak energy consumption from the grid per month must be calculated. The difference $P_{\text{g_in}}(t) - P_{\text{dch}}(t)$ can be seen as the net power drawn from the grid, and is used to find the peak energy consumption from the grid.

$$P_{\text{g_in}}(t) \leq P_{\text{g_in_max}}(t) \quad \text{for } t = 1, \dots, T \quad (4.24)$$

$$P_{\text{g_out}}(t) \leq P_{\text{g_out_max}}(t) \quad \text{for } t = 1, \dots, T \quad (4.25)$$

$$\begin{aligned} P_{\text{g_in_max_monthly}}(m) &\geq P_{\text{g_in}}(t) - P_{\text{dch}}(t), \\ \text{for } t &= 1, \dots, T \\ m &= 1, \dots, M \end{aligned} \quad (4.26)$$

4.3.9 Objective Functions

Three different objective functions were utilized in this thesis. The first one, Equation 4.29, aims to minimize the amount of curtailed power (P_d). This objective function finds the maximum storage capacity and rated power for all the scenarios. The results are then used to set the scenario's maximum rated power and battery capacity through constraints shown in Equation 4.22 and Equation 4.23.

Then, the objective function from Equation 4.30 is used to minimize the annual electricity bill from Equation 4.7 within the sizing limitations from Equation 4.22 and Equation 4.23. The aim of reducing costs ensures that the cheapest generation is set to satisfy the system load at each hour. Additionally, the sizing limitations from Equation 4.22 and Equation 4.23 were implemented with the aim of using as much of the locally produced solar power as possible.

Lastly, the objective function from Equation 4.31 is used to analyze how the model reacts to incorporating the initial investment costs of the two storage solutions. The initial investment costs (I_0) are calculated based on the cost-of-service tool methodology from page 126 in [82]. The calculation includes the cost of capacity components (E_{ec}) and cost of power components (E_{pc}) as shown in Equation 4.27. Capacity components include battery packs, storage management systems, etc., while power components include power electronic devices, balance-of-system components, etc. [83]. In addition to the energy and power-specific

costs, the investment costs also include the costs of engineering and other necessary labour. Due to the fact that the investment costs depend on a number of variables, it is an uncertain cost. Therefore, there is a chance that the cost values utilized in this thesis might be too optimistic or pessimistic.

As the investment costs often are a lump-sum payment, they are converted into annual costs using the annuity factor ϵ as illustrated in Equation 4.28 where E_{life} is the ESS lifetime and r is the discount rate. Other storage costs, such as operation and maintenance (OM) costs, are not included in the model as this would require a more in-depth economic analysis.

$$I_0 = (E_{ec} \cdot E_{cap} + E_{pc} \cdot P_{rated}) \cdot \epsilon \quad (4.27)$$

$$\epsilon = \frac{r}{1 - (1 + r)^{-E_{life}}} \quad (4.28)$$

$$\text{Minimize: } \sum_{t \in T} P_d(t) \quad (4.29)$$

$$\begin{aligned} \text{Minimize: } & E_{costs} - E_{revenues} \\ E_{costs} = & E_{fixed} + \sum_{t \in T} [(C_{ec}(t) + C_{ct}(t) + C_{spot}(t)) \cdot P_{g_in}(t)] \\ & + \sum_{m \in M} [C_{peak}(m) \cdot P_{g_in_max_monthly}(m)] \\ E_{revenues} = & \sum_{t \in T} [(C_{spot}(t) + C_{spot}(t) \cdot MLLR) \cdot P_{g_out}(t)] \end{aligned} \quad (4.30)$$

$$\begin{aligned} \text{Minimize: } & E_{costs} + I_0 - E_{revenues} \\ E_{costs} = & E_{fixed} + \sum_{t \in T} [(C_{ec}(t) + C_{ct}(t) + C_{spot}(t)) \cdot P_{g_in}(t)] \\ & + \sum_{m \in M} [C_{peak}(m) \cdot P_{g_in_max_monthly}(m)] \\ E_{revenues} = & \sum_{t \in T} [(C_{spot}(t) + C_{spot}(t) \cdot MLLR) \cdot P_{g_out}(t)] \end{aligned} \quad (4.31)$$

4.3.10 Overview of Input Data

The following table shows the input data used in the optimization models alongside the references from which these values were extracted.

Table 4.3.1: Storage inputs for the optimization models.

Parameter	VRFB	Ref	H2 storage	Ref
η_{ch} [%]	83.6	[41]	59 ^a	[84]
η_{dch} [%]	83.6	[41]	59	[84]
E_{DoD} [%]	90	[85]	83	[84]
$E_{\text{soc}_{\text{max}}}$ [%]	90	[79]	100	[84]
$E_{\text{soc}_{\text{min}}}$ [%]	10	[79]	0%	[81]
E_{life} [years]	20	[86]	18	[87]
$P_{\text{g_in_max}}(t)$ [kW]	100	[66]	100	[66]
$P_{\text{g_out_max}}(t)$ [kW]	$\max(P_{\text{load}})^{\text{b}}$	-	$\max(P_{\text{load}})$	-

^a Includes the efficiency of using a PEM electrolyzer and PEM fuel cell.

^b Maximum hourly electrical load at Skjetlein during the simulation period.

Table 4.3.2: Economic Parameters for the optimization models.

Parameter	VRFB	Ref	H2 storage	Ref
E_{fixed} [NOK]	8800 + 4800	[63], [64]	8800 + 4800	[63], [64]
MLR [%]	6 (winter), 4 (summer)	[62]	6 (winter), 4 (summer)	[62]
r [%]	4	[88]	4	[88]
E_{ec} [NOK/kWh]	2306	[43]	40 ^a	[89]
E_{pc} [NOK/kW]	9787	[43]	32118 ^b	[89]

^a Assumed equal to energy capacity cost of 2025 in [89]. 1 USD = 10.66 NOK used in the calculations.

^b Assumed equal to power capacity cost of 2025 in [89]. 1 USD = 10.66 NOK used in the calculations.

^c Calculated using cost-of-service tool from [43], assuming a cost reduction of 5.5% every year from 2016 to 2023. Inflation is taken into account, and 1 USD = 10.66 NOK is used in the calculations.

^d Calculated using cost-of-service tool from [43], assuming a cost reduction of 5.5% every year from 2016 to 2023. Inflation is taken into account, and 1 USD = 10.66 NOK is used in the calculations.

5 | Results

In this section, the results from the study are presented. First, the rooftop PV simulation results will be presented and compared to the actual monthly production data. Then, the APV simulation results will be presented through graphs. Afterwards, the storage optimization results will be presented.

5.1 PVSyst Simulations

This section will present all the results from the PVSyst simulations.

5.1.1 Existing Rooftop PV

Since the production from the existing PV systems at Skjetlein vary from year to year, it was decided to simulate all these installations in PVSyst to get the production from a "synthetic" year. The year is referred to as "synthetic" because the data does not represent an actual year but rather a "typical" year built on meteorological data from Meteonorm 8.1. To verify the simulated PV production data, the monthly values are compared with historical production data from Skjetlein. This is visually represented in Figure 20, Figure 21 and Figure 22.

For the PV system at the STO building, simulated production is generally higher than the real production. The only three months when the real production exceeds the simulated production are May 2021, September 2022, and November 2022. The production pattern is slightly different for the main building, where real production only exceeded the simulated production in November 2022. Historical production data is generally lacking for this PV system because it was installed in September 2022. The simulated PV production at the TIP building shows fluctuations compared to the actual production. There are some months where the simulation overestimates the PV production (e.g. July 2021 and April 2023), while in other months, the simulation underestimates the PV production. The total simulated solar PV production for existing installations constitutes the base case scenario. The total power output from this case throughout a year is illustrated in Figure 23. Details regarding the simulation of the rooftop PV systems can be found in the PVSyst reports in Appendix D.

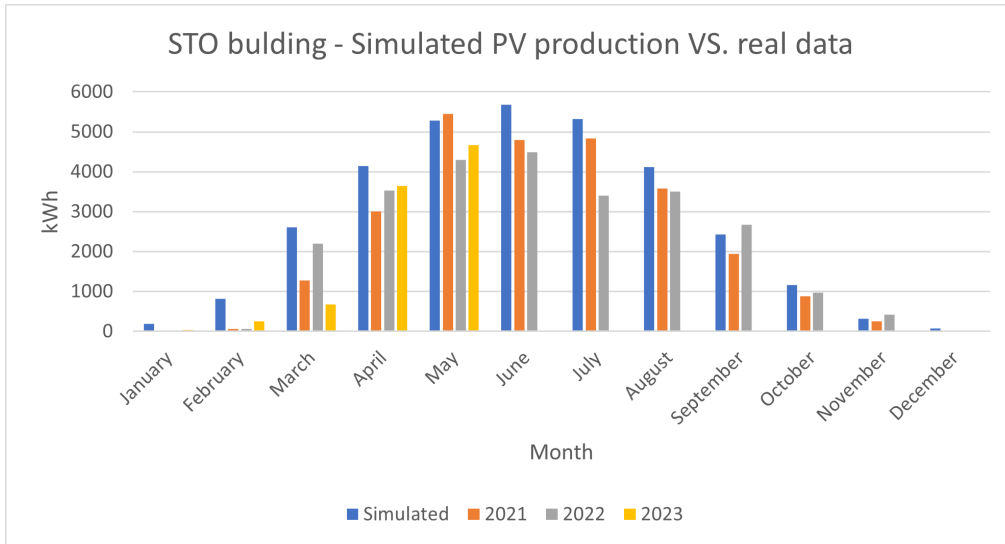


Figure 20: Simulated monthly production compared to real production [kWh] for STO building PV system (41.2 kWp).

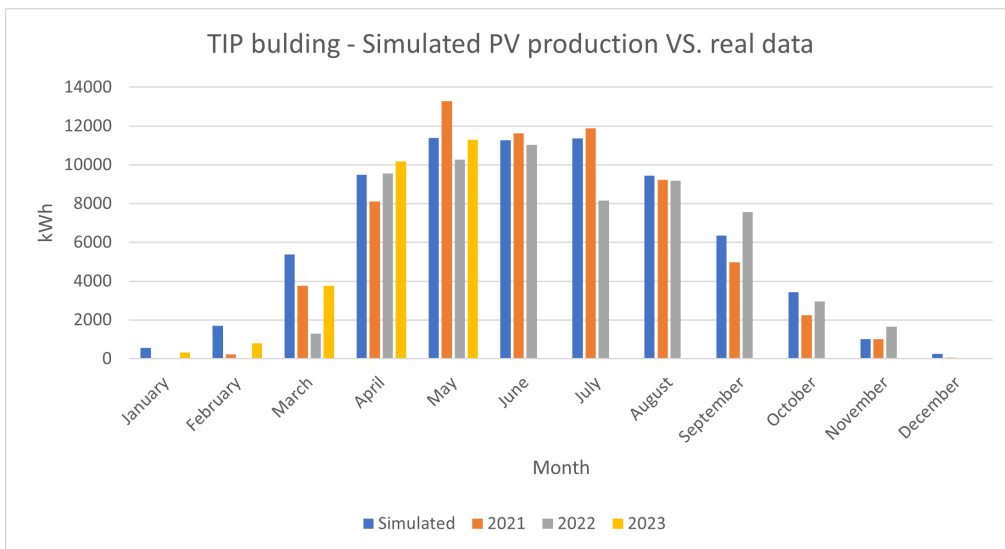


Figure 21: Simulated monthly production compared to real production [kWh] for TIP building PV system (84 kWp).

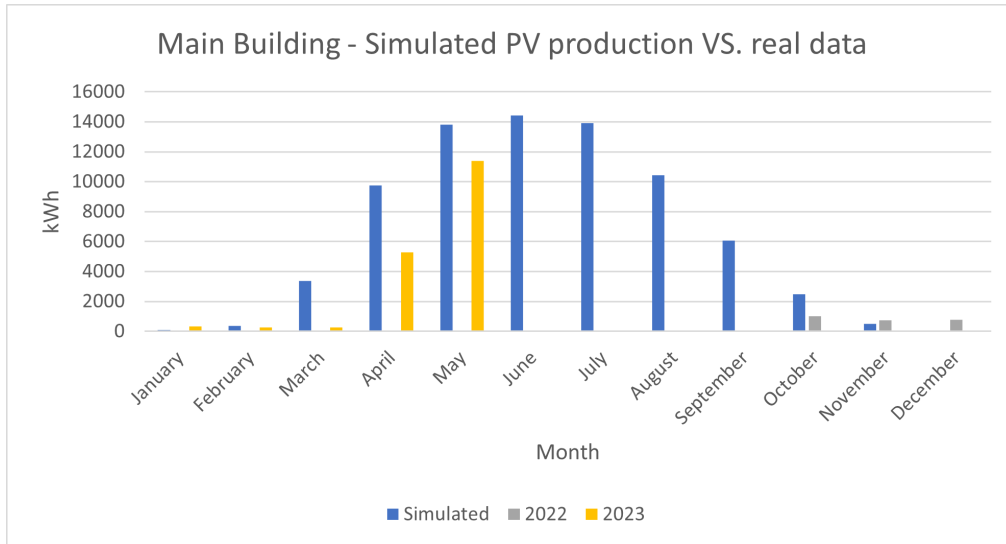


Figure 22: Simulated monthly production compared to real production [kWh] for the main building PV system (110 kWp).

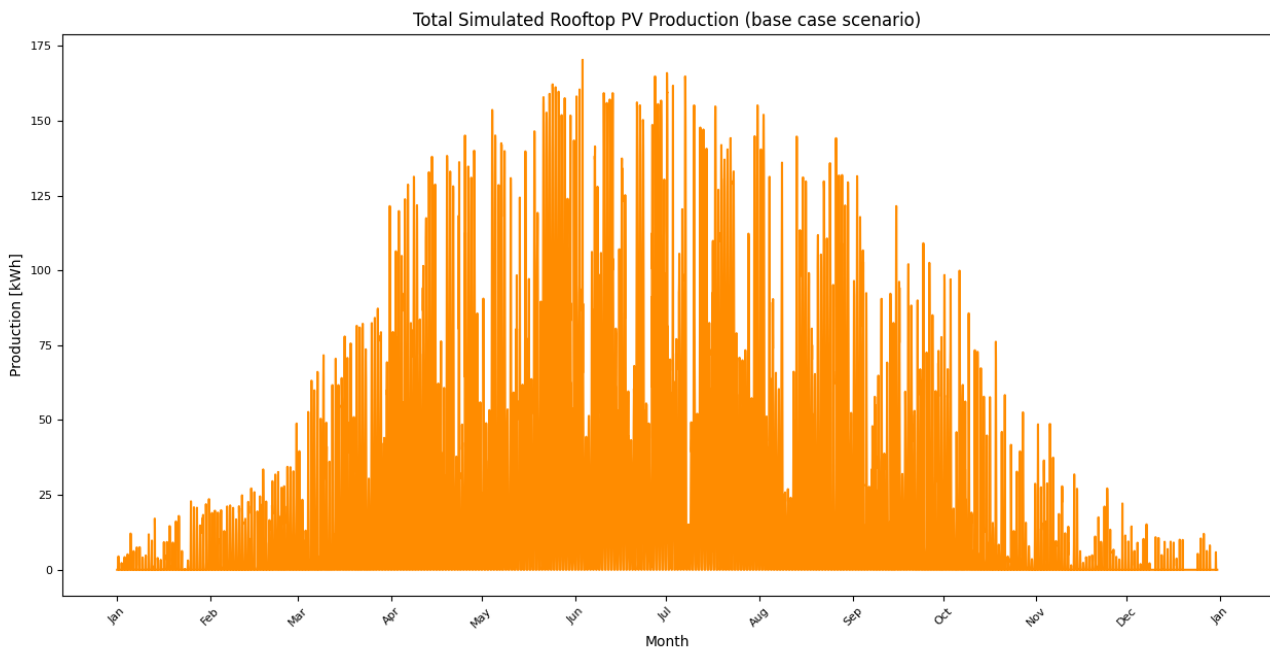


Figure 23: Total rooftop PV production [kWh] (base case scenario).

5.1.2 AgriPV Scenarios

As previously mentioned, three APV scenarios have been simulated as a part of this thesis. Two of the scenarios have an installed peak power of 711 kWp, while the last one has an installed peak power of 1.6 MWp. To get an overview of the total power production at the school, the power production from each APV scenario is added together with the simulated rooftop PV (base case scenario). In this way, we end up with three different scenarios for APV at Skjetlein, including the PV installations they already have. The power output from each of the APV

scenarios (including the base case scenario) are shown in Figure 24, Figure 25, and Figure 26. The power production is plotted together with Skjetlein High School's hourly electricity demand for 2021. The dashed line shows the 100 kW feed-in limit from the "Plus Consumer" scheme, which is almost constantly exceeded for all the scenarios.

From the plots, it is clear that the positioning and orientation of an APV system has an effect on power production. There is a significant difference in power production between the North S/N scenario (Figure 25) and the North E/W scenario (Figure 24), despite the fact that the systems have the exact same installed peak power. The North S/N scenario generally outperforms the North E/W scenario. This is also reflected in the specific yield and performance ratio shown in Table 5.1.1. A specific yield of $1082 \text{ kWh/kWp/year}$ was achieved for the North S/N scenario, which is even higher than typical specific yields for Norwegian PV systems, as mentioned in Section 2.5. Furthermore, the South E/W scenario (Figure 26) clearly has the highest power production, but this system also has the highest installed peak power. The PVSyst reports from the APV scenario simulations are shown in Appendix E.

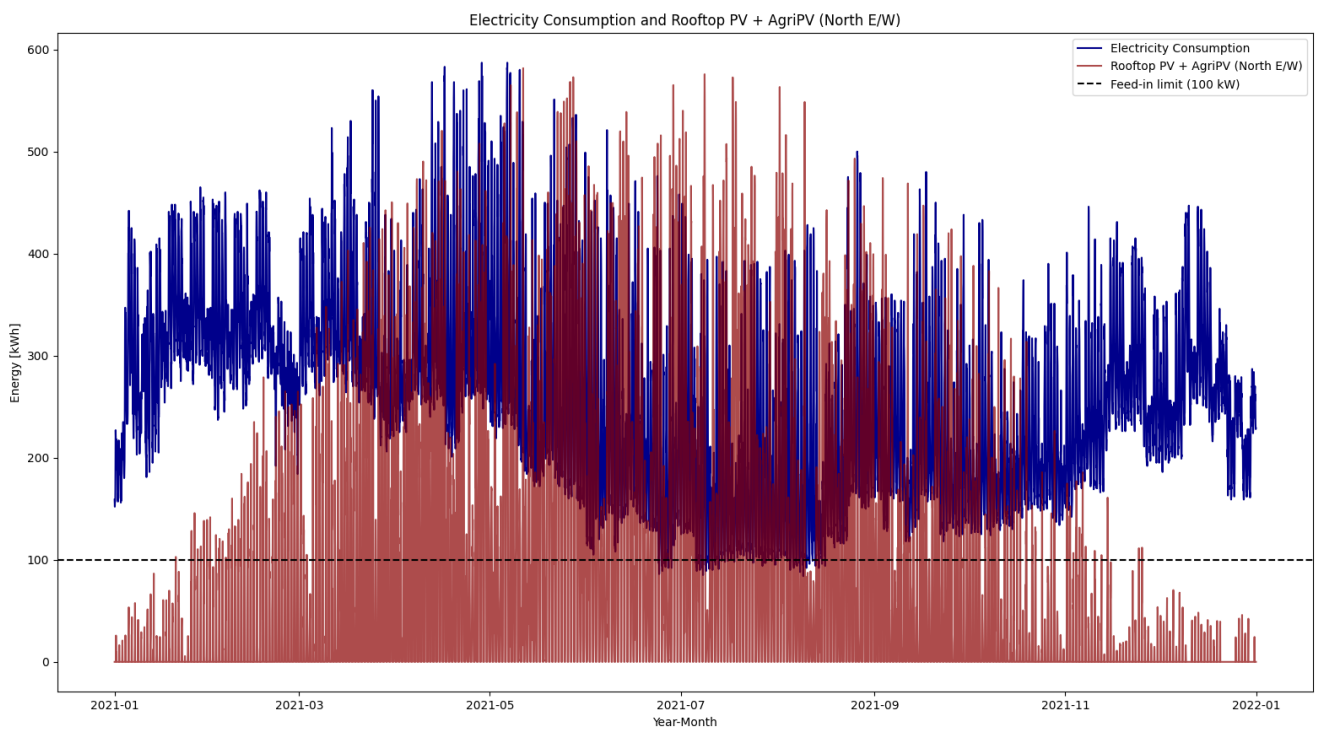


Figure 24: North E/W scenario including base case.

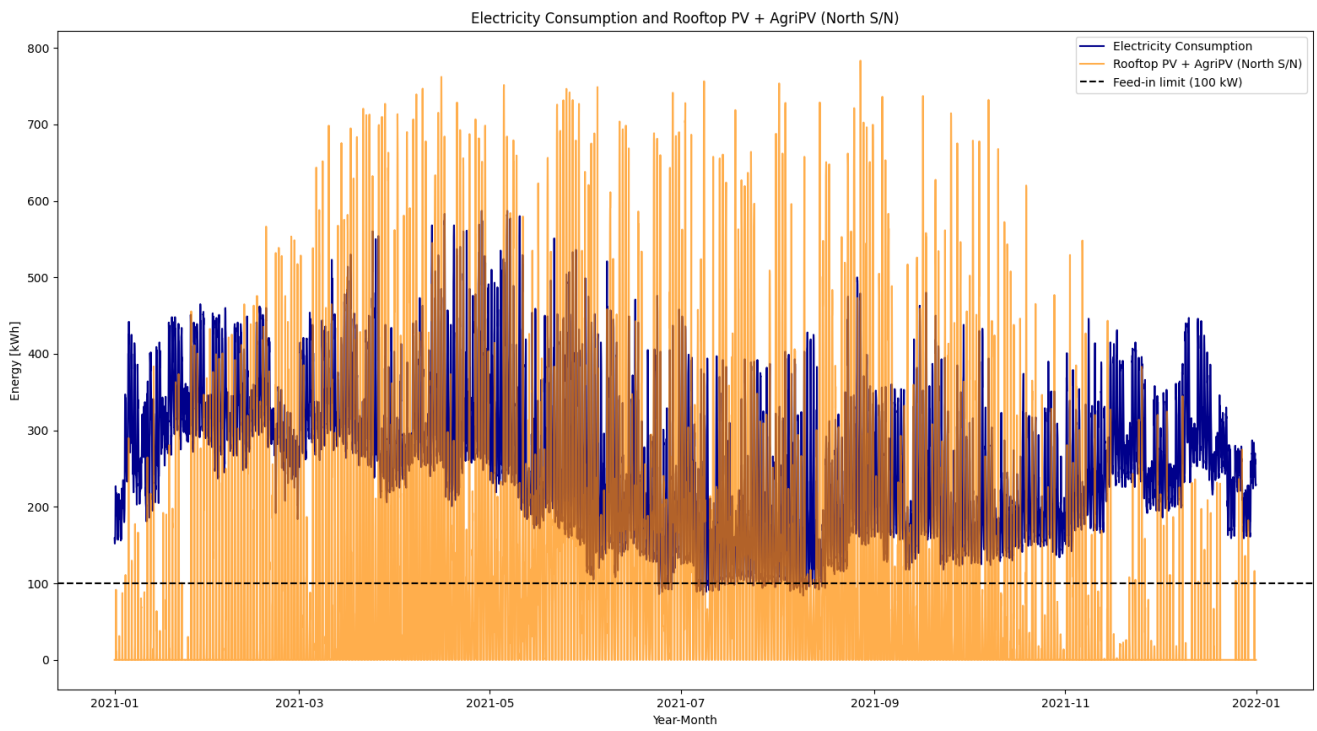


Figure 25: North S/N scenario including base case.

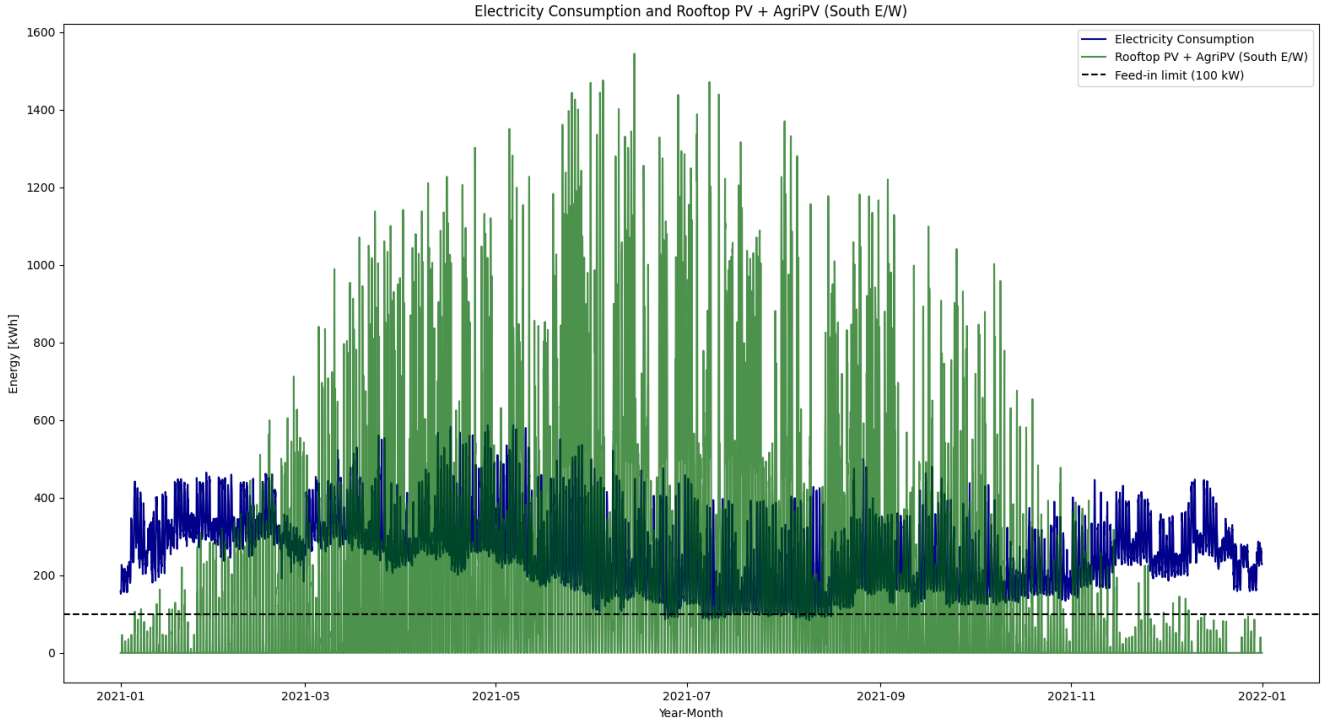


Figure 26: South E/W scenario including base case.

Table 5.1.1: Specific yields for different APV scenarios and their performance ratios.

Scenario	Specific yield [kWh/kWp/year]	Bifacial Performance Ratio [%]
North E/W	767	61
North S/N	1082	88
South E/W	989	77

5.2 VRFB Storage Optimization

This section will present all the results from the VRFB storage optimization.

5.2.1 Maximum Storage Capacity and Rated Power

The optimisation process's first step is determining the maximum storage capacity and rated power that the VRFB can have. This is done to make sure that the sizing of the battery stays within certain limits. If such limits do not exist, the optimization model can choose to size the battery in unrealistic manners to achieve high savings. By setting the objective function to minimize the curtailment, the model will try to use all of the excess solar PV production. This leads

to the maximum storage capacity and power rating as shown in Table 5.2.1. Keep in mind that the capacity and rating values are rounded up or down depending on the value.

Table 5.2.1: Maximum storage capacity and rated power for each APV scenario from minimizing curtailment.

	APV South E/W	APV North E/W	APV North S/N
$E_{\text{cap}_{\text{max}}}$	400 MWh	3 MWh	6 MWh
$P_{\text{rated}_{\text{max}}}$	1 ^a MW	300 kW	500 kW

^a Adjusted to 100 MW.

There is a notable difference in the capacity limitations for the scenarios. The scenario with the highest installed peak power (APV South E/W) achieves the highest maximum capacity and rated power. A 400 MWh, 1 MW battery yields an energy to power ratio (E/P) of 400 hours (16.7 days). In [90], an E/P of 100 is stated as the maximum ratio theoretically possible for a VRFB. VRFB projects normally have ratios ranging from 4 to 8 hours. To keep the E/P at a typical value, $P_{\text{rated}_{\text{max}}}$ is increased to 100 MW for the South E/W scenario. The E/P for the North E/W and S/N scenarios are 10 and 12 hours, respectively. Even though these ratios are not the most typical E/P for VRFB projects, they are acceptable for long-term storage and will therefore remain unchanged.

5.2.2 Control Strategy 1 - Minimize Total Electricity Costs

The first control strategy in the optimization model aims to minimize the total electricity costs. Since this control strategy does not include any costs related to the operation of the VRFB or investment costs, it must contain a storage size limitation. Energy and power-related limitations are set according to the results from minimizing the curtailed power (Table 5.2.1), except for the south E/W scenario where $P_{\text{rated}_{\text{max}}}$ was increased. The results from the optimization model are shown in Table 5.2.2.

Not surprisingly, the scenario with the highest installed peak power (South E/W) achieves the highest cost savings and curtailment. For the other two scenarios, the cost reductions are roughly 10% higher for the North S/N scenario than the North E/W scenario. The curtailment, however, is 0.082% higher for the North S/N scenario than the North E/W scenario. This may be related to the fact that an east-west oriented solar PV system provides two power peaks during the day (one in the morning and one in the evening), which indicates that the production profile from the North E/W scenario possibly may be a better fit for the electricity demand profile at Skjetlein High School.

Table 5.2.2: APV scenario results using control strategy 1.

	APV South E/W	APV North E/W	APV North S/N
$E_{\text{cap}_{\text{max}}}$	400 MWh	3 MWh	6 MWh
$P_{\text{rated}_{\text{max}}}$	100 MW	300 kW	500 kW
E_{cap}	400 MWh	3 MWh	6 MWh
P_{rated}	100 MW	300 kW	500 kW
Curtailed solar PV ^a	0.42%	0.013%	0.095%
Electricity cost savings ^b	78.33%	30.23%	40.32%

^a % of total PV power production.

^b % of the total electricity costs without PV and storage.

The following figures provide an overview of plots created as a result of implementing control strategy 1 in the optimization model. The plots include the following characteristics: battery discharging/charging dynamics, current energy stored in the battery, power import from the grid to the load, and power export from the PV system to the grid.

Figure 27 and Figure 28 shows the results from the South E/W scenario (400 MWh, 100 MW VRFB). As illustrated in Figure 27, the grid import has been reduced significantly. This is especially visible during the winter months. Additionally, Figure 28 shows that the optimization model favours the strategy of storing energy throughout the summer and discharging it during December and January, indicating a seasonal pattern. The discharge pattern appears to have a correlation to the Nord Pool spot prices, especially the highest values.

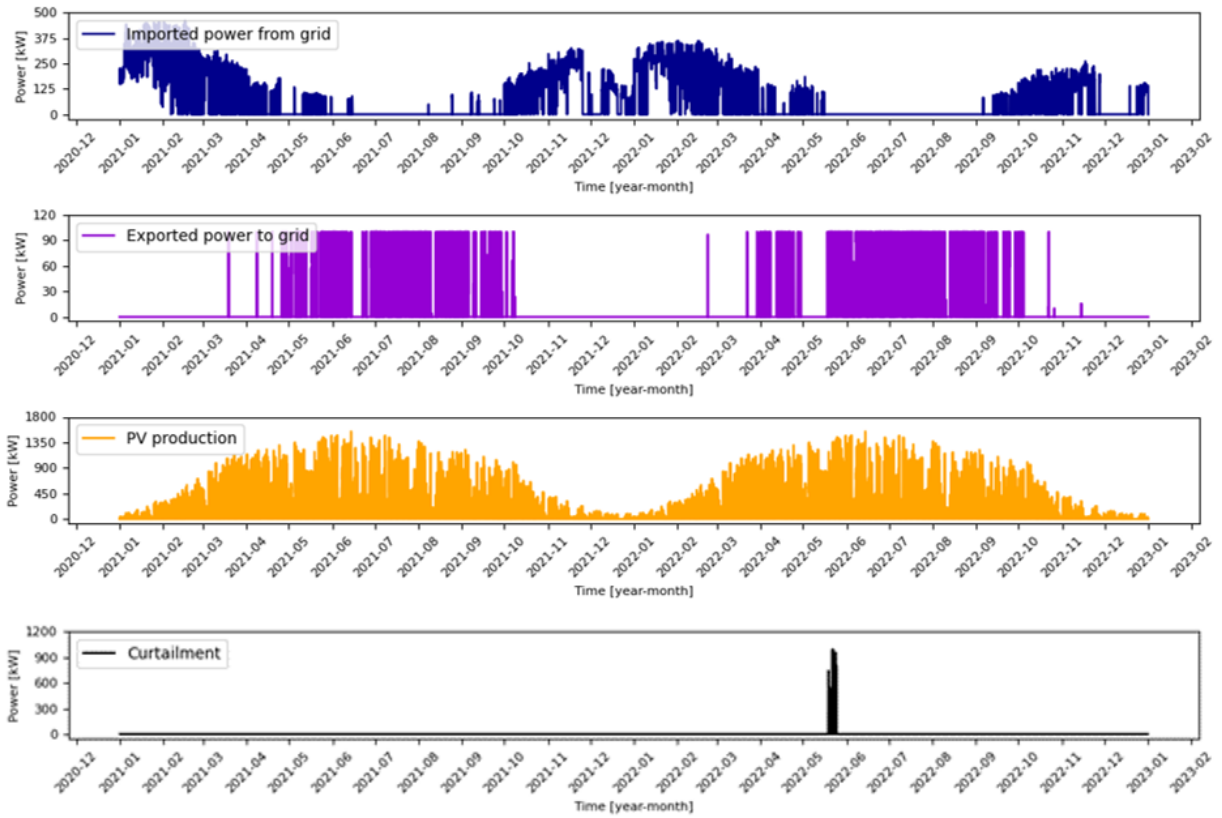


Figure 27: South E/W scenario - control strategy 1 - plots 1/2.

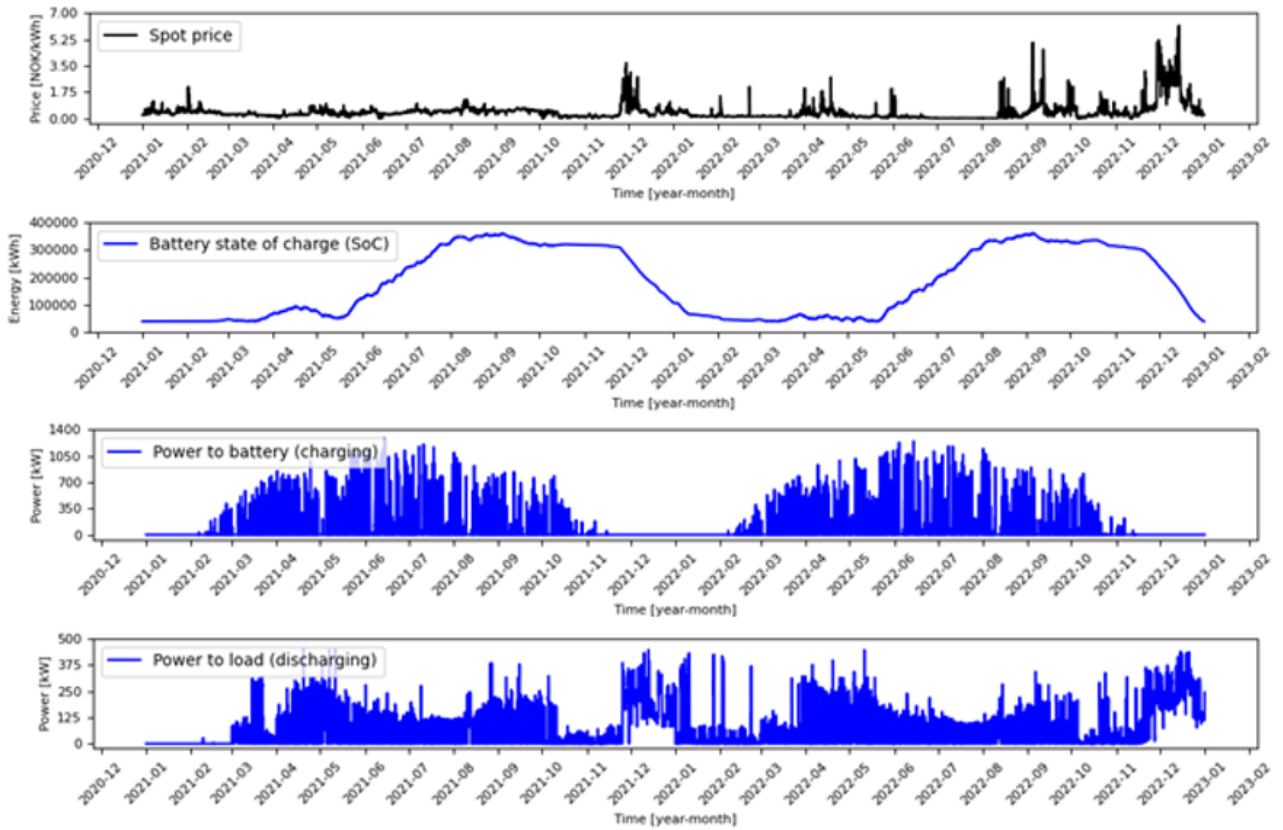


Figure 28: South E/W scenario - control strategy 1 - plots 2/2.

Figure 29 and Figure 30 illustrate the results from the North E/W scenario (3 MWh, 300 kW VRFB). In this scenario, the grid import is higher than in the South E/W scenario. This increase can likely be explained by the size of the battery, which is significantly smaller than the size from the South E/W scenario.

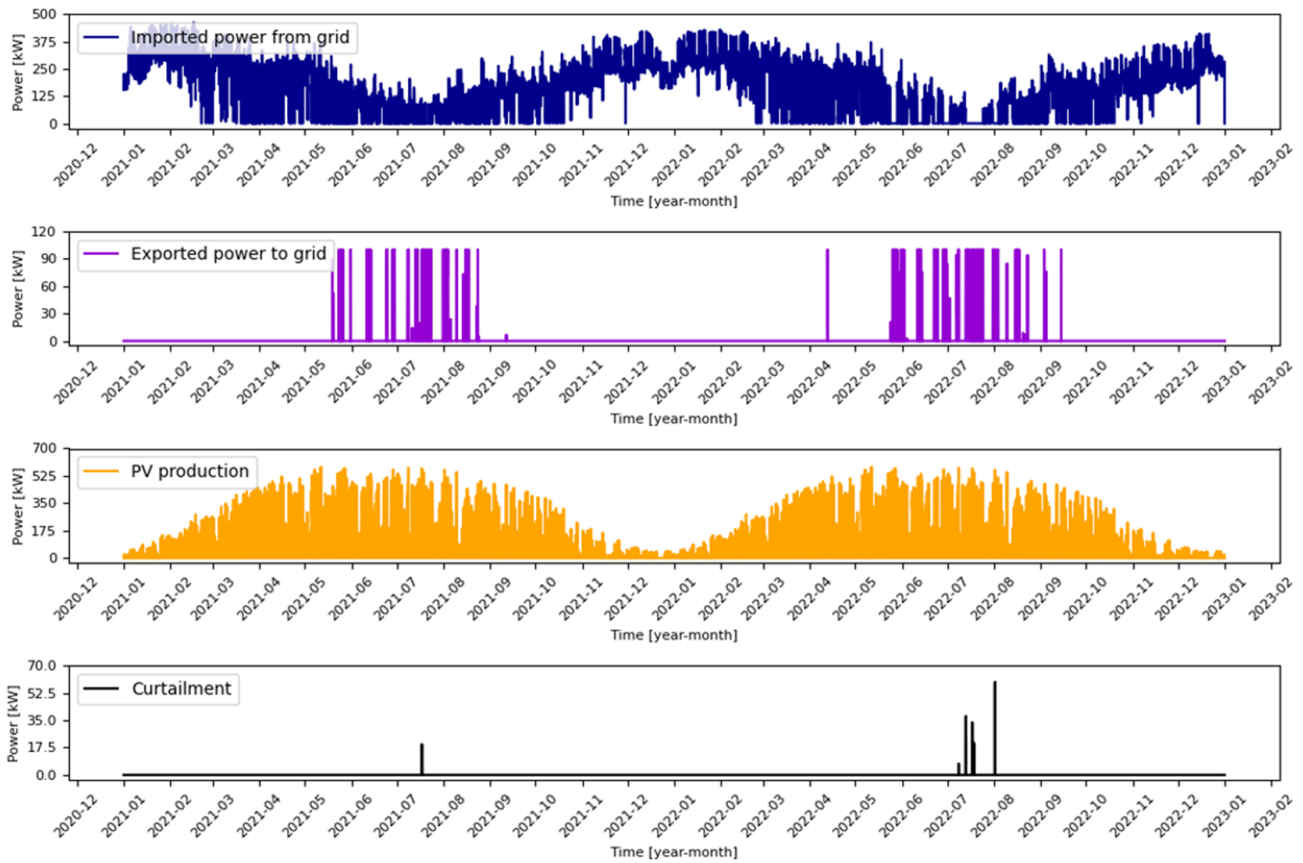


Figure 29: North E/W scenario - control strategy 1 - plots 1/2.

Since this battery has a lower capacity than the South E/W scenario, it discharges more often, as illustrated in Figure 30. Instead of following a seasonal pattern, the battery charges and discharges throughout the summer months and charges a lot during the end of October. Also, in this scenario, the discharge pattern appears to maintain a correlation with the highest Nord Pool spot prices.

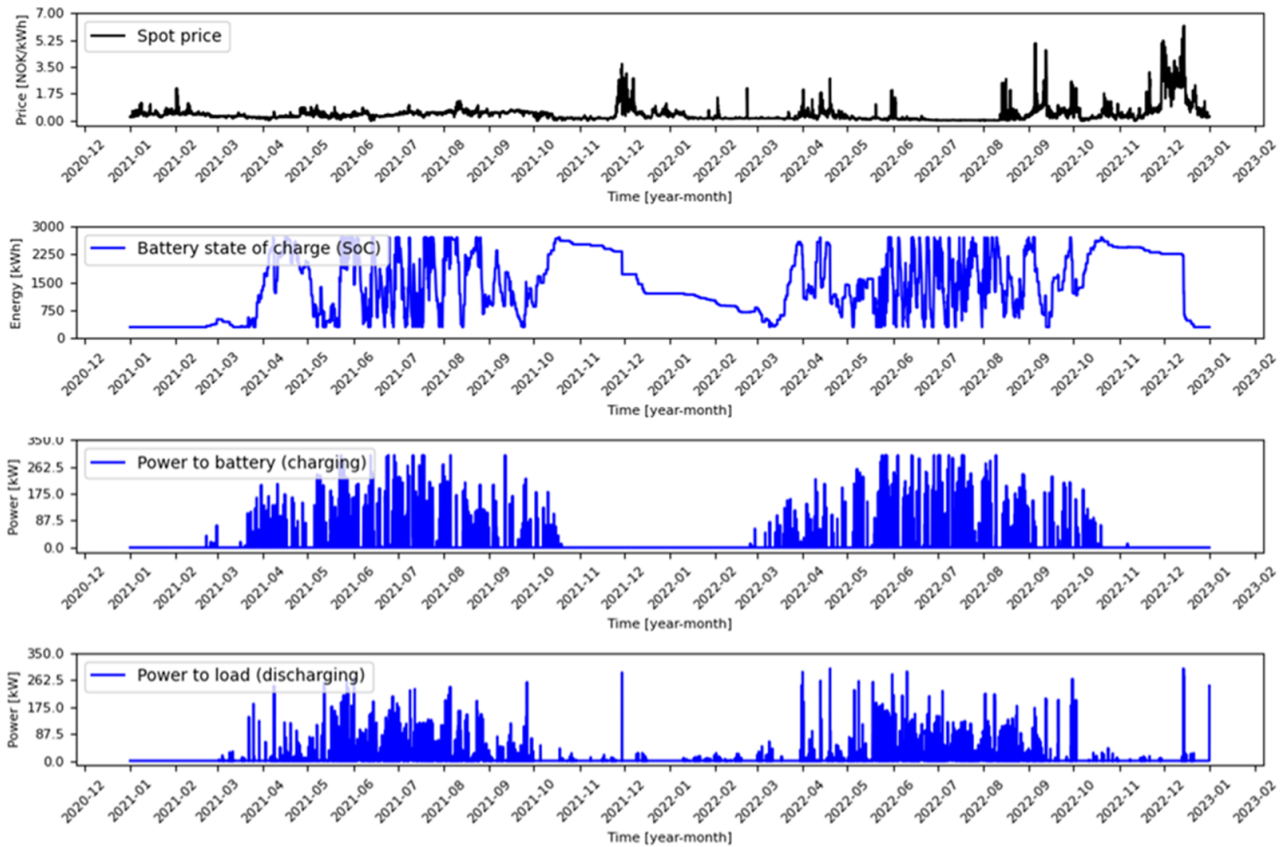


Figure 30: North E/W scenario - control strategy 1 - plots 2/2.

Figure 31 and Figure 32 illustrate the results from the North S/N scenario (6 MWh, 500 kW VRFB). This scenario appears to have characteristics from both the North E/W and the South E/W scenarios. This is logical because the battery capacity falls between the capacities used in the other two scenarios. Similarly to the North E/W scenario, this scenario often discharges throughout the year, except from October to December and December to February, as illustrated in Figure 32. The battery charges up in October and discharges a little bit during the beginning of November. Then, in December, at the point when the Nord Pool spot price is the highest, the battery discharges a lot. Some energy is still left in the battery, which gets discharged in February. This might be because there is a very small spot price peak at the beginning of February, which might make the optimization model hold on to the energy it has stored.

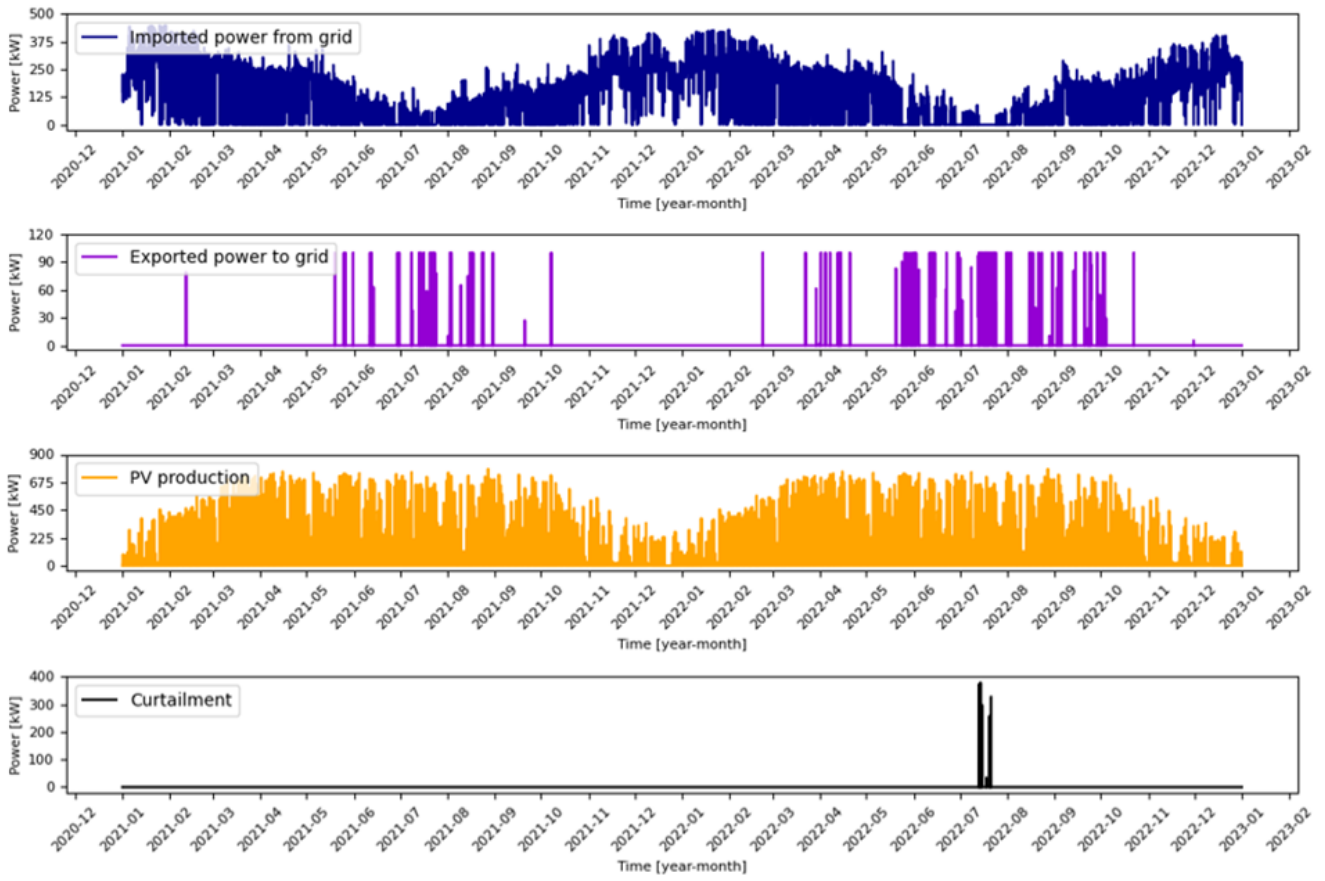


Figure 31: South E/W scenario - control strategy 1 - plots 1/2.

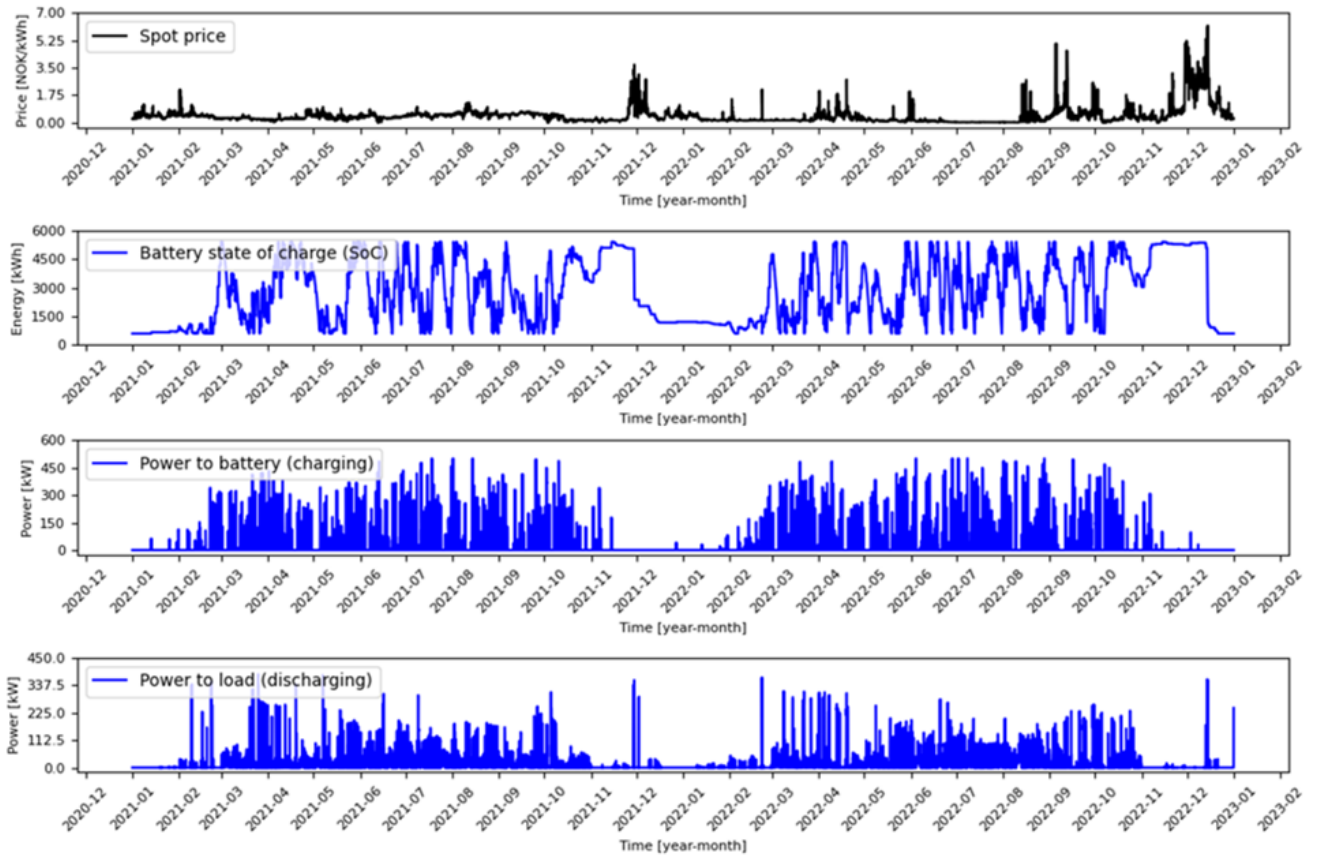


Figure 32: South E/W scenario - control strategy 1 - plots 2/2.

5.2.3 Control Strategy 2 - Minimize Total Electricity Costs and Investment Costs

The second control strategy aims to minimize the total electricity costs and the annual costs of the battery. Since this control strategy includes a cost related to the VRFB, the capacity and power constraints from control strategy 1 are removed. In this way, the model can decide on a suitable storage size based on the battery costs. The results from this control strategy are shown in Table 6.1.2.

The results from this control strategy are lower than the results from control strategy 1. This makes sense due to the incorporation of annual battery costs into the objective function. By lowering both the electricity bill and the annual VRFB costs, the optimization algorithm chooses a lower capacity and power rating, which results in increased total electricity costs and curtailed solar PV power compared to control strategy 1. However, a similarity between this control strategy and the previous one is the fact that the scenario with the highest installed peak power (South E/W) continues to achieve the highest installed capacity and rated power. This is logical because the scenario with the highest solar power output holds the most potential for achieving high electricity cost savings.

The North E/W scenario has a lower curtailment than the North S/N scenario. This observation highlights the assumption that the electricity demand at Skjetlein might better fit an east-west oriented PV system than a south-north oriented PV system.

Table 5.2.3: APV scenario results using control strategy 2.

	APV South E/W	APV North E/W	APV North S/N
E_{cap}	365 kWh	73 kWh	241 kWh
P_{rated}	70 kW	26 kW	54 kW
Curtailed solar PV ^a	36%	5%	9%
Electricity cost savings ^b	38%	24%	31%

^a % of total PV power production.

^b % of the total electricity costs without PV and storage.

Similarly to control strategy 1, the following figures provide an overview of plots created as a result of implementing control strategy 2 in the optimization model. The plots include the following characteristics: battery discharging/charging dynamics, current energy stored in the battery, power import from the grid to the load, and power export from the PV system to the grid.

Figure 33 and Figure 34 shows the results from the South E/W scenario (365 kWh, 70 kW VRFB). As illustrated in Figure 27, the curtailed power for this scenario is quite high, following the PV production pattern. Additionally, the import from the grid is reduced mostly during the summer months (June, July, and August). Figure 34 shows that the optimization model favours the charging and discharging strategy in a daily resolution except for during December. This

makes sense since the battery is considered relatively small for a use case such as Skjetlein, where the electricity demand is above 1 000 000 kWh per year. Even though such a battery only covers a fraction of the school's electricity demand, it could potentially be used for specific purposes, such as providing backup power for critical equipment.

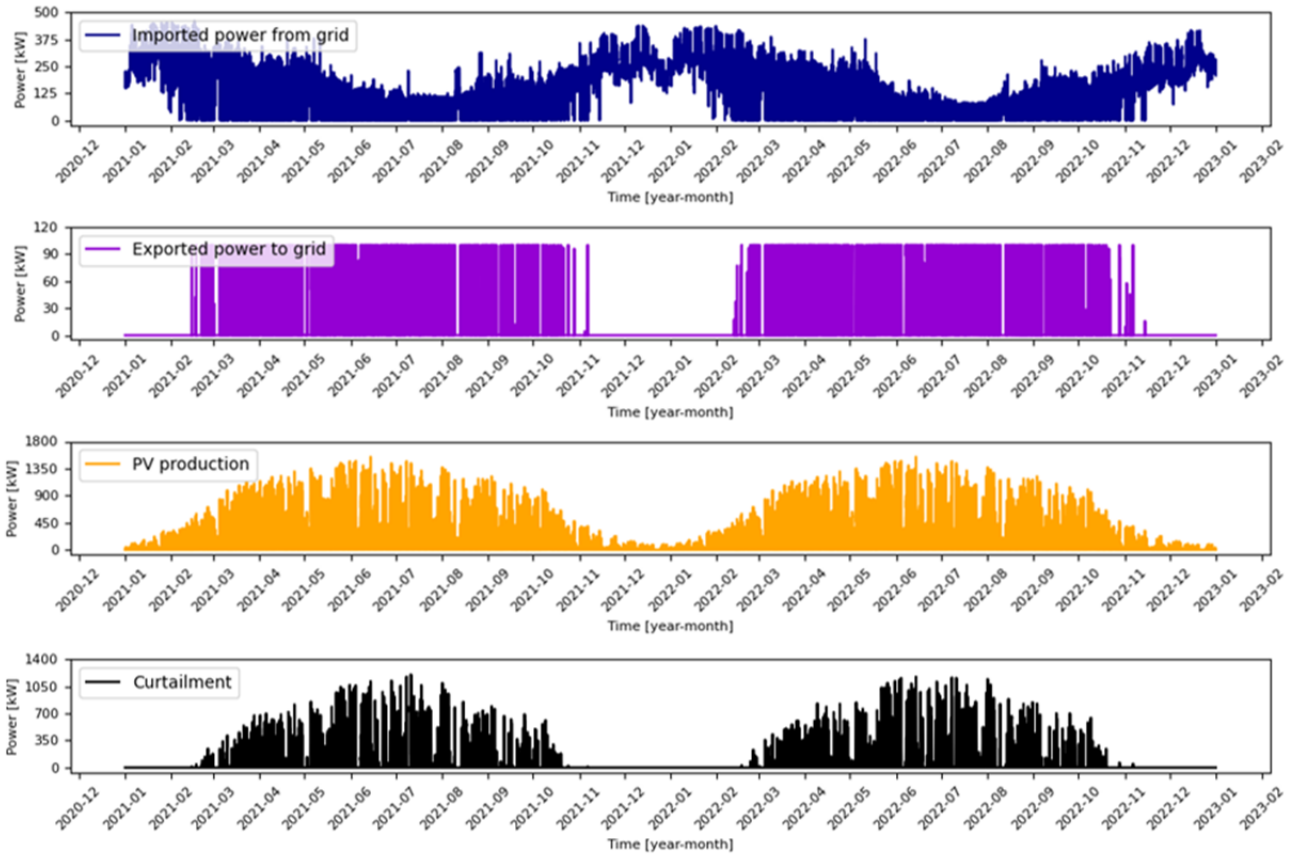


Figure 33: South E/W scenario - control strategy 2 - plots 1/2.

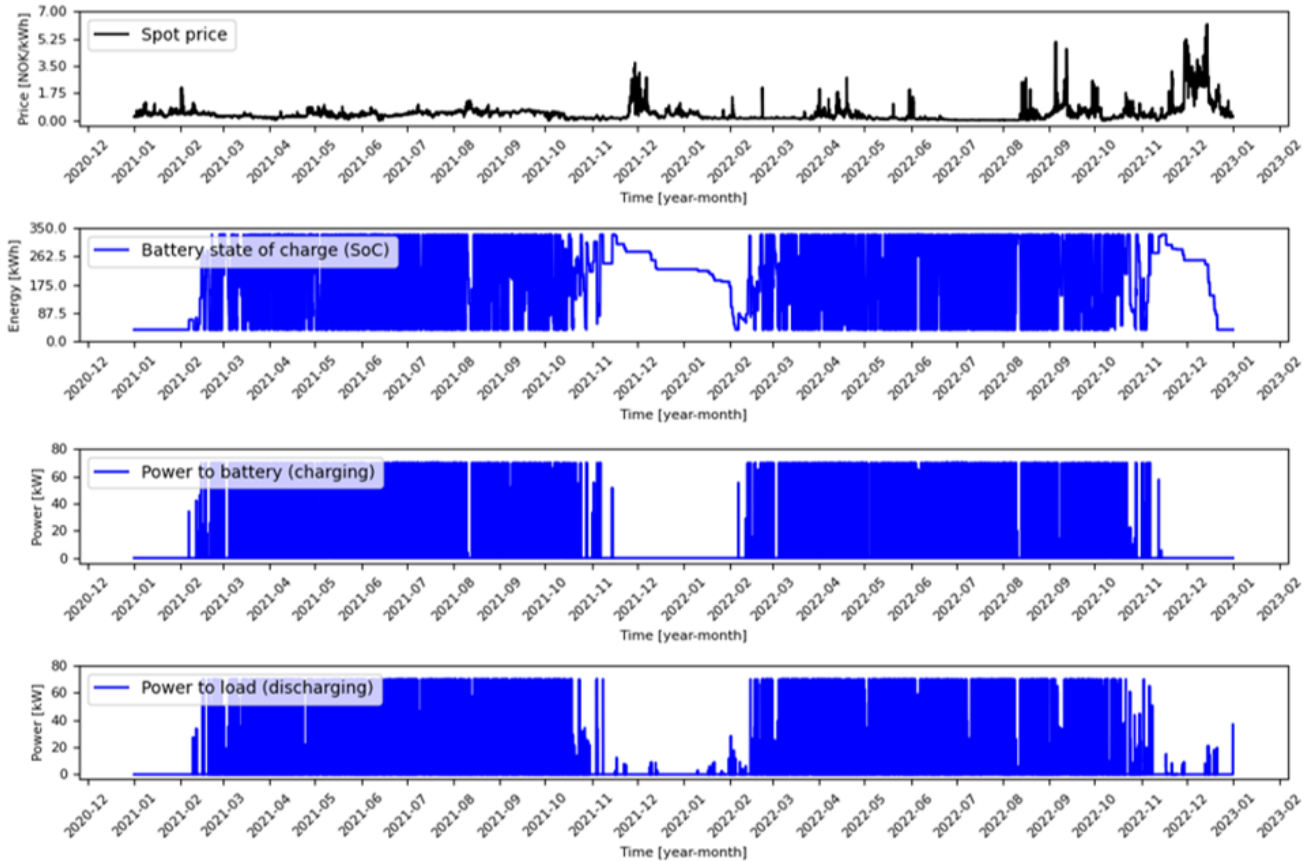


Figure 34: South E/W scenario - control strategy 2 - plots 2/2.

Figure 35 and Figure 36 illustrate the results from the North E/W scenario (73 kWh, 26 kW VRFB). This scenario has an even smaller capacity and power rating than the South E/W scenario and the North S/N scenario, which makes it charge/discharge often throughout the year except from October to March as seen in Figure 36.

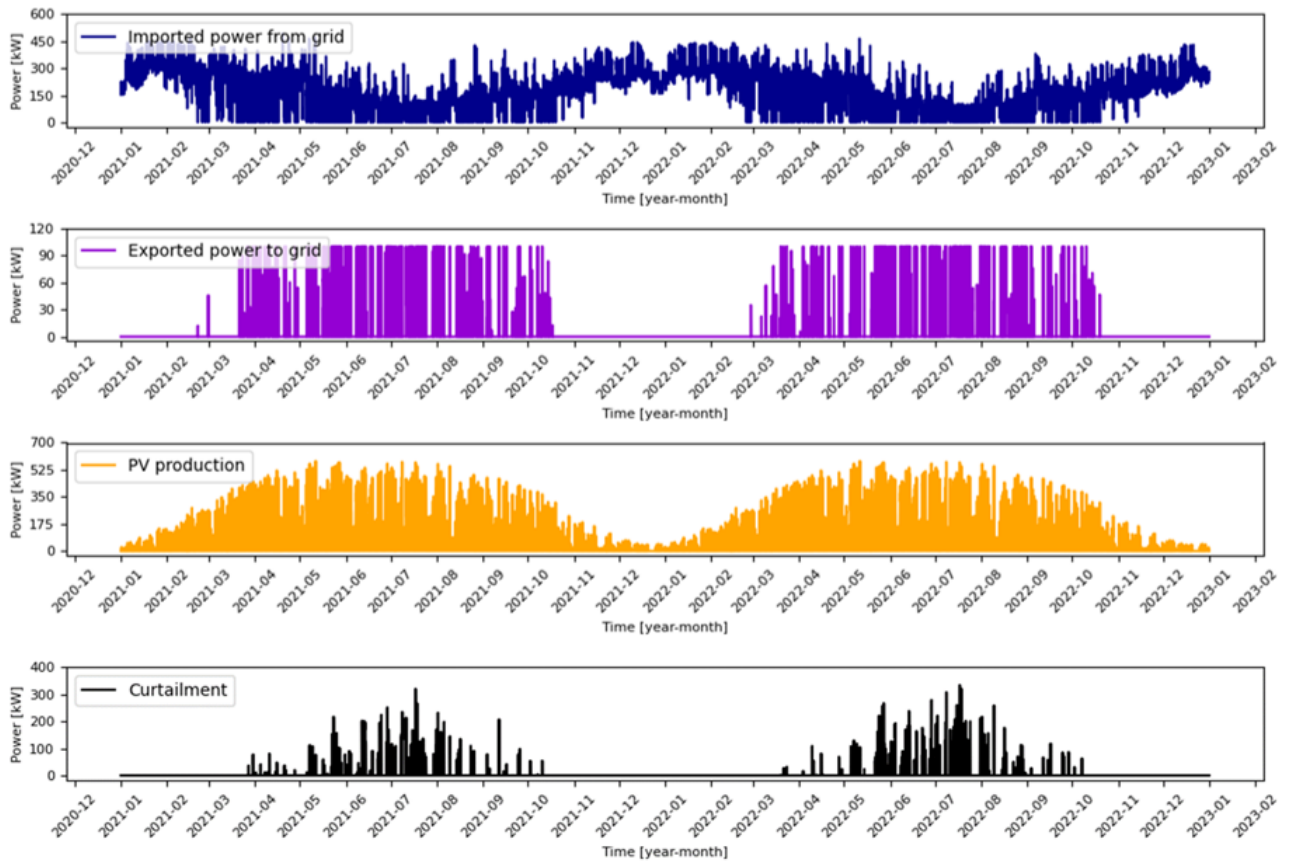


Figure 35: North E/W scenario - control strategy 2 - plots 1/2.

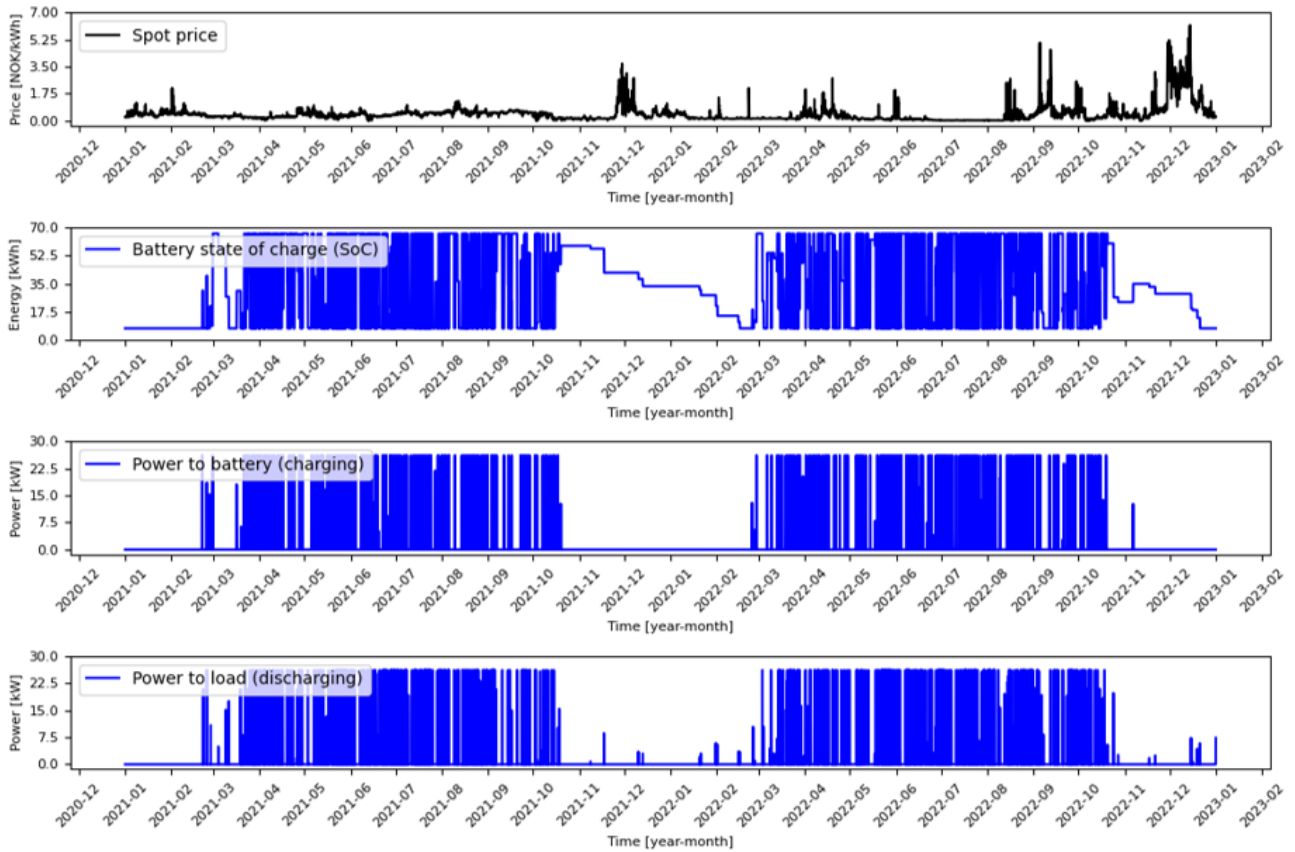


Figure 36: North E/W scenario - control strategy 2 - plots 2/2.

Figure 37 and Figure 38 illustrate the results from the North S/N scenario (241 kWh, 54 kW VRFB). In this scenario, the optimization model chooses to reduce the import from the grid during both the summer and the winter. Even though the storage capacity and power rating are lower than in the South E/W scenario, the optimization model chooses to reduce the import from the grid more during the winter for this scenario than for the South E/W scenario as seen in Figure 37.

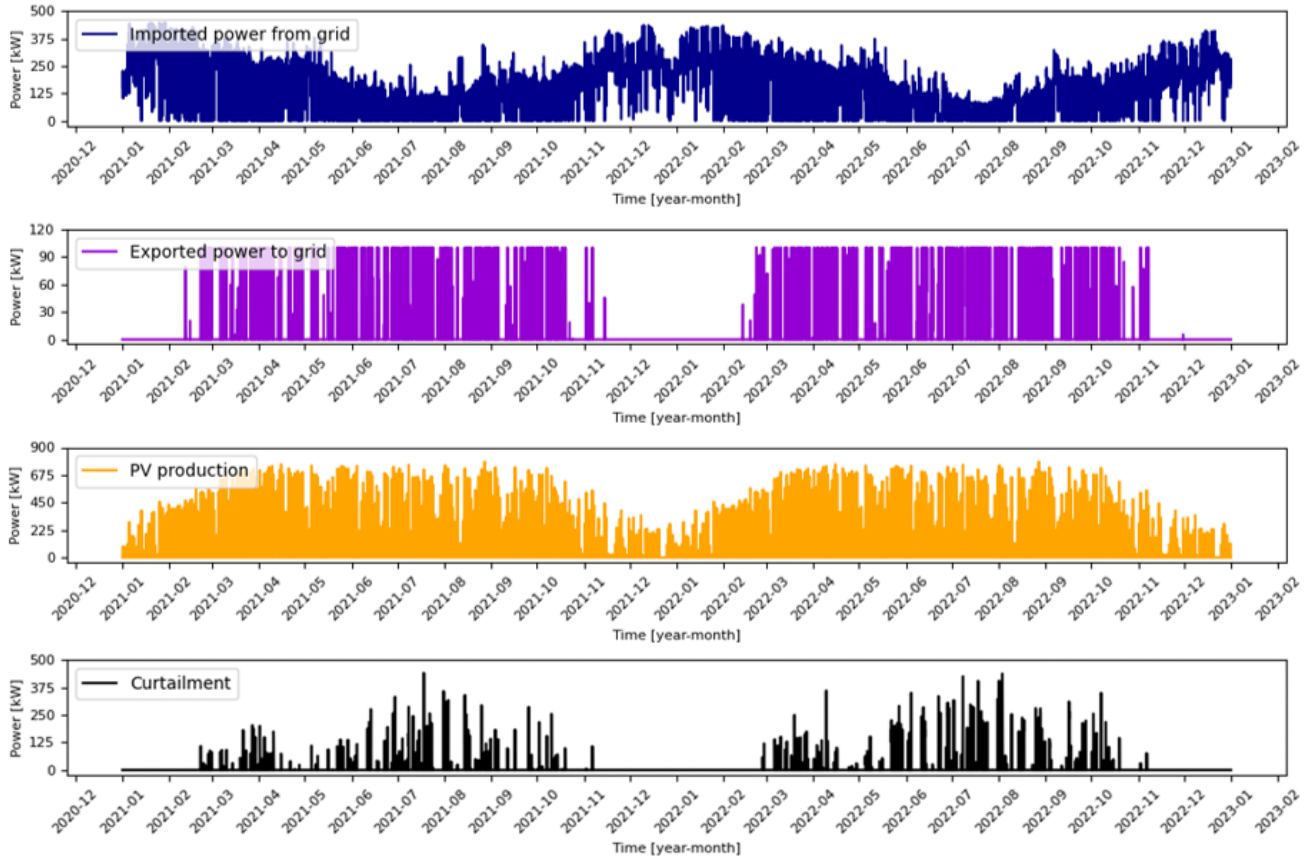


Figure 37: North S/N scenario - control strategy 2 - plots 1/2.

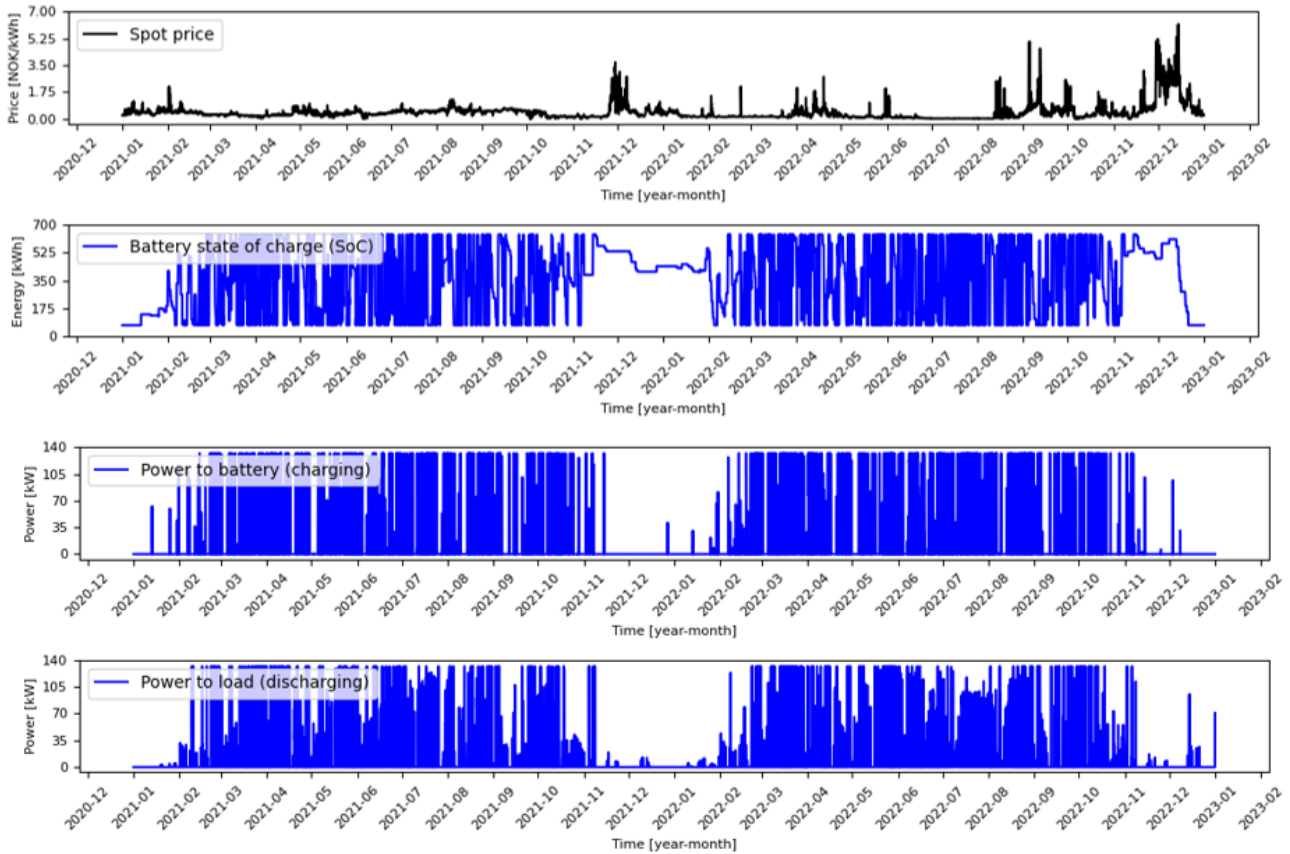


Figure 38: North S/N scenario - control strategy 2 - plots 2/2.

5.3 Hydrogen Storage Optimization

This section will present all the results from the hydrogen storage optimization.

5.3.1 Control Strategy 1 - Minimize Total Electricity Costs

The maximum storage capacity and rating are set according to the procedure in Section 5.2.1. The results from implementing control strategy 1 using a hydrogen storage system are shown in Table 5.3.1. The plots from the simulations are illustrated in Figure 39, 40, 41, 42, 43 and 44. This section does not provide a detailed explanation of these figures because the plots share many similarities with figures from the VRFB simulation. The results will, however, be discussed further in Section 6.1.3.

Table 5.3.1: APV scenario results using control strategy 1.

	APV South E/W	APV North E/W	APV North S/N
$E_{\text{cap}_{\text{max}}}$	200 MWh	4 MWh	8 MWh
$E_{\text{rated}_{\text{p}_{\text{max}}}}$	1 MW	400 kW	600 kW
E_{cap}	200 MWh	4 MWh	8 MWh
$E_{\text{rated}_{\text{p}}}$	1 MW	400 kW	600 kW
Curtailed solar PV ^a	0.19%	0%	0%
Electricity cost savings ^b	61.85%	28.58%	37.07%

^a % of total PV power production.

^b % of the total electricity costs without PV and storage.

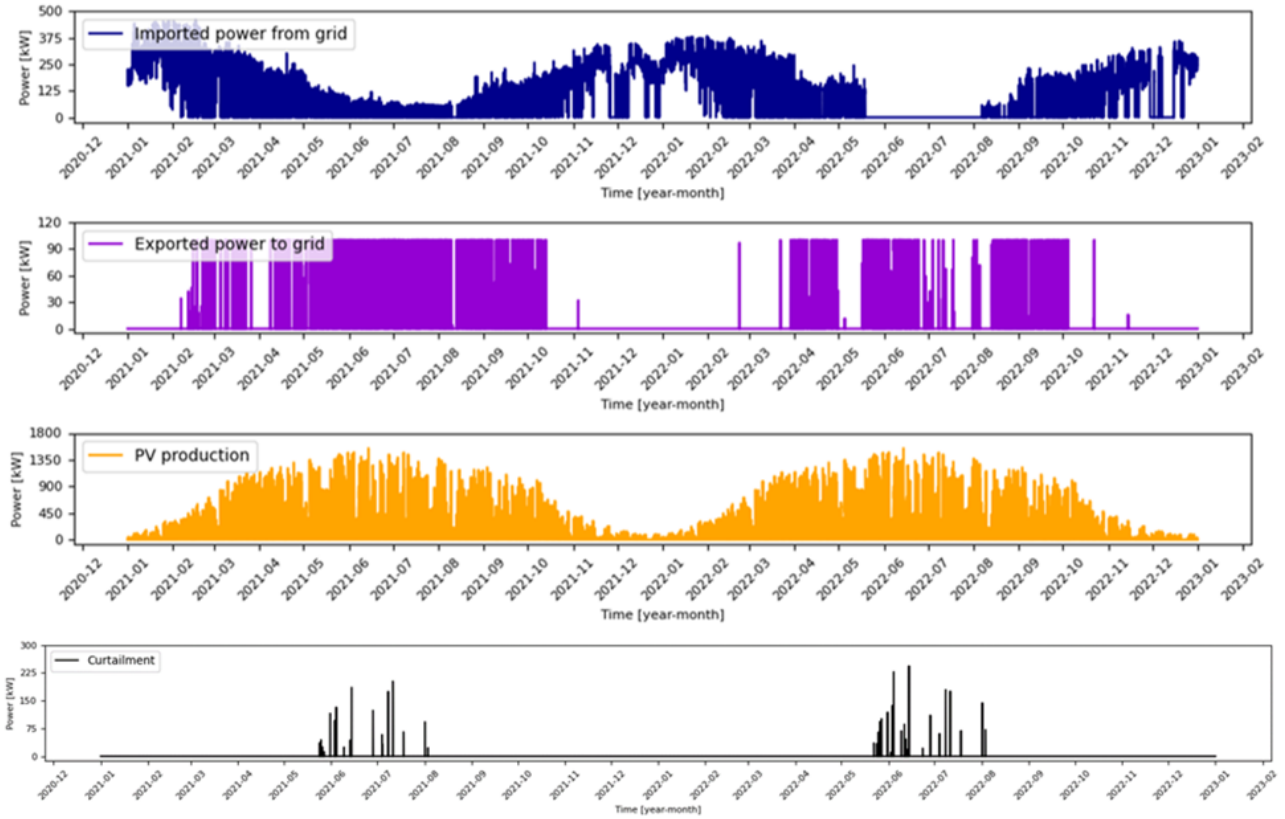


Figure 39: South E/W Scenario - control strategy 1 - plots 1/2.

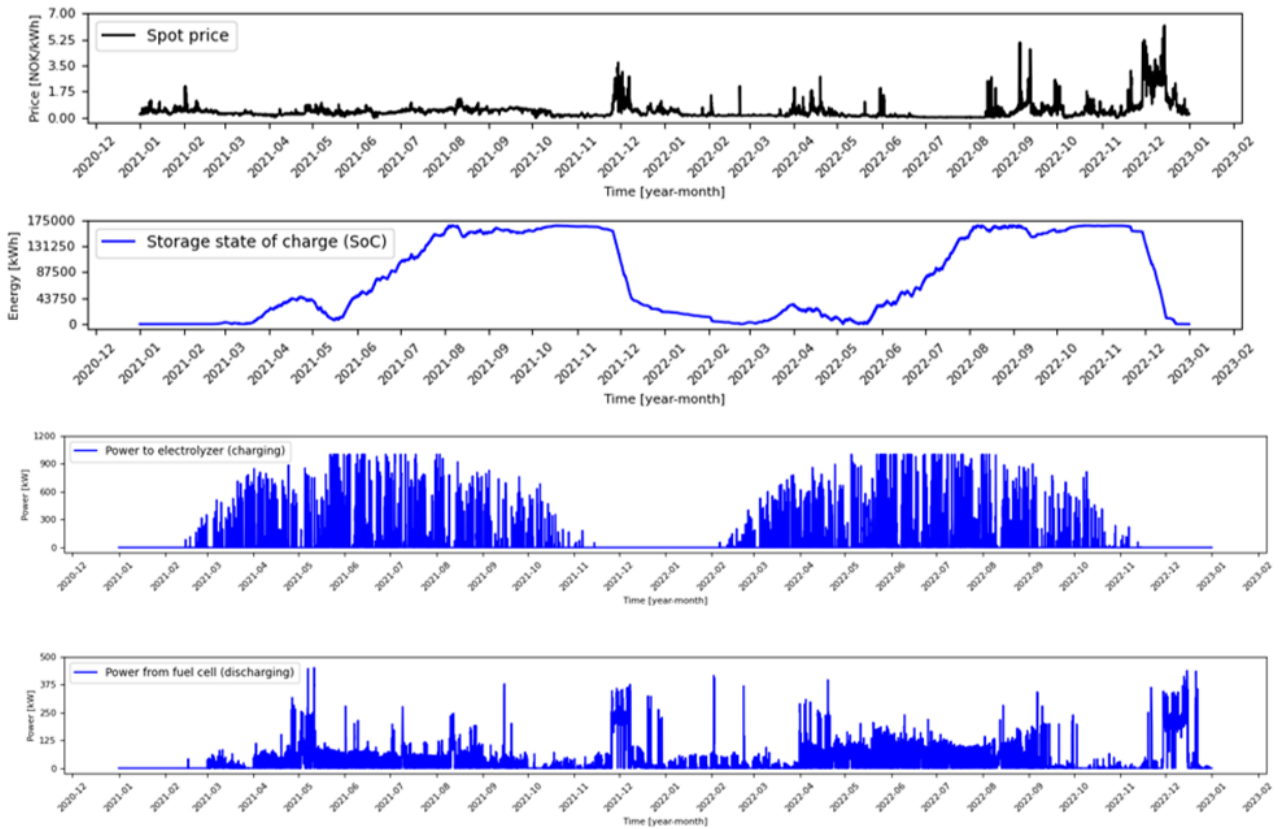


Figure 40: South E/W Scenario - control strategy 1 - plots 2/2.

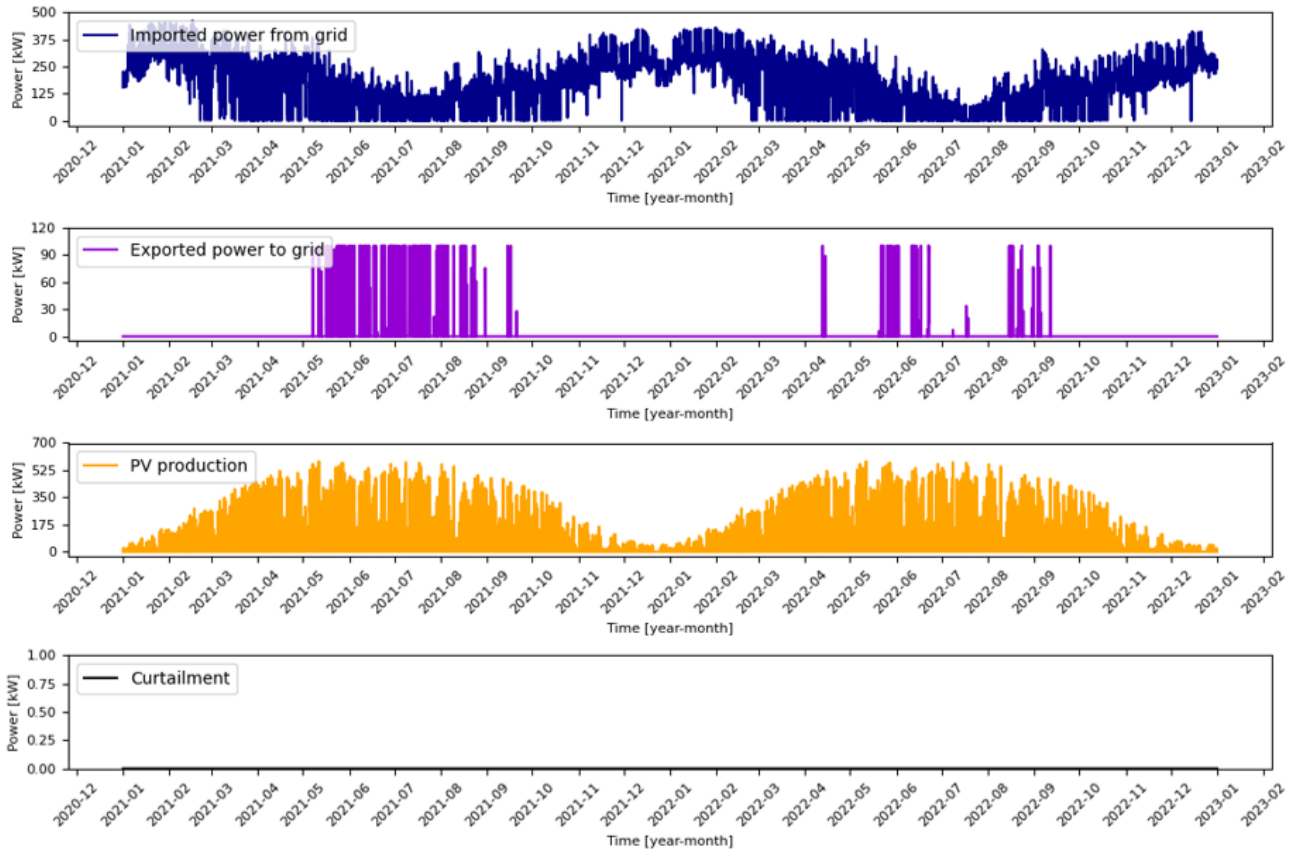


Figure 41: North E/W Scenario - control strategy 1 - plots 1/2.

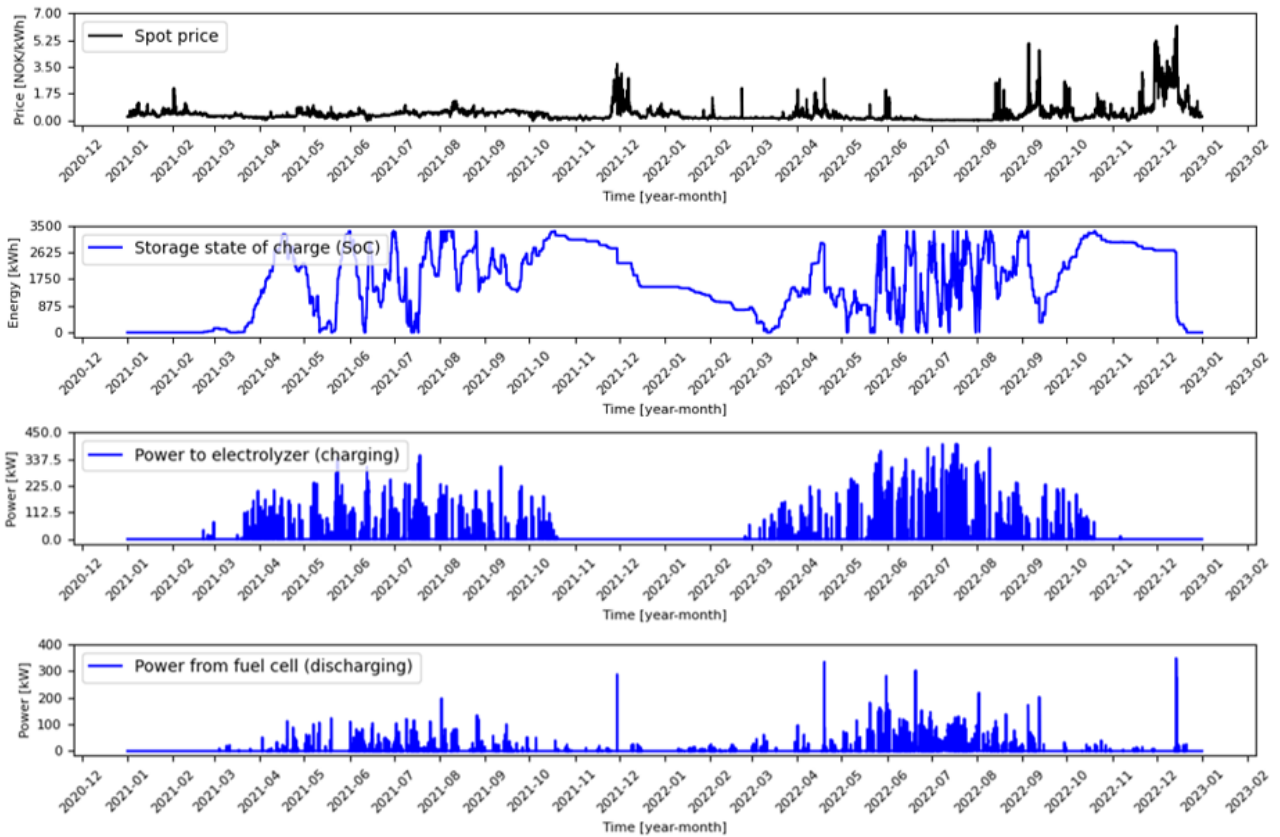


Figure 42: North E/W Scenario - control strategy 1 - plots 2/2.

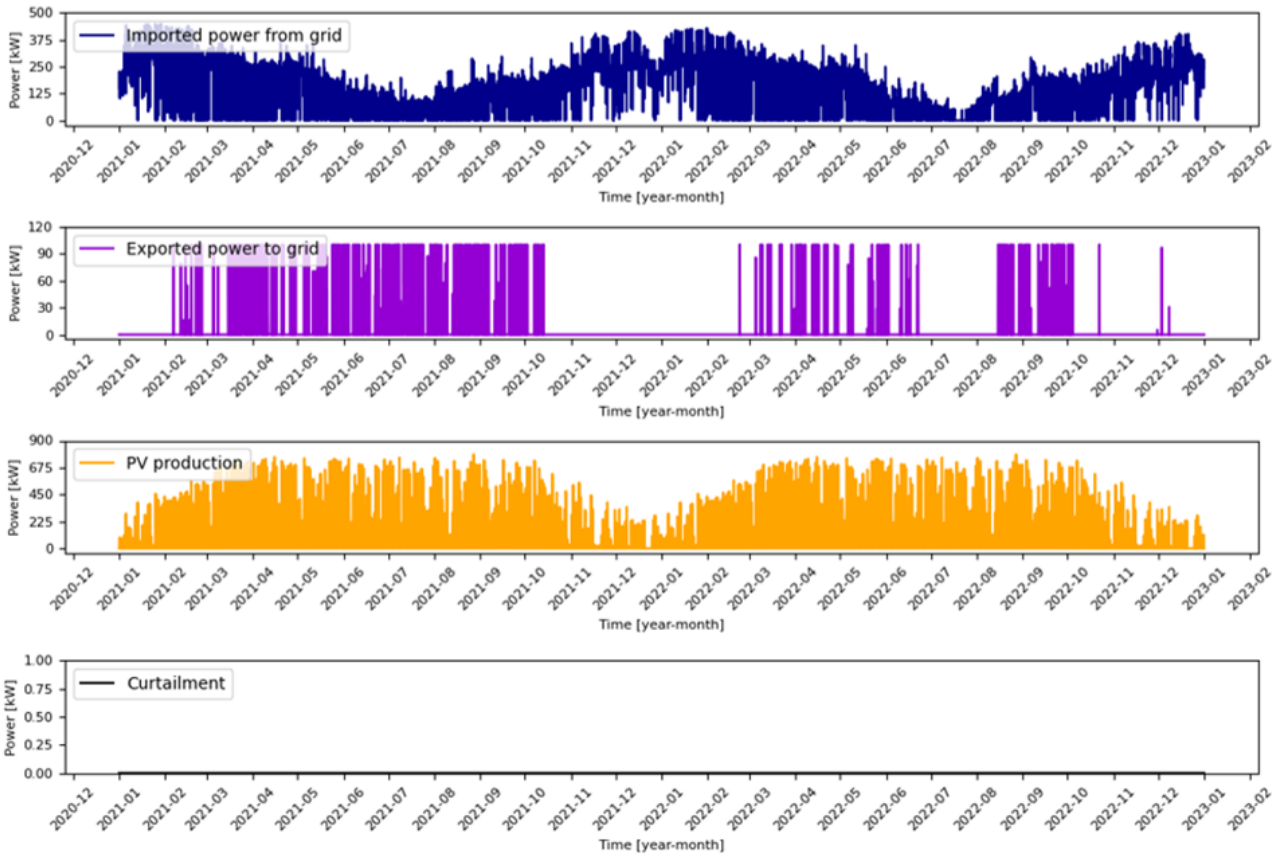


Figure 43: North S/N Scenario - control strategy 1 - plots 1/2.

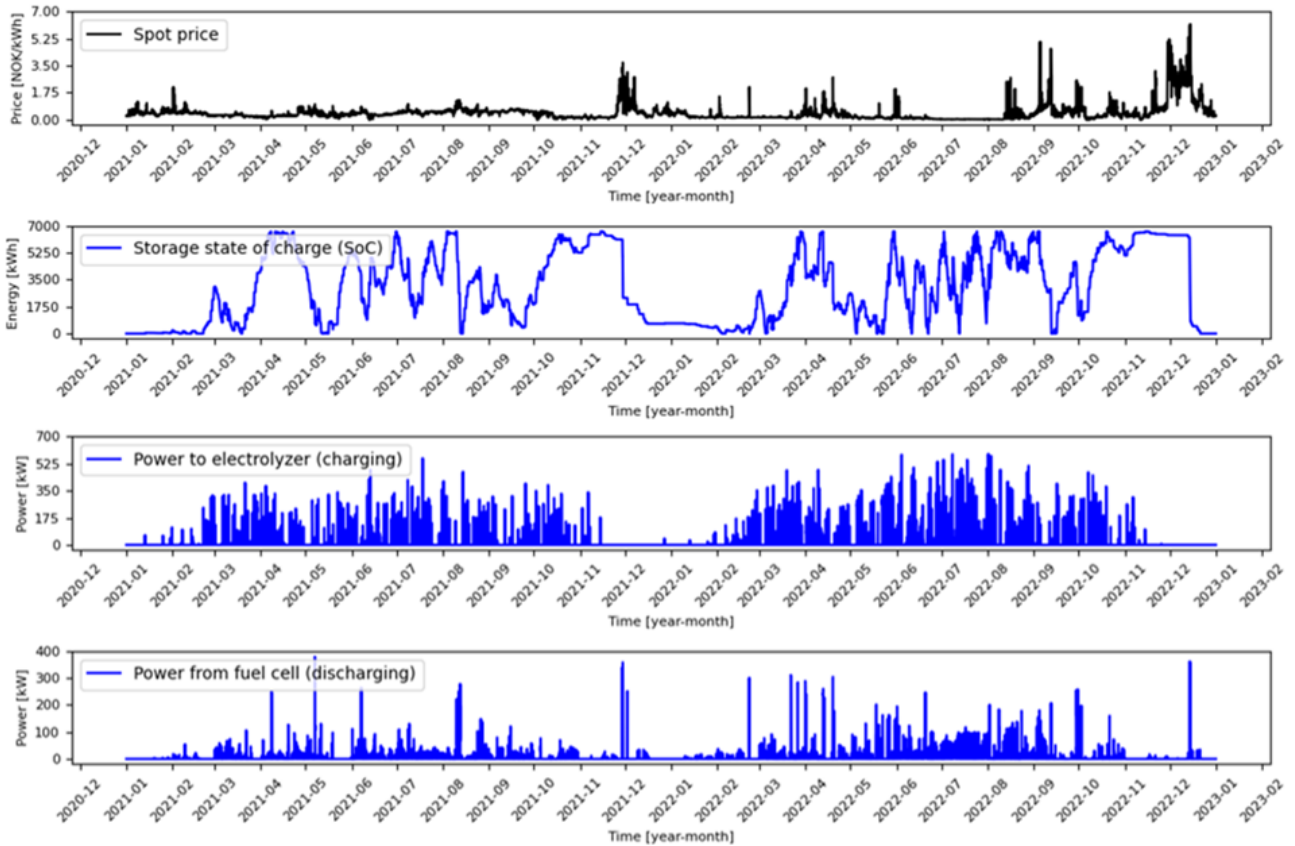


Figure 44: North S/N Scenario - control strategy 1 - plots 2/2.

5.3.2 Control Strategy 2 - Minimize Total Electricity Costs and Investment Costs

The results from implementing control strategy 2 for a hydrogen storage system are shown below in Table 5.3.2. The plots from the simulations are illustrated in Figure 45, 46, 47, 48, and 48. In this control strategy, the North E/W scenario causes the optimization model not to suggest any storage solution. Thus, the capacity and power rating are set to zero. This means that the optimization model does not find it profitable enough to invest in a hydrogen storage system when Skjetlein has the PV systems from scenario North E/W. Interestingly, the cost savings from the North E/W scenario are 24%, only 5.6% less than the North S/N cost savings for this control strategy. Furthermore, as these results differ quite a lot from the VRFB simulation, they will be compared and discussed in Section 6.1.4.

Table 5.3.2: APV Scenario results using control strategy 2.

	APV South E/W	APV North E/W	APV North S/N
E_{cap}	2.9 MWh	0 MWh	919 kWh
E_{rated_p}	20 kW	0 kW	8.328 kW
Curtailed solar PV ^a	37.46%	5%	12%
Electricity cost savings ^b	36.98%	24.10%	29.75%

^a % of total PV power production.

^b % of the total electricity costs without PV and storage.

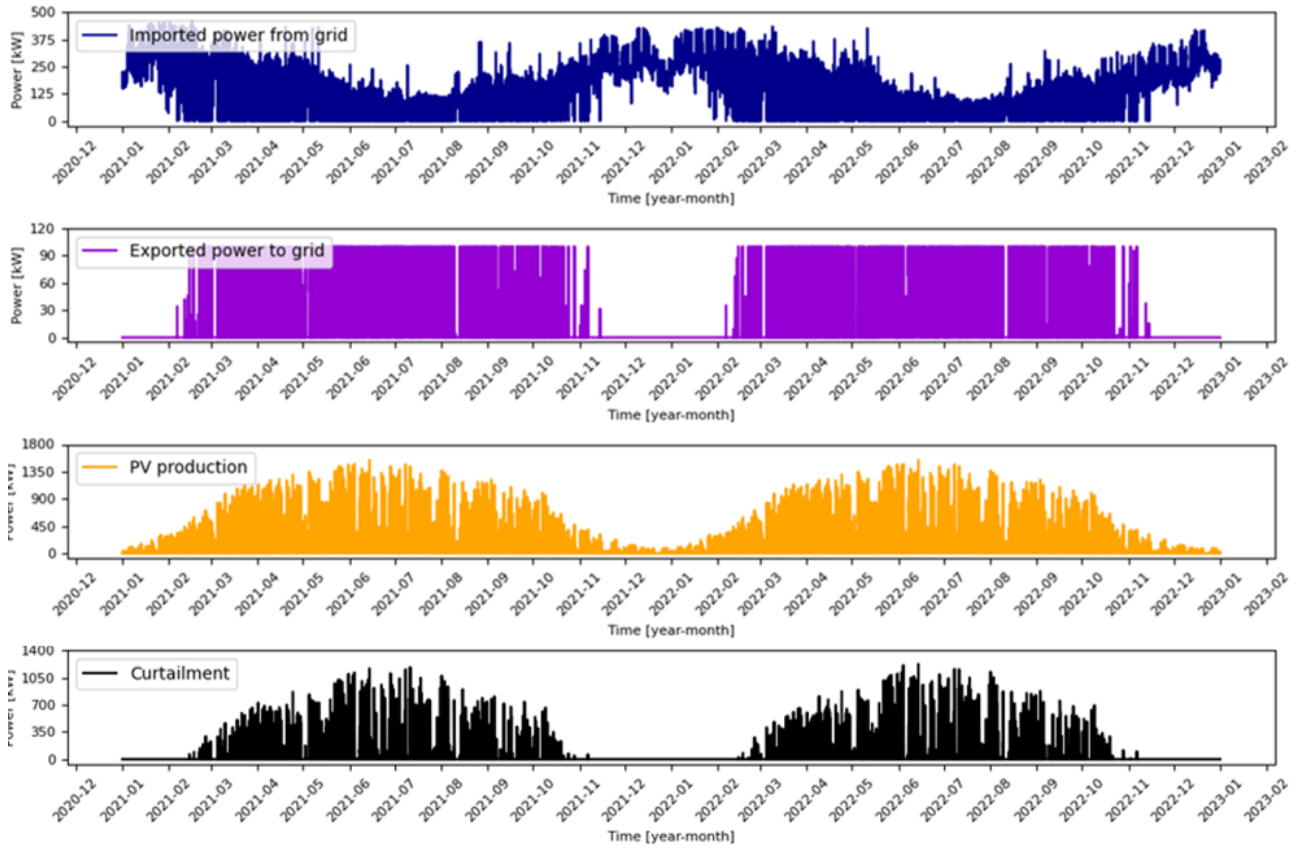


Figure 45: South E/W Scenario - control strategy 2 - plots 1/2.

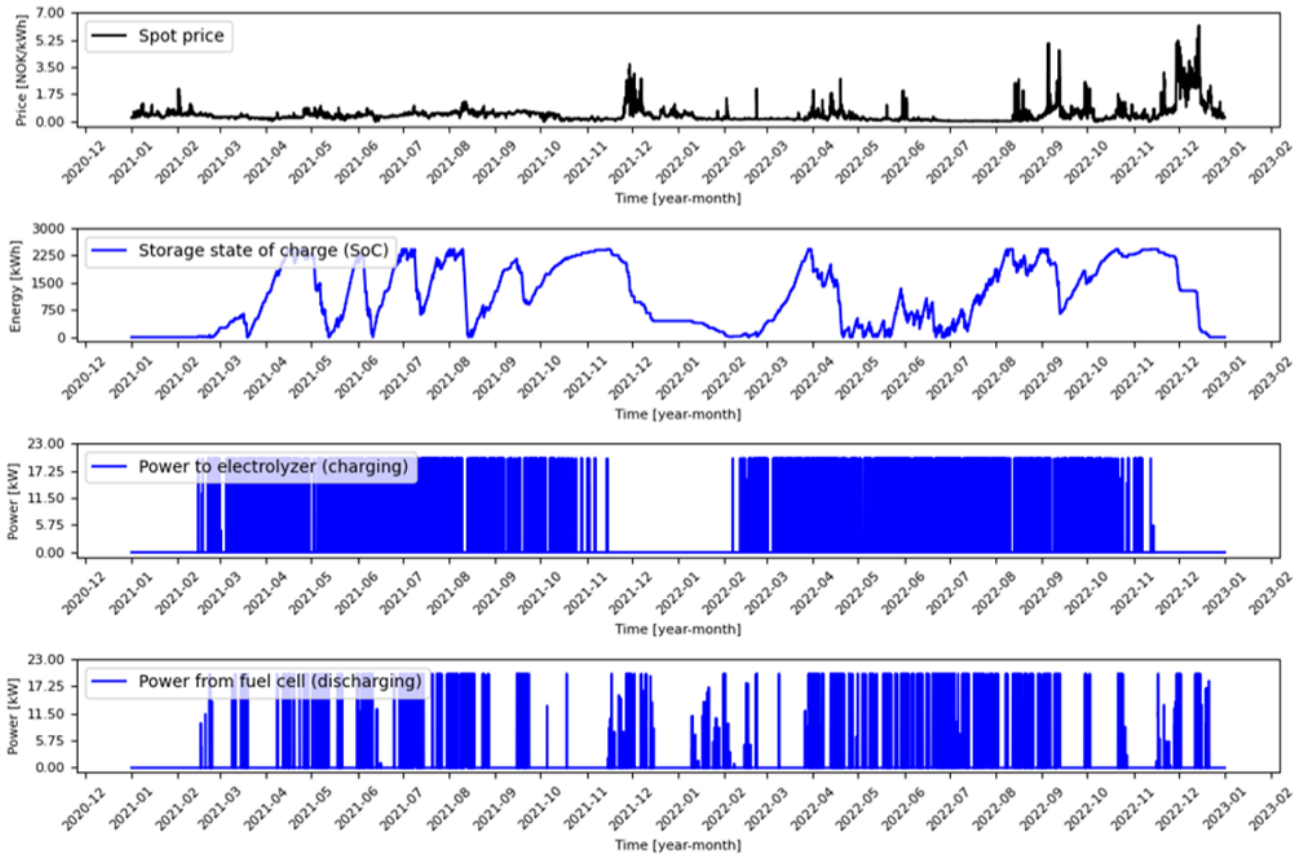


Figure 46: South E/W Scenario - control strategy 2 - plots 2/2.

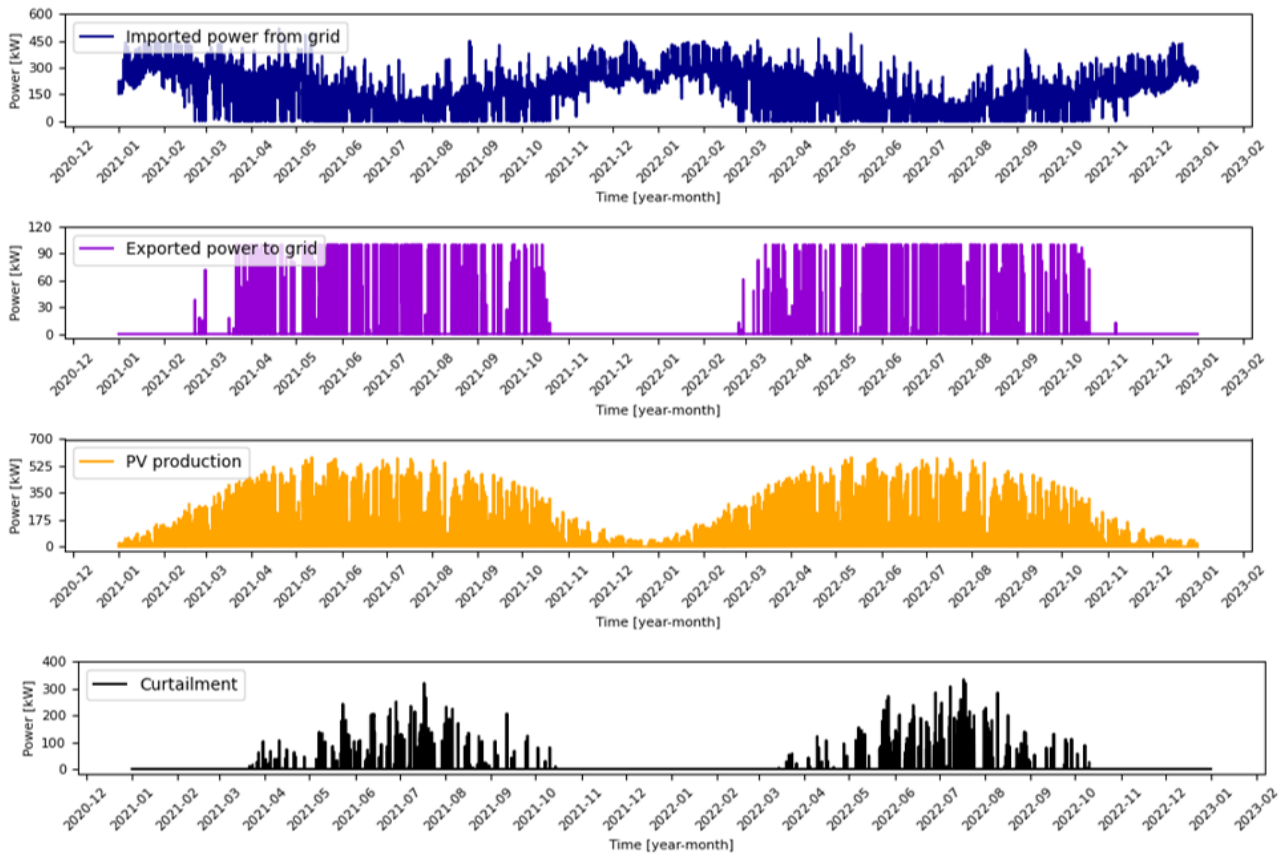


Figure 47: North E/W Scenario - control strategy 2 - plots 1/1.

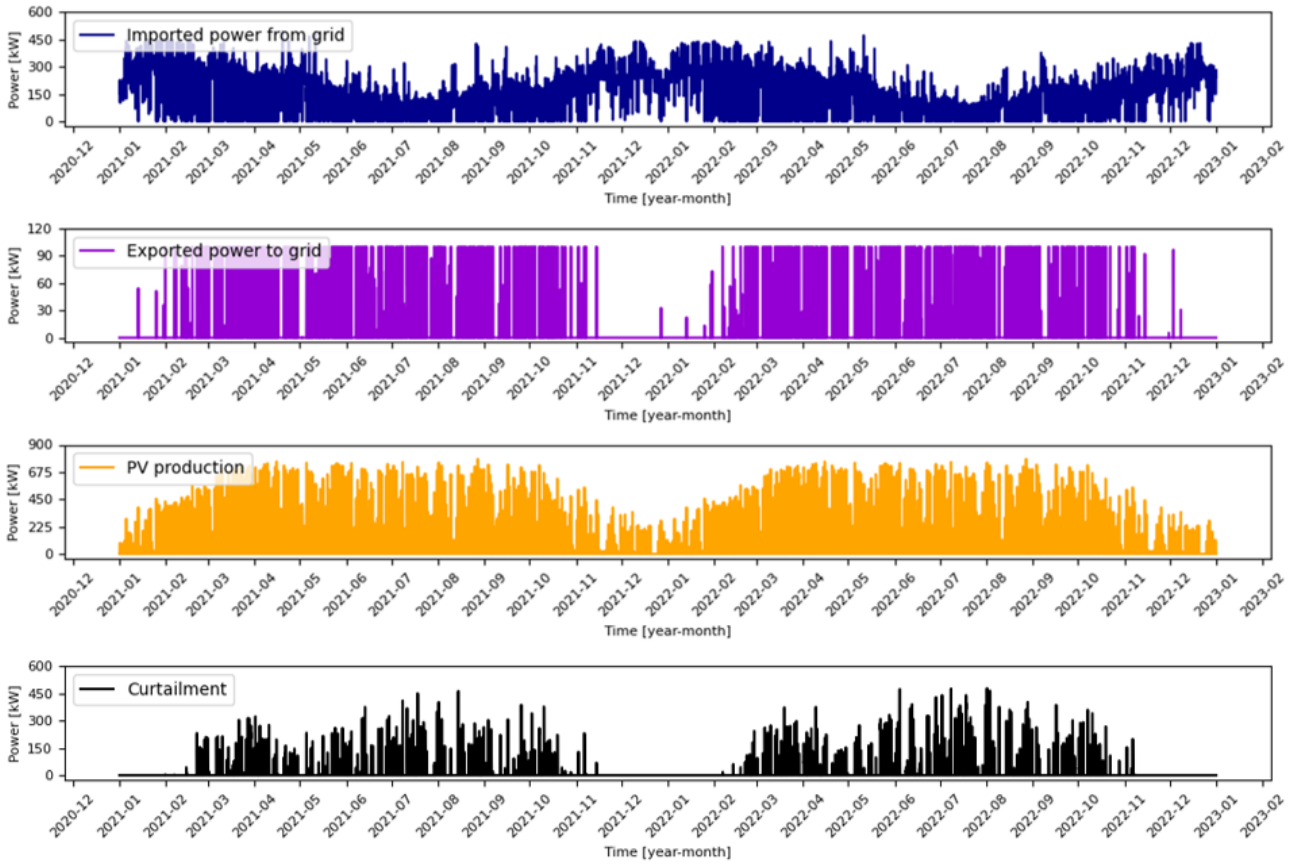


Figure 48: North S/N Scenario - control strategy 2 - plots 1/2.

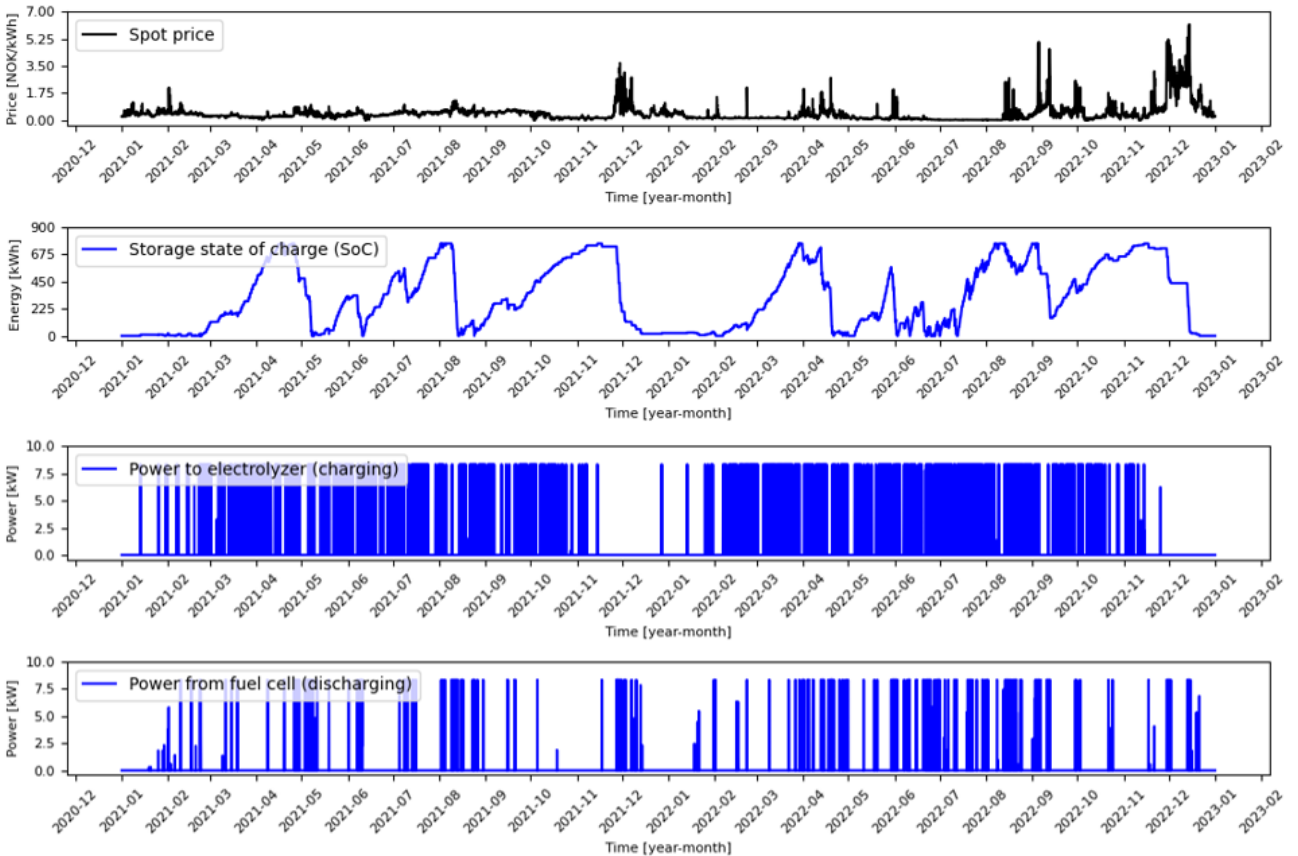


Figure 49: North S/N Scenario - control strategy 2 - plots 2/2.

6 | Discussion

This thesis aims to analyze the sizing and utilization of seasonal storage in combination with APV at Skjetlein High School. When analyzing the results, it is crucial to keep in mind the assumptions and simplifications made when creating the APV scenarios and the storage optimization model, as they may have significantly impacted the findings. In this chapter, the results will be discussed while considering the purpose of the thesis.

6.1 PV System Modelling

This section will discuss the results from simulating APV and existing rooftop PV systems at Skjetlein.

6.1.1 Rooftop PV

The simulated PV system at the STO building resulted in a generally higher power production than the actual measurements from 2021, 2022, and 2023. This is especially evident for January, February, and March. One explanation may be that the soiling factor (explained in Section 4.2.4) was set too low. Snow coverage on the panels may have been more frequent than what was accounted for in the inserted soiling loss factors for the installation. Another factor that might have influenced the results is the irradiation data from Meteonorm. As mentioned in Section 4.2.2, the largest uncertainty of Meteonorm is regarding its irradiance data. Thus, it might have happened that the irradiance from Meteonorm was too high in comparison with the real irradiance. Another source of uncertainty may also be the albedo factors.

For the PV system at the TIP building, the produced power aligned a lot more with the real data from Skjetlein. This suggests that the input parameters of this simulation are a better fit for this installation. Lastly, the PV system of the main building was investigated. Since there is a lack of historical data for this system, there is little basis for discussing possible causes of inaccuracies. However, the available historical data shows a clear discrepancy between the simulated PV production and the real production. Similarly to the STO building, the soiling values, albedo factors, and irradiance data may be sources of potential error.

6.1.2 Agrivoltaics

A weakness in designing the APV scenarios is the fact that the crops at the locations are not modelled. Since APV aims to reduce the negative effect on crops, it is essential to have them modelled to investigate the negative effects and to find the most suitable scenario for dual use. However, since this was not a part of the thesis scope, it was not carried out. Additionally, since the ground albedo plays an important role in the bifacial performance, measured values are preferred instead of estimated values.

6.1.3 Storage Control Strategy 1

The findings from control strategy 1 are summarized in Table 6.1.1. As mentioned in Section 4.3.9, this control strategy aims to minimize the total electricity costs while having storage size limits. An observable trend in Table 6.1.1 is that the capacities and rated power values are set to the upper limits in the model. Since the storage costs are not included in this control strategy, the model will make the storage sizing as big as possible to achieve the highest savings.

Table 6.1.1: Summary of results for control strategy 1.

	VRFB Case			H2 Case		
	South E/W	North E/W	North S/N	South E/W	North E/W	North S/N
Maximum capacity ($E_{\text{cap,max}}$) [MWh]	400	3	6	200	4	8
Maximum power rating ($P_{\text{rated,max}}$) [MW]	100	0.3	0.5	1	0.4	0.6
Capacity (E_{cap}) [MWh]	400	3	6	200	4	8
Rated power (P_{rated}) [MW]	100	0.3	0.5	1	0.4	0.6
Curtailed solar PV^a [%]	0.4	0.01	0.09	0.2	0	0
Electricity cost savings^b [%]	78	30	40	62	29	37

^a % of total PV power production.

^b % of the total electricity costs without PV and storage.

For both VRFB and hydrogen storage, the smallest storage sizes are in relation to the North E/W scenario. As mentioned in Section 4.2.5, this scenario has an East/West orientation and a power installation of 711 kWp. The power production profile of an East/West PV system is described in Section 4.2.2, along with an explanation of how such a profile may match Skjetleins' electricity consumption. The results from Table 6.1.1 suggest that larger storage is not necessary for the North E/W scenario, which may imply that the electricity consumption profile of Skjetlein aligns, to some extent, with the power production profile. Additionally, both the North E/W scenario and the North S/N scenario have the same installed power, but the curtailment percentage ended up being nine times higher for the North S/N scenario in the VRFB case. This indicates that the

electricity consumption profile of Skjetlein has some correlation with the power production profile of the North E/W scenario, which reduces curtailment and the need for storage.

According to Section 4.3.9, the storage size limits were set using an objective function that minimizes curtailment. For the scenario with the highest installed peak power, South E/W, the optimization model set maximum capacities of 400 and 200 MWh. As mentioned in Section 3.2, the world's largest VRFB has a capacity of 800 MWh [48], which is twice as big as one of the capacities proposed by the model. Hydrogen storage systems can also be of this size. However, the implementation of such large-scale systems may not be possible at Skjetlein due to various reasons such as available space and project budget. Other storage sizes proposed by the model (3-8 MWh) seem to be more feasible. This suggests that a 1600 kWp APV system may not be the optimal choice for Skjetlein if their aim is to utilize as much of the generated PV as possible.

6.1.4 Storage Control Strategy 2

The findings from control strategy 2 are summarized in Table 6.1.2.

Table 6.1.2: Summary of APV Scenario Results using Control Strategy 2.

	VRFB Case			H2 Case		
	South E/W	North E/W	North S/N	South E/W	North E/W	North S/N
Capacity (E_{cap}) [MWh]	0.3	0.07	0.2	2.9	0	0.9
Rated power (P_{rated}) [kW]	70	26	54	20	0	8.3
Curtailed solar PV^a [%]	36	5	9	37	5	12
Electricity cost savings^b [%]	38	24	31	37	24	30

^a % of total PV power production.

^b % of the total electricity costs without PV and storage.

The storage sizes are heavily reduced in comparison to control strategy 1. This suggests that storing excess PV over seasons may not be cost-effective for Skjetlein. It should be noted that the model does not consider that storage projects in agriculture can get funding from Innovation Norway and Enova. Therefore, it is not entirely impossible that seasonal storage at Skjetlein could be cost-effective if sufficient funding is given. Moreover, the costs regarding energy and power installations are subject to considerable variability, which contributes to the uncertainty of the results in control strategy 2.

6.2 Spot Prices

The results of the storage optimization model are highly dependent on the spot prices used. In this thesis, the spot prices for 2021 and 2022 were chosen due

to the fact that they align with the electricity demand collected from Skjetlein. However, as mentioned in Section 4.1.3, these prices have been record-high compared to historical prices. Therefore, they may not paint an accurate picture of the future prices.

6.3 General Reflections

The optimization model demonstrates the potential benefits of utilizing seasonal storage at Skjetlien High School. However, only the two largest storages from control strategy 1 obtained a clear seasonal storage charge/discharge pattern. This might imply that seasonal storage at Skjetlein requires high solar PV production (1600 kWp in this thesis). When incorporating the investment costs into the model, the storage sizes are reduced significantly, and none of the storage sizes shows a clear seasonal charge/discharge pattern. This may imply that the size needed for seasonal storage may not be cost-effective at Skjetlein High School.

It is important to note that directly relying on the model for storage sizing and/or charge/discharge characteristics is not advisable. This is primarily due to the unrealistic assumption that the Nord Pool spot prices and Skjetleins' electricity consumption for two years can be accurately predicted, which is highly unlikely.

A constant round-trip efficiency and a 100% inverter efficiency are appropriate for the optimization model's intended application. In reality, the round-trip efficiency will be influenced by a number of factors, such as ageing, temperature, SoC and charging rates. The model would become far more complicated if these effects were included, which would not be practical. However, the model would not become more advanced by including the inverter efficiency. Therefore, this may be conducted in future works. Furthermore, the storage lifespan is heavily dependent on the amount of charge-discharge cycles. Therefore, using a constant storage lifespan can be an overestimation of the actual storage life. Although the cycle life could have been incorporated, such integration would have drastically made the model more advanced.

6.4 Comment on Cost Calculation Error

A misunderstanding of the power charge was discovered late in the project period. Instead of being calculated as explained in Section 4.1.3, the power charge was assumed to be constant at the 100-400 NOK/kW/month level in the optimization model. So, if Skjetlein has a maximum power output of 390 kW during a month, this value was simply multiplied by either the winter or summer charge for the 100-400 NOK/kW/month level instead of being calculated as explained in Section 4.1.3. Implementing the power charge calculation shown in Section 4.1.3 would most likely lead to reductions in the grid import peaks for the graphs shown in and instead of reducing some of them to zero.

6.5 Suggestions for Future Work

Some potential improvements were found during the work on the optimization model and PVSyst simulations. The following points present some of the possibilities for further research:

- **Improving albedo accuracy:** Since the albedo value is one of the most critical parameters for bifacial PV power production, this value should be improved (ideally by using measured data) to increase the PVSyst simulation's accuracy.
- **Conduct crop modelling:** This should be carried out to find the most suitable scenario for PV production and crop production in the chosen scenario locations of this thesis.
- **Conduct a sensitivity analysis and case study:** A continuation of the work conducted in this thesis can be to conduct a sensitivity analysis of the spot price and grid tariff. Additionally, a case study of the spot prices involving the prices of other countries could have provided more insight.
- **Maximize the net present value:** Since only the storage investment costs are implemented in the model, it would have been interesting to investigate a net present value maximization model using costs of the entire project (APV and storage).
- **Implementing stochasticity and/or forecasting:** The model's input data is based on historical time series and is therefore known before the optimization. To make the model more realistic, the implementation of a forecasting technique and/or stochasticity should be considered.
- **Implement constraints related to the distribution grid:** The optimization model does not include bus voltage and line power flow operational limits. Such constraints can, for example, ensure that the voltage levels are maintained within permissible limits.
- **Implement correct calculation of power charge:** As mentioned in Section 6.4, the calculated power charge was not calculated correctly in this thesis. Therefore, further work should implement the correct calculation.

7 | Conclusions

This thesis has investigated the implementation of seasonal storage in combination with APV at Skjetlein High School. The study has evaluated two storage technologies, VRFB and hydrogen storage. Each storage technology has been evaluated in combination with three possible APV scenarios.

The overall results showed that the integration of long-term storage could increase electricity cost savings from 24-78%. The storage capacities and power ratings ranged from 0-400 MWh and 0-100 MW, respectively. The biggest storage systems (capacity of 200 and 400 MWh) obtained a clear seasonal storage pattern, storing excess electricity from the summer and discharging it in the winter. However, such systems are excessively large and might not be possible to install at Skjetlein due to available space and project budget. The smallest storage systems (73 - 365 kWh) were obtained from the VRFB, resulting in daily storage except during the winter when the battery holds onto the storage capacity for the highest Nord Pool spot prices. The smallest hydrogen storage systems achieved a capacity ranging from (0 - 300 kWh). These storage systems store energy from weeks to months, which is a clear difference from the smallest VRFBs. Some of the weaknesses of the optimization model include the exclusion of OM costs, the efficiency of the inverter and an error in the calculation of the power charge. This can be included in future analysis.

According to this thesis, seasonal storage in combination with APV at Skjetlein is not a possible solution due to their needed size. Additionally, the model suggests that such large storage systems are not cost-effective. However, long-term storage over several weeks or a few months (capacity of 3-8 MWh) can be cost-effective if sufficient funding is given, but it is dependent on the Nord Pool spot prices.

Bibliography

- [1] *Håndbok til energidebatten*. [Online]. Available: <https://klimastiftelsen.no/publikasjoner/handbok-til-energidebatten/> (visited on 16/03/2023).
- [2] P. B. Ulvin, *Vil 33-doble solkraft i Norge på syv år: – Realistisk*, Section: annet, Feb. 2023. [Online]. Available: https://www.nrk.no/klima/vil-33-doble-solkraft-i-norge-pa-syv-ar_-_-realistisk-1.16279839 (visited on 18/03/2023).
- [3] Oda Andrea Hjelme, Bjørn Thorud, Torje Evensen and et al., “Norsk solkraft 2022 – innenlands og eksport”, Market report, Aug. 2022. [Online]. Available: <https://www.solenergiklyngen.no/wp-content/uploads/2022/08/220815-markedsrapport-solenergiklyngen-final-.pdf>.
- [4] Beatriz Santos, *Norway to nearly triple annual PV additions in 2022, says research firm*, en-US, Nov. 2022. [Online]. Available: <https://www.pv-magazine.com/2022/11/28/norway-to-nearly-triple-annual-pv-additions-in-2022-says-research-firm/> (visited on 17/06/2023).
- [5] O. Pfeiffer, C. Marks, J. Hanneforth, E.-M. Grommes and U. Blieske, “Validation of a Bifacial Simulation Software against measured Energy yield from a utility-scale vertical fixed-tilt Agrophotovoltaic Plant”, Sep. 2022.
- [6] Gaute Stokkan, *Agrivoltaics*. [Online]. Available: <https://www.sintef.no/ekspertise/sintef-industri/agrivoltaics/> (visited on 24/03/2023).
- [7] F. Berglund, “Optimal Operation of Battery Storage for Peak Shaving Applications - A Norwegian Case Study for a Medium-Scale Swimming Facility”, M.S. thesis, NTNU, 2018. [Online]. Available: <https://ntnuopen.ntnu.no/ntnu-xmlui/handle/11250/2566723>.
- [8] S. Schindele, M. Trommsdorff, A. Schlaak *et al.*, “Implementation of agrophotovoltaics: Techno-economic analysis of the price-performance ratio and its policy implications”, en, *Applied Energy*, vol. 265, p. 114 737, May 2020, ISSN: 0306-2619. DOI: 10 . 1016 / j . apenergy . 2020 . 114737. [Online]. Available: <https://www.sciencedirect.com/science/article/pii/S030626192030249X> (visited on 29/05/2023).
- [9] J. F. Weaver, *Half of US electricity CO2-free in May?*, Jun. 2021. [Online]. Available: <https://commercialsolarguy.com/half-of-us-electricity-co2-free-in-may/> (visited on 19/06/2023).
- [10] SolarPower Europe, “Agri-PV: How solar enables the energy transition in rural areas”, Tech. Rep., Sep. 2020.
- [11] Miguel Herrero, *Agrisolar: Win-wins for farmers and photovoltaics*.

- [12] M. Trommsdorff, *Performance Indices for Parallel Agriculture and PV*, Oct. 2020. [Online]. Available: https://iea-pvps.org/wp-content/uploads/2020/09/07_M.-Trommsdorff_A-PV_T13-Workshop.pdf.
- [13] P. E. Campana, B. Stridh, S. Amaducci and M. Colauzzi, “Optimisation of vertically mounted agrivoltaic systems”, *Journal of Cleaner Production*, vol. 325, p. 129 091, Nov. 2021, ISSN: 0959-6526. DOI: 10.1016/j.jclepro.2021.129091. [Online]. Available: <https://www.sciencedirect.com/science/article/pii/S0959652621032807> (visited on 24/02/2023).
- [14] Ravi Kumar, Ronald Reagon, “Modelling and Analysis of vertical bifacial agrivoltaic test system at Skjetlein high school, Norway”, Accepted: 2022-07-29T17:19:31Z, M.S. thesis, NTNU, 2022. [Online]. Available: <https://ntnuopen.ntnu.no/ntnu-xmlui/handle/11250/3009234> (visited on 11/04/2023).
- [15] Joshua S. Stein, Sandia National Laboratories, USA, Christian Reise, Fraunhofer ISE, Freiburg, Germany, Johanna Bonilla Castro, TÜV Rheinland, Cologne, Germany *et al.*, “Bifacial Photovoltaic Modules and Systems”, Tech. Rep. Report IEA-PVPS T13-14:2021, Apr. 2021. [Online]. Available: <https://iea-pvps.org/key-topics/bifacial-photovoltaic-modules-and-systems/> (visited on 03/06/2023).
- [16] EMILIANO BELLINI, *Optimal topology for agrivoltaics based on bifacial PV modules*, en-US, Jan. 2022. [Online]. Available: <https://www.pv-magazine.com/2022/01/21/optimal-topology-for-agrivoltaics-based-on-bifacial-pv-modules/> (visited on 03/06/2023).
- [17] S. Guo, T. M. Walsh and M. Peters, “Vertically mounted bifacial photovoltaic modules: A global analysis”, en, *Energy*, vol. 61, pp. 447–454, Nov. 2013, ISSN: 0360-5442. DOI: 10.1016/j.energy.2013.08.040. [Online]. Available: <https://www.sciencedirect.com/science/article/pii/S0360544213007275> (visited on 03/06/2023).
- [18] Tommy Engvik, *Energy yield from vertically mounted bifacial solar panels*, Jul. 2022. [Online]. Available: <https://overeasy.no/2022/07/22/energy-yield-from-vertically-mounted-bifacial-solar-panels/> (visited on 11/04/2023).
- [19] Emiliano Bellini, *High-latitude tests show vertical rooftop PV yields 30% more energy*, en-US, Apr. 2023. [Online]. Available: <https://www.pv-magazine-india.com/2023/04/03/high-latitude-tests-show-vertical-rooftop-pv-yields-30-more-energy/> (visited on 03/06/2023).
- [20] J. Mamen, *Köppens klimaklassifikasjon*, Jan. 2023. [Online]. Available: https://snl.no/K%C3%B6ppens_klimaklassifikasjon.
- [21] V. Omubo-Pepple, C. Israel-Cookey and G. Alaminiookuma, “Effects of Temperature, Solar Flux and Relative Humidity on the Efficient Conversion of Solar Energy to Electricity”, *European Journal of Scientific Research*, pp. 173–180, Oct. 2009.
- [22] M. Hefte, “Energy system planning of Zero Emission Neighborhood in Bodø combined with hydrogen ferries”, Accepted: 2021-09-15T17:19:12Z, M.S. thesis, NTNU, 2021. [Online]. Available: <https://ntnuopen.ntnu.no/ntnu-xmlui/handle/11250/2778279> (visited on 04/06/2023).

- [23] M. Manni, M. C. Failla, A. Nocente, G. Lobaccaro and B. P. Jelle, “The influence of icephobic nanomaterial coatings on solar cell panels at high latitudes”, *Solar Energy*, pp. 76–87, Dec. 2022. DOI: 10.1016/j.solener.2022.11.005. [Online]. Available: <https://www.sciencedirect.com/science/article/pii/S0038092X22008076> (visited on 30/05/2023).
- [24] R. Garner, *Solar Irradiance*, Text, Apr. 2015. [Online]. Available: http://www.nasa.gov/mission_pages/sdo/science/solar-irradiance.html.
- [25] A. E. O. Kheddioui and M. F. Smiej, “Estimation of the global horizontal solar irradiation GHI for the Moroccan national territory from meteorological satellite images of the Second Generation Meteosat series MSG”, *European Journal of Molecular & Clinical Medicine*, pp. 2814–2826, Jun. 2021. [Online]. Available: https://ejmcm.com/article_11528.html (visited on 30/05/2023).
- [26] Ingrid Brøndbo, “Analysis of the potential from agrophotovoltaics and hydrogen production/use - A study on seasonal energy storage at Norwegian farms”, NTNU, Trondheim, Norway, Tech. Rep.
- [27] International Finance Corporation, “Utility-Scale Solar Photovoltaic Power Plants”, Jun. 2015, Publisher: Washington, DC. [Online]. Available: <http://hdl.handle.net/10986/22797> (visited on 08/06/2023).
- [28] Multiconsult, “Kostnadsstudie, Solkraft i Norge 2013”, Tech. Rep., 2013.
- [29] *Standard Test Conditions - HOMER Energy*. [Online]. Available: https://www.homerenergy.com/products/pro/docs/3.11/standard_test_conditions.html (visited on 29/05/2023).
- [30] PVSyst, *Project design > Results > Performance Ratio PR*. [Online]. Available: https://www.pvsyst.com/help/performance_ratio.htm (visited on 14/06/2023).
- [31] *NEK EN IEC 61724-1:2021*, Aug. 2021. [Online]. Available: <https://handle.standard.no/no/Nettbutikk/produktkatalogen/Produktpresentasjon/?ProductID=1376143> (visited on 04/06/2023).
- [32] H. N. Riise, M. Øgaard, J. Zhu *et al.*, “Performance analysis of a BAPV bifacial system in Norway”, in *2021 IEEE 48th Photovoltaic Specialists Conference (PVSC)*, ISSN: 0160-8371, Jun. 2021, pp. 1304–1308. DOI: 10.1109/PVSC43889.2021.9518963.
- [33] J. Stein, C. Reise, J. Castro *et al.*, “Bifacial Photovoltaic Modules and Systems: Experience and Results from International Research and Pilot Applications”, Tech. Rep., Apr. 2021. DOI: 10.2172/1779379. [Online]. Available: <https://www.osti.gov/servlets/purl/1779379/> (visited on 05/06/2023).
- [34] J. Ying, Z. Li, L. Yang, Y. Jiang, Y. Luo and X. Gao, “The characteristics and parameterizations of the surface albedo of a utility-scale photovoltaic plant in the Gobi Desert”, *Theoretical and Applied Climatology*, Feb. 2023. DOI: 10.1007/s00704-022-04337-5. [Online]. Available: <https://doi.org/10.1007/s00704-022-04337-5> (visited on 29/05/2023).
- [35] G. M. Masters, *Renewable and Efficient Electric Power Systems*, en. John Wiley & Sons Inc, 2013.
- [36] *Module Structure | PVEducation*. [Online]. Available: <https://www.pveducation.org/pvcdrom/modules-and-arrays/module-structure> (visited on 29/05/2023).
-

- [37] K. Ramalingam and C. Indulkar, “Chapter 3 - Solar Energy and Photovoltaic Technology”, in *Distributed Generation Systems*, Jan. 2017. [Online]. Available: <https://www.sciencedirect.com/science/article/pii/B9780128042083000030> (visited on 29/05/2023).
- [38] M. M. Rahman, A. O. Oni, E. Gemechu and A. Kumar, “Assessment of energy storage technologies: A review”, *Energy Conversion and Management*, Nov. 2020. DOI: 10.1016/j.enconman.2020.113295. [Online]. Available: <https://www.sciencedirect.com/science/article/pii/S0196890420308347> (visited on 01/03/2023).
- [39] N. Gupta, N. Kaur, S. K. Jain and K. Singh Joshal, “Chapter 3 - Smart grid power system”, en, in *Advances in Smart Grid Power System*, A. Tomar and R. Kandari, Eds., Academic Press, Jan. 2021, pp. 47–71, ISBN: 978-0-12-824337-4. DOI: 10.1016/B978-0-12-824337-4.00003-5. [Online]. Available: <https://www.sciencedirect.com/science/article/pii/B9780128243374000035> (visited on 16/05/2023).
- [40] A. Chauhan and R. P. Saini, “A review on Integrated Renewable Energy System based power generation for stand-alone applications: Configurations, storage options, sizing methodologies and control”, en, *Renewable and Sustainable Energy Reviews*, vol. 38, pp. 99–120, Oct. 2014, ISSN: 1364-0321. DOI: 10.1016/j.rser.2014.05.079. [Online]. Available: <https://www.sciencedirect.com/science/article/pii/S1364032114004043> (visited on 28/02/2023).
- [41] Frida Berglund, James Lam and Kjersti Aarrestad, “DNV GL - Lagringsteknologier for fleksibilitet i energisystemet”, Høvik, Studie og kunnskapsgrunnlag 2020-0919, Nov. 2020.
- [42] *Megapack*. [Online]. Available: <https://www.tesla.com/megapack> (visited on 05/06/2023).
- [43] IRENA, “Battery Storage for Renewables: Market Status and Technology Outlook”, en, Tech. Rep., Jan. 2015. [Online]. Available: <https://www.irena.org/publications/2015/Jan/Battery-Storage-for-Renewables-Market-Status-and-Technology-Outlook> (visited on 05/06/2023).
- [44] A. A. Kebede, T. Kalogiannis, J. Van Mierlo and M. Berecibar, “A comprehensive review of stationary energy storage devices for large scale renewable energy sources grid integration”, *Renewable and Sustainable Energy Reviews*, vol. 159, May 2022, ISSN: 1364-0321. DOI: 10.1016/j.rser.2022.112213. [Online]. Available: <https://www.sciencedirect.com/science/article/pii/S1364032122001368> (visited on 05/06/2023).
- [45] H. R. Jiang, W. Shyy, Y. X. Ren, R. H. Zhang and T. S. Zhao, “A room-temperature activated graphite felt as the cost-effective, highly active and stable electrode for vanadium redox flow batteries”, *Applied Energy*, vol. 233-234, pp. 544–553, Jan. 2019, ISSN: 0306-2619. DOI: 10.1016/j.apenergy.2018.10.059. [Online]. Available: <https://www.sciencedirect.com/science/article/pii/S0306261918316192> (visited on 28/02/2023).
- [46] Eduardo Sanchez-Diez, Edgar Ventosa, Massimo Guarnieri *et al.*, “Redox flow batteries: Status and perspective towards sustainable stationary energy storage | Elsevier Enhanced Reader”, en, Aug. 2020. DOI: 10.1016/j.jpowsour.2020.228804. [Online]. Available: <https://www.sciencedirect.com/science/article/pii/S0378775320311083> (visited on 08/12/2022).

- [47] Natalie Filatoff, *Large-scale vanadium redox flow battery takes shape in Australia*, en-US, May 2021. [Online]. Available: <https://www.pv-magazine.com/2021/05/10/large-scale-vanadium-redox-flow-battery-takes-shape-in-australia/> (visited on 08/12/2022).
- [48] Beatriz Santos, *China connects world's largest redox flow battery system to grid*, en-US, Sep. 2022. [Online]. Available: <https://www.pv-magazine.com/2022/09/29/china-connects-worlds-largest-redox-flow-battery-system-to-grid/> (visited on 14/06/2023).
- [49] *Hydrogen – Analysis*. [Online]. Available: <https://www.iea.org/reports/hydrogen> (visited on 04/06/2023).
- [50] C. J. Greiner, “Sizing and Operation of Wind-Hydrogen Energy Systems”, Accepted: 2014-12-19T13:52:28Z ISBN: 9788247120194, Doctoral thesis, Norges teknisk-naturvitenskapelige universitet, Fakultet for informasjonsteknologi, matematikk og elektroteknikk, Institutt for elkraftteknikk, 2010. [Online]. Available: <https://ntnuopen.ntnu.no/ntnu-xmlui/handle/11250/256981> (visited on 04/06/2023).
- [51] *Fuel Cells*. [Online]. Available: <https://www.energy.gov/eere/fuelcells/fuel-cells> (visited on 04/06/2023).
- [52] T. Heimvik, I. G. Folkestad and J. W. Ingebretsen, “A Feasibility Study of Hydrogen Production at Hitra”, Accepted: 2020-07-07T16:04:38Z, Bachelor thesis, NTNU, 2020. [Online]. Available: <https://ntnuopen.ntnu.no/ntnu-xmlui/handle/11250/2661143> (visited on 19/06/2023).
- [53] *Ørn Optima - Innlogging*. [Online]. Available: <https://login.entro.no/> (visited on 17/06/2023).
- [54] *The power market*. [Online]. Available: <https://energifaktanorge.no/en/norsk-energiforsyning/kraftmarkedet/> (visited on 07/06/2023).
- [55] *Bind strømprisen med Lyse Fastpris | Lyse*. [Online]. Available: <https://www.lyse.no/strom/fastpris> (visited on 07/06/2023).
- [56] Statnett, “Langsiktig markedsanalyse - Norge, Norden og Europa 2022-2050”, Market report, Mar. 2023.
- [57] Trym Kristian Økland, *Strømprisene preget KPI i 2021*, nb, Jan. 2022. [Online]. Available: <https://www.ssb.no/priser-og-prisindekser/konsumpriser/statistikk/konsumprisindeksen/artikler/stromprisene-preget-kpi-i-2021> (visited on 15/06/2023).
- [58] Silje Skjolden Thorsnes and Trym Kristian Økland, *Ekstraordinært år for prisveksten i 2022*. [Online]. Available: <https://www.ssb.no/priser-og-prisindekser/konsumpriser/statistikk/konsumprisindeksen/artikler/ekstraordinaert-ar-for-prisveksten-i-2022> (visited on 15/06/2023).
- [59] Henriette Birkelund, Fredrik Arnesen, Jarand Hole *et al.*, “Langsiktig kraftmarkedsanalyse 2021-2040”, Norges vassdrags- og energidirektorat, Oslo, Tech. Rep., 2019. [Online]. Available: https://publikasjoner.nve.no/rapport/2021/rapport2021_29.pdf.
- [60] Nord Pool, *See market data for all areas*. [Online]. Available: <https://www.nordpoolgroup.com/en/Market-data1/> (visited on 10/06/2023).
- [61] *Regulation of grid operations*. [Online]. Available: <https://energifaktanorge.no/en/regulation-of-the-energy-sector/regulering-av-nettvirksomhet/> (visited on 07/06/2023).

- [62] Tensio AS, *Nettleie, priser og avtaler*, no. [Online]. Available: <https://ts.tensio.no/kunde/nettleie-priser-og-avtaler> (visited on 07/06/2023).
- [63] *2021 nettleie bedrift*. [Online]. Available: <https://ts.tensio.no/kunde/nettleie-priser-og-avtaler/2021-nettleie-bedrift> (visited on 16/06/2023).
- [64] *2022 nettleie Bedrift*. [Online]. Available: <https://ts.tensio.no/kunde/nettleie-priser-og-avtaler/2022-nettleie-bedrift> (visited on 16/06/2023).
- [65] *Electricity certificates - Skagerak Kraft*, en, Nov. 2017. [Online]. Available: https://www.skagerakkraft.no/krafthandel_2/electricity-certificates/ (visited on 18/06/2023).
- [66] *Plusskunder - NVE*, Jan. 2023. [Online]. Available: <https://www.nve.no/reguleringsmyndigheten/regulering/nettvirksomhet/nettleie/tariffer-for-produksjon/plusskunder/> (visited on 23/03/2023).
- [67] Erlend Hustad Honningdalsnes, “Autonomous Optimization of Agrivoltaic Systems in Norway”, Accepted: 2022-07-29T17:19:31Z, M.S. thesis, NTNU, 2022. (visited on 11/04/2023).
- [68] NIBIO, *LMT Skjetlein*. [Online]. Available: <https://lmt.nibio.no/station/43/> (visited on 07/06/2023).
- [69] *Invalid Meto file: The clearness index is to high*, Aug. 2016. [Online]. Available: <https://forum.pvsyst.com/topic/1058-invalid-meto-file-the-clearness-index-is-to-high/>.
- [70] H. Andersen, P. Ravibalan, S. Myklebost and H. Ø. Røisgård, “Analyse av reell solenergiproduksjon og simuleringer i PVsyst”, nob, Accepted: 2021-09-15T17:23:39Z, Bachelor thesis, NTNU, 2021. [Online]. Available: <https://ntnuopen.ntnu.no/ntnu-xmlui/handle/11250/2778303> (visited on 11/06/2023).
- [71] I. Frimannslund, T. Thiis, L. V. Skjøndal and T. Marke, “Energy demand and yield enhancement for roof mounted photovoltaic snow mitigation systems”, en, *Energy and Buildings*, vol. 278, p. 112602, Jan. 2023, ISSN: 0378-7788. DOI: 10.1016/j.enbuild.2022.112602. [Online]. Available: <https://www.sciencedirect.com/science/article/pii/S0378778822007733> (visited on 16/06/2023).
- [72] S. Jouttijärvi, G. Lobaccaro, A. Kamppinen and K. Miettunen, “Benefits of bifacial solar cells combined with low voltage power grids at high latitudes”, en, *Renewable and Sustainable Energy Reviews*, vol. 161, p. 112354, Jun. 2022, ISSN: 1364-0321. DOI: 10.1016/j.rser.2022.112354. [Online]. Available: <https://www.sciencedirect.com/science/article/pii/S1364032122002659> (visited on 14/06/2023).
- [73] Sunstream Energy, *Cleaner, Greener, Better Energy Solutions*. [Online]. Available: <https://sunstreamenergy.ie/> (visited on 14/06/2023).
- [74] Chris Deline, Silvana Ayala Peláez, Bill Marion, Bill Sekulic, Michael Woodhouse and Josh Stein, *Bifacial PV System Performance: Separating Fact from Fiction*, 2019.
- [75] Standard Norge, *Energy performance of buildings — Calculation of energy needs and energy supply (SN-NSPEK 3031:2021)*. [Online]. Available: <https://handle.standard.no/no/Nettbutikk/produktkatalogen/Produktpresentasjon/?ProductID=1393607> (visited on 07/06/2023).
-

- [76] Martin Brunstad Høydal, *Albedo og soiling spørsmål*, Apr. 2023.
- [77] Christine Forsetlund Solbakken, *Spør en forsker: Hvorfor er det mer støv i lufta om våren?*, no, Section: miljø, Mar. 2015. [Online]. Available: <https://forskning.no/spor-en-forsker-bil-og-trafikk-forurensning/spor-en-forsker-hvorfor-er-det-mer-stov-i-lufta-om-varen/506014> (visited on 07/06/2023).
- [78] Next2Sun, *References Agri-Photovoltaic Projects | Next2Sun Agri-PV Concept*. [Online]. Available: <https://next2sun.com/en/testimonials/agripv-systems/> (visited on 08/06/2023).
- [79] D. Cremoncini, G. F. Frate, A. Bischi and L. Ferrari, “Mixed Integer Linear Program model for optimized scheduling of a vanadium redox flow battery with variable efficiencies, capacity fade, and electrolyte maintenance”, Mar. 2023. [Online]. Available: <https://www.sciencedirect.com/science/article/pii/S2352152X22024896> (visited on 09/06/2023).
- [80] Pyomo, *About Pyomo*. [Online]. Available: <http://www.pyomo.org/about> (visited on 10/06/2023).
- [81] M. Korpås, “Distributed Energy Systems with Wind Power and Energy Storage”, Doctoral thesis, 2004. [Online]. Available: <https://ntnuopen.ntnu.no/ntnu-xmlui/handle/11250/249683>.
- [82] IRENA, “Battery Storage and Renewables: Costs and Markets to 2030”, en, Tech. Rep., Oct. 2017. [Online]. Available: <https://www.irena.org/publications/2017/oct/electricity-storage-and-renewables-costs-and-markets> (visited on 05/06/2023).
- [83] T. Heimvik, “Battery for Capacity Expansion: A Techno-Economic Case Study in Trøndelag”, eng, Accepted: 2023-05-27T17:19:23Z, M.S. thesis, NTNU, 2023. [Online]. Available: <https://ntnuopen.ntnu.no/ntnu-xmlui/handle/11250/3069205> (visited on 12/06/2023).
- [84] Michael Penev, *NREL - Energy Storage Analysis*, Apr. 2019.
- [85] A. Bergström, “Techno-economic analysis of commercial battery storage systems in Northern Europe”, M.S. thesis, 2020. [Online]. Available: <https://www.semanticscholar.org/paper/Techno-economic-analysis-of-commercial-battery-in-Bergstr%C3%B6m/58d7231979538b6de04a5fb15626412306eb0806> (visited on 12/06/2023).
- [86] Visblue, *Container Module*. [Online]. Available: <https://www.visblue.com/product/container-module>.
- [87] O. J. Guerra, J. Zhang, J. Eichman, P. Denholm, J. Kurtz and B.-M. Hodge, “The value of seasonal energy storage technologies for the integration of wind and solar power”, en, *Energy & Environmental Science*, vol. 13, no. 7, pp. 1909–1922, Jul. 2020, Publisher: The Royal Society of Chemistry, ISSN: 1754-5706. DOI: 10.1039/D0EE00771D. [Online]. Available: <https://pubs.rsc.org/en/content/articlelanding/2020/ee/d0ee00771d> (visited on 18/06/2023).
- [88] T. G. Hansen, “Utilization of energy storage systems in ports”, en, M.S. thesis, NTNU, 2020. [Online]. Available: <https://ntnuopen.ntnu.no/ntnu-xmlui/handle/11250/2778219>.

- [89] J. Dycus, *NREL study backs hydrogen for long-duration storage*, Jul. 2020. [Online]. Available: <https://pv-magazine-usa.com/2020/07/03/nrel-study-backs-hydrogen-for-long-duration-storage/> (visited on 18/06/2023).
- [90] M. Ceraolo, G. Lutzemberger, D. Poli, S. Salamone and C. Scarpelli, “Redox-flow batteries for high energy-to-power ratio storage: A preliminary experimental study”, in *2021 IEEE International Conference on Environment and Electrical Engineering and 2021 IEEE Industrial and Commercial Power Systems Europe (EEEIC / I&CPS Europe)*, Sep. 2021, pp. 1–6. DOI: 10.1109/EEEIC/ICPSEurope51590.2021.9584820.

Appendix A - Python Script for Data Aggregation

```
1 import csv
2 import os
3
4 year = "2020" #Change year here
5 site = "TIP" #Change site here
6 #Folder either TIP or ST0
7 for i in range(1,54): # 1 to 53 weeks
8     with open(os.path.join(os.getcwd(),site,year)+"\\"+str(i)+".csv
9         ") as csv_file:
10         csv_reader = csv.reader(csv_file, delimiter=',')
11         line_count = 0
12         aggregatedData = 0
13         main_time = ""
14         for row in csv_reader:
15             if line_count == 0:
16                 print(i)
17             else:
18                 selectedRow = row[0].split(",")
19                 updatedRow = [selectedRow[0],selectedRow[1].replace
20 ("\"",",")]
21                 if(line_count % 4 == 0):
22                     # print(main_time, aggregatedData + float(
23 updatedRow[1])) # print the aggregated data
24                     with open(os.path.join(os.getcwd(),"Output",
25 site+"_"+year+".csv"), "a+") as myfile:
26                         if os.path.getsize(os.path.join(os.getcwd()
27 ,"Output",site+"_"+year+".csv")) == 0:
28                             myfile.write("Time, System Production (W
29 )\n")
30                             myfile.write('{0},"{1}"'.format(
31 main_time, aggregatedData + float(updatedRow[1]))+"\n")
32                             aggregatedData = 0
33                             elif(line_count % 4 == 1):
34                                 main_time = updatedRow[0]
35                                 aggregatedData += float(updatedRow[1])
36                             else:
37                                 aggregatedData += float(updatedRow[1])
38                             line_count += 1
39                             print(f'Processed {line_count} lines.')
```

Listing B.1: Python script used to aggregate 15-minute resolution data into hourly data for years 2021 and 2022.

Appendix B - Simulation Recommendations by Next2Sun and Component Data Sheets

B1 - PVSyst APV Simulation recommendations by Next2Sun


Key Facts Simulation of N2S System to be used with Simulation Software PVSyst		Next2Sun																					
																							
Header																							
Document name	Key-Facts Simulation																						
Version	1.4																						
Date	2021-01-13																						
Created by	P. Bendix																						
Review by	H. Hildebrandt																						
PVSyst Version	7.1.3																						
Utilisation Purpose	<p>This document describes the guidelines and parameter settings to simulate PV-Systems with the vertical and bifacial Next2Sun concept.</p> <p>The given recommended parameter settings should be used for correct yield expectations concerning upcoming projects. The data is validated by measured data in 5 minutes resolution of the Next2Sun Pilot plant with data from 2016-2019.</p> <p>The validation data based on our pilot plant concerning the simulation is listed below. Validated with Meteonorm 7.2 year and site-specific irradiation and weather data</p> <table border="1"> <thead> <tr> <th></th> <th>2019</th> <th>2018</th> <th>2017</th> <th>2016</th> </tr> </thead> <tbody> <tr> <td>Measured</td> <td>1102</td> <td>1159</td> <td>1083</td> <td>1036</td> </tr> <tr> <td>Simulation</td> <td>1070</td> <td>1134</td> <td>1086</td> <td>1074</td> </tr> <tr> <td>Difference</td> <td>-2,90 %</td> <td>-2,16 %</td> <td>+0,27 %</td> <td>+3,66 %</td> </tr> </tbody> </table>				2019	2018	2017	2016	Measured	1102	1159	1083	1036	Simulation	1070	1134	1086	1074	Difference	-2,90 %	-2,16 %	+0,27 %	+3,66 %
	2019	2018	2017	2016																			
Measured	1102	1159	1083	1036																			
Simulation	1070	1134	1086	1074																			
Difference	-2,90 %	-2,16 %	+0,27 %	+3,66 %																			
Grid System Definition																							
Parameter	Value	Description																					
PV Module	The used PV Module needs to be entered	See document: Specification Solarmodules for further details of Modules which are usable																					
Inverter	The used Inverter needs to be entered	We are working by default with the Huawei Inverter SUN2000 KTL																					
Multi-MPPT feature	Disabled	Inverters with power sharing for different MPPT inputs should be used. With the possibility to share the total inverter power for different MPPT inputs the power produced by strings facing frontside east and frontside west can be shared. With this setup the Pnom ratio can be chosen high to minimize system costs by still earning full power.																					
Pnom ratio	1.35-1.45																						
Bifacial System Definition																							
Parameter	Value	Description																					
Bifacial Model	Use unlimited sheds 2D-Model	System based on unlimited sheds																					
Shed transparent fraction	13.1 %	$1 - \frac{\text{Wafersurface PV Module} + \text{crossbeam} + \text{post}}{\text{post distance} \cdot \text{shed height}}$ <p>Concerning Jollywood Modules:</p> $1 - \frac{3,52 \text{ m}^2 + 0,15 \text{ m}^2 + 0,16 \text{ m}^2}{2,15 \text{ m} \cdot 2,05 \text{ m}} = 13.1\%$																					

Figure C.1: PVSyst simulation recommendations from Next2Sun [67].

B2 - Bifacial PV Panel Data Sheet

CHASER-M6/144P
455-475W
 HJT 9BB HALF-CUT BIFACIAL
 DOUBLE GLASS MODULE

Hi-Chaser
 SK8612HDGDC

30
 30-year quality warranty with longer operational life

1500V
 1500V high system voltage design



Fire class A, harsh environment adaptability

Consist of double-glass, with special design cells, Outstanding anti-PID performance.



30 -year power warranty

Bifacial module ensures 30-year outdoor operation, longer than the conventional type of normally 25 years.



Elegant appearance & high performance

The bifacial module is of high light transmittance to ensure good performance, an advanced solution that enables more energy generation, light capturing and elegant appearance.



1500V system voltage

Maximum 1500V DC system voltage , excellent insulation performance and lower total system cost.

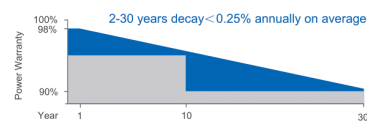
LINEAR PERFORMANCE WARRANTY



Product warranty on materials and workmanship



Linear power output warranty



CERTIFICATES

ISO 9001: 2015
 Quality Management System

IEC 61215 / IEC 61730

ISO 14001: 2015
 Environmental Management System

OHSAS 18001: 2007
 Occupational Health &
 Safety Management System

*Certification requirements vary in different markets, please consult with Akcome Optronics sales team for appropriate certification.



Figure C.2: Bifacial PV panel data sheet page 1/2.

ELECTRICAL PARAMETERS @ STC

	455	367	460	371	465	375	470	379	475	383
	Front	Back	Front	Back	Front	Back	Front	Back	Front	Back
Max. Power Output Pmax (W)	0~+3%		0~+3%		0~+3%		0~+3%		0~+3%	
Power Tolerance	45.10	45.52	45.30	45.72	45.50	45.92	45.70	46.12	45.90	46.32
Max. Power Voltage Vmp (V)	10.09	8.07	10.15	8.12	10.22	8.18	10.28	8.23	10.35	8.28
Max. Power Current Imp (A)	53.05	52.61	53.35	52.91	53.65	53.21	53.95	53.51	54.25	53.81
Open Circuit Voltage Voc (V)	10.90	8.77	10.94	8.81	10.98	8.84	11.02	8.87	11.06	8.90
Short Circuit Current Isc (A)	20.36	16.44	20.59	16.62	20.81	16.80	21.04	16.98	21.26	17.16
Module Efficiency (%)										

*STC (Standard Test Condition): Irradiance 1000W/m², Cell Temperature 25°C, Air Mass 1.5
*Measurement Tolerance (±3.0%)

Integrated Power @ STC (Reference to 465W front)

Power Gains	5%	10%	15%	20%	25%
Max. Power Output Pmax (W)	488	512	534	557	580
Max. Power Voltage Vmp (V)	45.50	45.50	45.40	45.40	45.40
Max. Power Current Imp (A)	10.73	11.24	11.75	12.26	12.77
Open Circuit Voltage Voc (V)	53.65	53.65	53.75	53.75	53.75
Short Circuit Current Isc (A)	11.53	12.08	12.63	13.18	13.73

TEMPERATURE COEFFICIENTS

Temperature Coefficients of Pmp	-0.24%/°C
Temperature Coefficients of Voc	-0.22%/°C
Temperature Coefficients of Isc	+0.047%/°C

MECHANICAL PARAMETERS

Cell Type	HJT 166x83mm
Number of Cells	144pcs(6x24)
Dimensions (L*W*H)	2132x1048x30mm
Weight	29.0kg
Frame	Anodised Aluminium
Junction Box	IP67, 3 bypass diodes
Cable, Length	4.0mm ² , 300mm

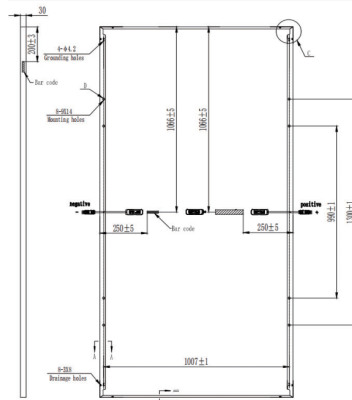
OPERATING CONDITION

Maximum System Voltage(V)	1500(DC)
Operating Temperature(°C)	-40~+85
Max. Wind Load / Snow Load(pa)	2400/5400
Max. Over Current(A)	20
Fire Rating	Class A
NOCT(°C)	45±2

PACKAGE INFORMATION

Container 40'HQ	700pcs
Quantity / Pallet	CTNR: 35pcs

ASSEMBLY DRAWING (Unit:mm)



I-V CURVES

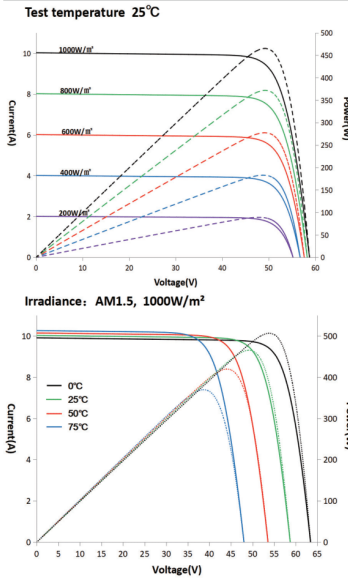


Figure C.3: Bifacial PV panel data sheet page 2/2.

B3 - Inverter Data Sheet



PVsyst V7.3.4

Ingrid Brøndbo (Norway)

Inverter - SUN2000-100KTL-INM0-415Vac

Manufacturer	Generic		
Model	SUN2000-100KTL-INM0-415Vac		
Commercial data			
Availability :	Prod. Since 2019	Data source :	Manufacturer 2019
Remarks			
Technology:	Dual stage, Transformerless		
Protection:	IP66		
Control:	LED indicator, Bluetooth/WLAN + APP, USB data cable+APP		
Input characteristics (PV array side)			
Operating mode	MPPT		
Minimum MPP Voltage (Vmin)	200 V	Power Threshold (Pthresh.)	150 W
Maximum MPP Voltage (Vmax)	1000 V		
Absolute max. PV Voltage (Vmax array)	1100 V		
"String" inverter with input protections			
Number of string inputs	20		
Behaviour at Vmin/Vmax	Limitation		
Behaviour at Pnom	Limitation		
Output characteristics (AC grid side)			
Grid voltage (Imax)	Triphased 415 V	Nominal AC Power (Pnom AC)	100 kWac
Grid frequency	50/60 Hz	Maximum AC Power (Pmax AC)	110 kWac
		Nominal AC current (Inom AC)	139 A
		Maximum AC current (Imax AC)	155 A
Multi MPPT capability			
		Number of MPPT inputs	10

Efficiency defined for 3 voltages

	V	Maximum efficiency	European average efficiency
		%	%
Low voltage	540	98.0	97.7
Medium voltage	620	98.8	98.6
High voltage	800	98.5	98.3

Remarks and Technical features

Array isolation monitoring
Internal DC switch
Output Voltage disconnect adjustment
ENS protection

Efficiency profile vs Input power

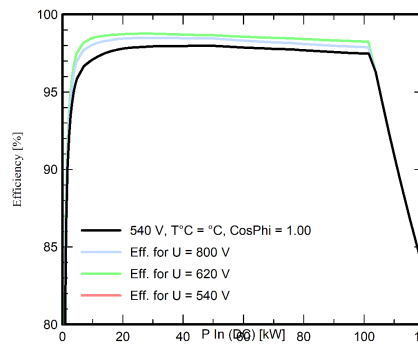


Figure C.4: Inverter data sheet page 1/1.

Appendix C - GitHub Repository

The code and data used in this thesis for optimization and plotting are included in the GitHub repository linked below. Further explanations are given in the README-file.

GitHub repository link

- <https://github.com/Ingridbro/Master-s-thesis-code>

Appendix D - PVsyst Reports from Base Case Scenario

D1 - PVsyst Report STO Building



Version 7.3.4

PVsyst - Simulation report

Grid-Connected System

Project: Skjetlein_scenario1

Variant: STO_bygg

Tables on a building

System power: 41.2 kWp

Nypan - Norway

Author
Ingrid Brøndbo (Norway)

Figure E.1: PVsyst report STO building page 1/9.



PVsyst V7.3.4

VCD, Simulation date:
10/06/23 23:18
with v7.3.4

Project: Skjetlein_scenario1

Variant: STO_bygg

Ingrid Brøndbo (Norway)

Project summary

Geographical Site	Situation	Meteo data
Nypan Norway	Latitude 63.34 °N Longitude 10.30 °E Altitude 58 m Time zone UTC+1	Nypan Meteonorm 8.1 (1991-2013) - Synthetic

Monthly albedo values

	Jan.	Feb.	Mar.	Apr.	May	June	July	Aug.	Sep.	Oct.	Nov.	Dec.
Albedo	0.70	0.70	0.40	0.20	0.20	0.20	0.20	0.20	0.20	0.20	0.40	0.70

System summary

Grid-Connected System	Tables on a building	User's needs
PV Field Orientation Fixed plane Tilt/Azimuth 25 / -66.7 °	Near Shadings Detailed electrical calculation acc. to module layout	Unlimited load (grid)
System information	Inverters	
PV Array Nb. of modules 147 units Pnom total 41.2 kWp	Nb. of units 2 units Pnom total 55.0 kWac Pnom ratio 0.748	

Results summary

Produced Energy	32140 kWh/year	Specific production	781 kWh/kWp/year	Perf. Ratio PR	80.36 %
-----------------	----------------	---------------------	------------------	----------------	---------

Table of contents

Project and results summary	2
General parameters, PV Array Characteristics, System losses	3
Horizon definition	5
Near shading definition - Iso-shadings diagram	6
Main results	7
Loss diagram	8
Predef. graphs	9
Single-line diagram	10

Figure E.2: PVSyst report STO building page 2/9.



PVsyst V7.3.4

VCD, Simulation date:
10/06/23 23:18
with v7.3.4

Project: Skjetlein_scenario1

Variant: STO_bygg

Ingrid Brøndbo (Norway)

General parameters

Grid-Connected System		Tables on a building	
PV Field Orientation		Sheds configuration	
Orientation			Models used
Fixed plane			Transposition Perez
Tilt/Azimuth	25 / -66.7 °		Diffuse Perez, Meteonorm Circumsolar separate
Horizon		Near Shadings	
Average Height	3.5 °	Detailed electrical calculation acc. to module layout	
		User's needs	
		Unlimited load (grid)	

PV Array Characteristics

PV module		Inverter	
Manufacturer	Generic	Manufacturer	Generic
Model	LX-280M/156-60+ GG	Model	SUN2000-28KTL
(Original PVsyst database)		(Original PVsyst database)	
Unit Nom. Power	280 Wp	Unit Nom. Power	27.5 kWac
Number of PV modules	147 units	Number of inverters	2 units
Nominal (STC)	41.2 kWp	Total power	55.0 kWac
Modules	7 Strings x 21 In series	Operating voltage	200-950 V
At operating cond. (50°C)		Pnom ratio (DC:AC)	0.75
Pmpp	37.1 kWp	Power sharing within this inverter	
U mpp	583 V		
I mpp	64 A		
Total PV power		Total inverter power	
Nominal (STC)	41 kWp	Total power	55 kWac
Total	147 modules	Number of inverters	2 units
Module area	247 m ²	Pnom ratio	0.75
Cell area	214 m ²		

Array losses

Array Soiling Losses												
Average loss Fraction 8.2 %												
Jan.	Feb.	Mar.	Apr.	May	June	July	Aug.	Sep.	Oct.	Nov.	Dec.	
20.0%	25.0%	15.0%	3.0%	2.0%	2.0%	2.0%	2.0%	2.0%	2.0%	5.0%	18.0%	
Thermal Loss factor			DC wiring losses				Series Diode Loss					
Module temperature according to irradiance			Global array res. 154 mΩ				Voltage drop 0.7 V					
Uc (const) 20.0 W/m ² K			Loss Fraction 1.5 % at STC				Loss Fraction 0.1 % at STC					
Uv (wind) 0.0 W/m ² K/m/s												
LID - Light Induced Degradation			Module Quality Loss				Module mismatch losses					
Loss Fraction 2.0 %			Loss Fraction -0.6 %				Loss Fraction 2.0 % at MPP					
Strings Mismatch loss												
Loss Fraction 0.2 %												

Figure E.3: PVsyst report STO building page 3/9.



PVsyst V7.3.4
VCD, Simulation date:
10/06/23 23:18
with v7.3.4

Project: Skjetlein_scenario1

Variant: STO_bygg

Ingrid Brøndbo (Norway)

Array losses

IAM loss factor

Incidence effect (IAM): Fresnel smooth glass, n = 1.526

0°	30°	50°	60°	70°	75°	80°	85°	90°
1.000	0.998	0.981	0.948	0.862	0.776	0.636	0.403	0.000

System losses

Unavailability of the system

Time fraction 0.5 %
1.8 days,
3 periods

Figure E.4: PVSyst report STO building page 4/9.



PVsyst V7.3.4
 VCD, Simulation date:
 10/06/23 23:18
 with v7.3.4

Project: Skjetlein_scenario1
 Variant: STO_bygg

Ingrid Brøndbo (Norway)

Horizon definition

Horizon from Meteornorm web service, lat=63,3426, lon=10,301

Average Height 3.5 ° Albedo Factor 0.84
 Diffuse Factor 0.98 Albedo Fraction 100 %

Horizon profile

Azimuth [°]	-180	-149	-148	-146	-145	-141	-140	-137	-136	-134	-133	-128	-127	-121
Height [°]	6.0	6.0	5.0	5.0	6.0	6.0	5.0	5.0	6.0	6.0	5.0	5.0	4.0	4.0
Azimuth [°]	-120	-113	-112	-100	-99	-63	-62	-59	-58	-48	-47	-46	-32	-31
Height [°]	5.0	5.0	4.0	4.0	3.0	3.0	2.0	2.0	3.0	3.0	4.0	3.0	3.0	4.0
Azimuth [°]	-17	-16	-4	-3	1	2	23	24	25	33	34	65	66	100
Height [°]	4.0	3.0	3.0	2.0	2.0	1.0	1.0	2.0	1.0	2.0	2.0	2.0	1.0	1.0
Azimuth [°]	101	107	108	112	113	119	120	131	132	149	150	175	176	179
Height [°]	2.0	2.0	3.0	3.0	4.0	4.0	5.0	5.0	6.0	6.0	5.0	5.0	6.0	6.0

Sun Paths (Height / Azimuth diagram)

Fixed plane, Tilts/azimuths: 25° -67°

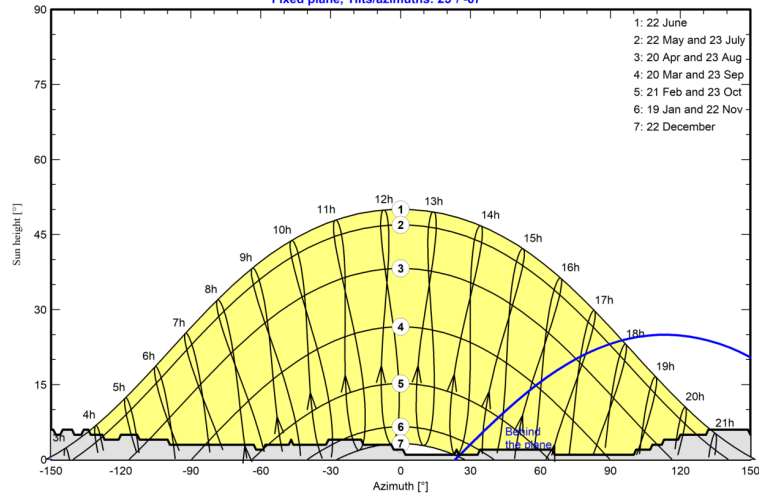


Figure E.5: PVsyst report STO building page 5/9.

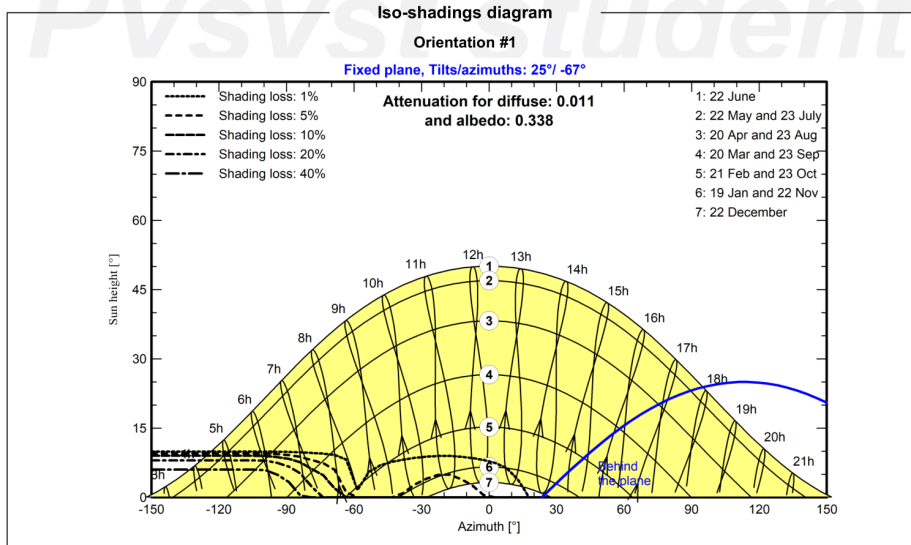
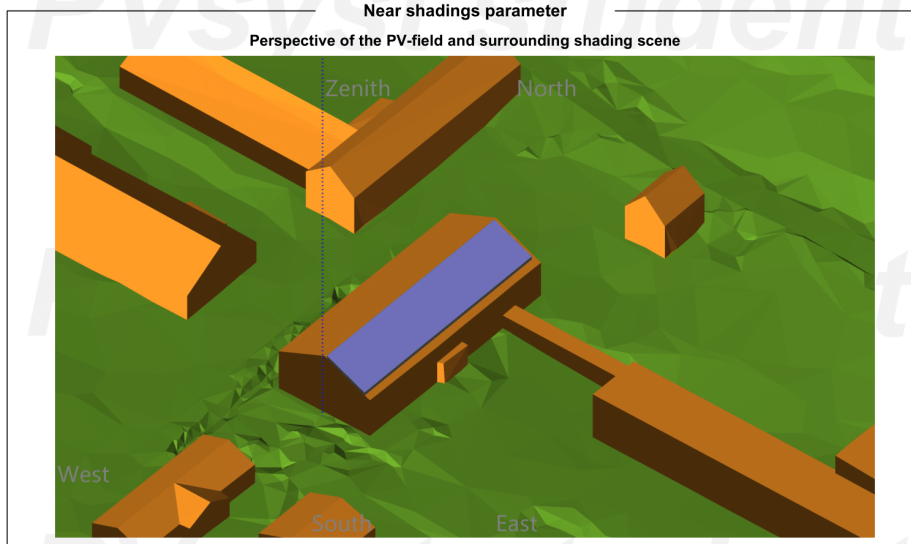


PVsyst V7.3.4
VCD, Simulation date:
10/06/23 23:18
with v7.3.4

Project: Skjetlein_scenario1

Variant: STO_bygg

Ingrid Brøndbo (Norway)



10/06/23

PVsyst Student License for Ingrid Brøndbo (Norway)

Page 6/10

Figure E.6: PVSyst report STO building page 6/9.



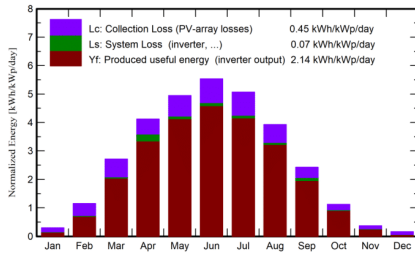
Main results

System Production

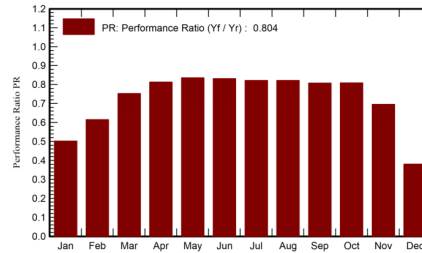
Produced Energy 32140 kWh/year

Specific production 781 kWh/kWp/year
Perf. Ratio PR 80.36 %

Normalized productions (per installed kWp)



Performance Ratio PR



Balances and main results

	GlobHor kWh/m ²	DiffHor kWh/m ²	T_Amb °C	GlobInc kWh/m ²	GlobEff kWh/m ²	EArray kWh	E_Grid kWh	PR ratio
January	5.8	3.90	-1.06	9.1	5.6	208	188	0.502
February	22.9	11.74	-0.97	32.3	21.2	845	818	0.615
March	67.0	25.70	0.92	84.2	66.9	2671	2611	0.753
April	111.6	44.99	5.22	123.7	113.8	4441	4143	0.814
May	151.1	64.36	9.43	153.5	142.7	5400	5282	0.836
June	159.5	72.78	12.22	166.0	154.6	5807	5680	0.831
July	154.8	79.90	15.61	157.2	146.2	5438	5316	0.822
August	116.1	57.06	14.94	121.9	112.7	4220	4124	0.822
September	67.8	36.75	10.95	72.9	66.8	2559	2426	0.808
October	29.6	16.65	6.26	34.8	30.8	1196	1158	0.809
November	8.1	5.66	2.26	11.0	8.7	333	315	0.696
December	2.7	2.05	-0.24	5.0	2.5	88	78	0.380
Year	896.9	421.55	6.34	971.6	872.6	33205	32140	0.804

Legends

GlobHor	Global horizontal irradiation	EArray	Effective energy at the output of the array
DiffHor	Horizontal diffuse irradiation	E_Grid	Energy injected into grid
T_Amb	Ambient Temperature	PR	Performance Ratio
GlobInc	Global incident in coll. plane		
GlobEff	Effective Global, corr. for IAM and shadings		

Figure E.7: PVSyst report STO building page 7/9.



PVsyst V7.3.4
VCD, Simulation date:
10/06/23 23:18
with v7.3.4

Project: Skjetlein_scenario1

Variant: STO_bygg

Ingrid Brøndbo (Norway)

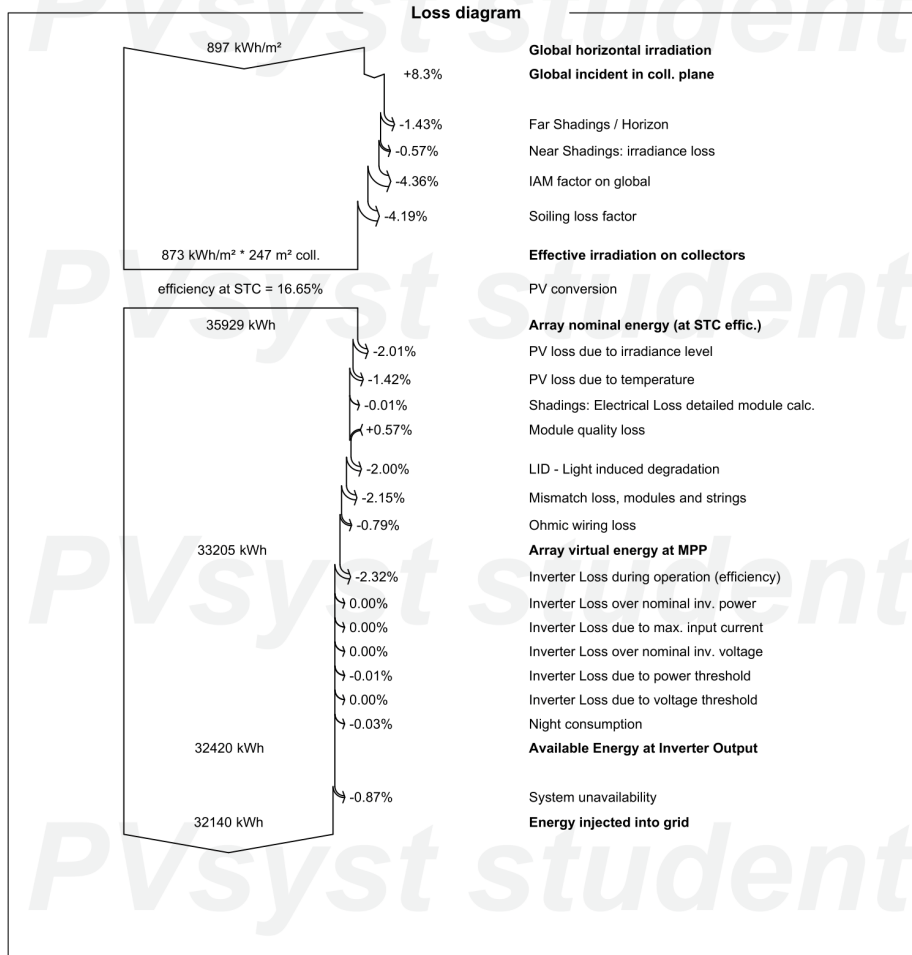


Figure E.8: PVsyst report STO building page 8/9.

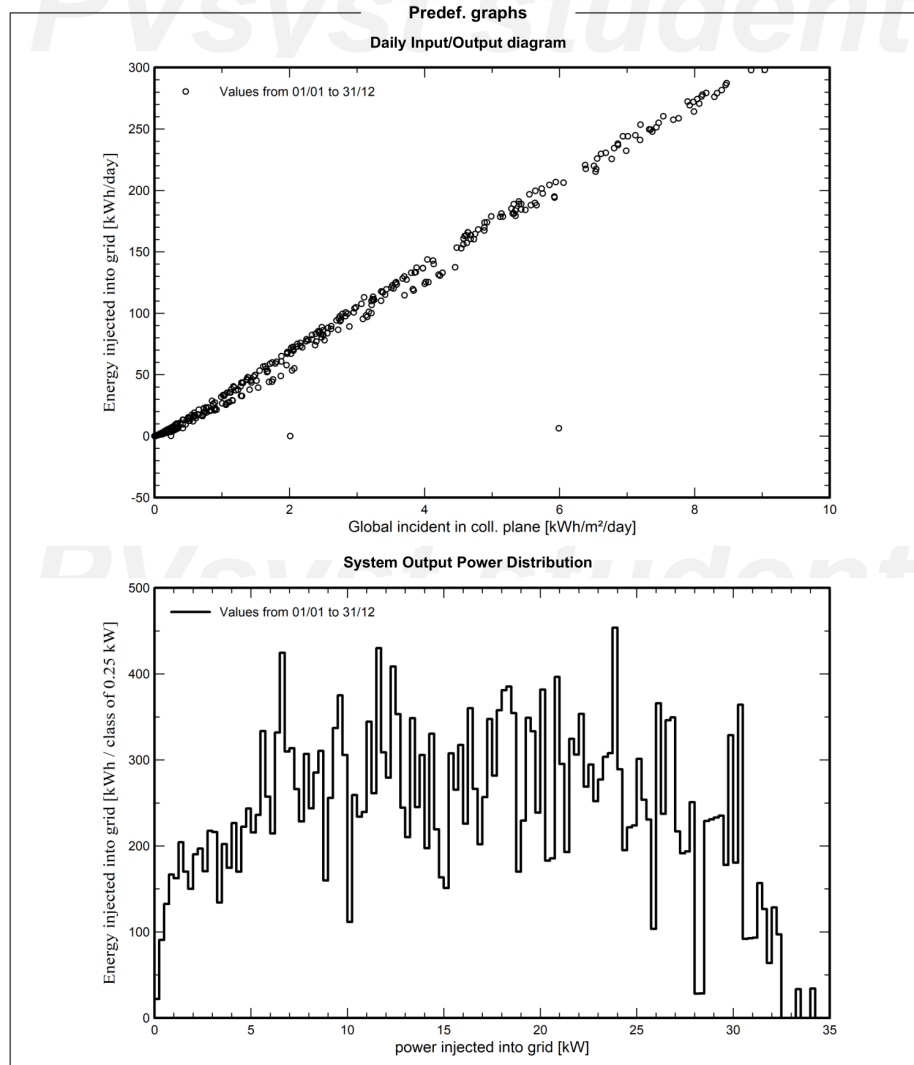


PVsyst V7.3.4
VCD, Simulation date:
10/06/23 23:18
with v7.3.4

Project: Skjetlein_scenario1

Variant: STO_bygg

Ingrid Brøndbo (Norway)



10/06/23

PVsyst Student License for Ingrid Brøndbo (Norway)

Page 9/10

Figure E.9: PVSyst report STO building page 9/9.

D2 - PVSyst Report TIP Building



Version 7.3.4

PVsyst - Simulation report

Grid-Connected System

Project: Skjetlein_scenario1

Variant: TIP_bygg

Tables on a building

System power: 84.0 kWp

Nypan - Norway

Author
Ingrid Brøndbo (Norway)

Figure E.10: PVSyst report TIP building page 1/9.



PVsyst V7.3.4

VCE, Simulation date:
10/06/23 23:43
with v7.3.4

Project: Skjetlein_scenario1

Variant: TIP_bygg

Ingrid Brøndbo (Norway)

Project summary

Geographical Site	Situation	Meteo data
Nypan Norway	Latitude 63.34 °N Longitude 10.30 °E Altitude 58 m Time zone UTC+1	Nypan Meteonorm 8.1 (1991-2013) - Synthetic

Monthly albedo values

	Jan.	Feb.	Mar.	Apr.	May	June	July	Aug.	Sep.	Oct.	Nov.	Dec.
Albedo	0.70	0.70	0.40	0.20	0.20	0.20	0.20	0.20	0.20	0.20	0.40	0.70

System summary

Grid-Connected System	Tables on a building	User's needs
PV Field Orientation Fixed plane Tilt/Azimuth 24 / 24.9 °	Near Shadings Detailed electrical calculation acc. to module layout	Unlimited load (grid)

System information		Inverters	
PV Array		Nb. of units	2 units
Nb. of modules	280 units	Pnom total	55.2 kWac
Pnom total	84.0 kWp	Pnom ratio	1.522

Results summary

Produced Energy	71649 kWh/year	Specific production	853 kWh/kWp/year	Perf. Ratio PR	78.32 %
-----------------	----------------	---------------------	------------------	----------------	---------

Table of contents

Project and results summary	2
General parameters, PV Array Characteristics, System losses	3
Horizon definition	5
Near shading definition - Iso-shadings diagram	6
Main results	7
Loss diagram	8
Predef. graphs	9

Figure E.11: PVsyst report TIP building page 2/9.



PVsyst V7.3.4
 VCE, Simulation date:
 10/06/23 23:43
 with v7.3.4

Project: Skjetlein_scenario1
 Variant: TIP_bygg

Ingrid Brøndbo (Norway)

General parameters

Grid-Connected System		Tables on a building	
PV Field Orientation		Sheds configuration	Models used
Orientation			Transposition Perez
Fixed plane			Diffuse Perez, Meteonorm
Tilt/Azimuth	24 / 24.9 °		Circumsolar separate
Horizon		Near Shadings	User's needs
Average Height	3.4 °	Detailed electrical calculation acc. to module layout	Unlimited load (grid)

PV Array Characteristics

PV module		Inverter	
Manufacturer	Generic	Manufacturer	Generic
Model	LX-300M/156-60+ GG Full Black	Model	SE55K/SE82.8K Unit
(Original PVsyst database)		(Original PVsyst database)	
Unit Nom. Power	300 Wp	Unit Nom. Power	27.6 kWac
Number of PV modules	280 units	Number of inverters	2 units
Nominal (STC)	84.0 kWp	Total power	55.2 kWac
SolarEdge Power Optimizer			
Model	P950 Worldwide		
Unit Nom. Power	950 W		
Input modules	2 in series		
Array #1 - PV Array		Array #2 - Sub-array #2	
Number of PV modules	160 units	Number of inverters	0.6 unit
Nominal (STC)	48.0 kWp	Total power	31.5 kWac
Optimizer Array	5 Strings x 16 In series	Operating voltage	750 V
At operating cond. (50°C)		Pnom ratio (DC:AC)	1.35
Pmpp	43.3 kWp		
Output of optimizers			
Voper	750 V		
I at Poper	58 A		
Total PV power		Total inverter power	
Nominal (STC)	84 kWp	Total power	55.2 kWac
Total	280 modules	Number of inverters	2 units
Module area	471 m ²	Pnom ratio	1.52
Cell area	408 m ²		

Figure E.12: PVsyst report TIP building page 3/9.



PVsyst V7.3.4

VCE, Simulation date:
10/06/23 23:43
with v7.3.4

Project: Skjetlein_scenario1

Variant: TIP_bygg

Ingrid Brøndbo (Norway)

Array losses

Array Soiling Losses

Average loss Fraction 15.2 %

Jan.	Feb.	Mar.	Apr.	May	June	July	Aug.	Sep.	Oct.	Nov.	Dec.
40.0%	50.0%	30.0%	5.0%	2.0%	2.0%	2.0%	2.0%	2.0%	2.0%	10.0%	35.0%

Thermal Loss factor

Module temperature according to irradiance
Uc (const) 20.0 W/m²K
Uv (wind) 0.0 W/m²K/m/s

Serie Diode Loss

Voltage drop 0.7 V
Loss Fraction 0.1 % at STC

LID - Light Induced Degradation

Loss Fraction 2.0 %

Module Quality Loss

Loss Fraction -0.6 %

Module mismatch losses

Loss Fraction 0.6 % at MPP

IAM loss factor

Incidence effect (IAM): Fresnel smooth glass, n = 1.526

0°	30°	50°	60°	70°	75°	80°	85°	90°
1.000	0.998	0.981	0.948	0.862	0.776	0.636	0.403	0.000

DC wiring losses

Global wiring resistance 10 mΩ
Loss Fraction 1.5 % at STC

Array #1 - PV Array

Global array res. 176 mΩ
Loss Fraction 1.5 % at STC

Array #2 - Sub-array #2

Global array res. 234 mΩ
Loss Fraction 1.5 % at STC

System losses

Unavailability of the system

Time fraction 0.5 %
1.8 days,
3 periods

Figure E.13: PVsyst report TIP building page 4/9.



PVsyst V7.3.4
 VCE, Simulation date:
 10/06/23 23:43
 with v7.3.4

Project: Skjetlein_scenario1

Variant: TIP_bygg

Ingrid Brøndbo (Norway)

Horizon definition

Horizon from Meteornorm web service, lat=63,3403, lon=10,2973

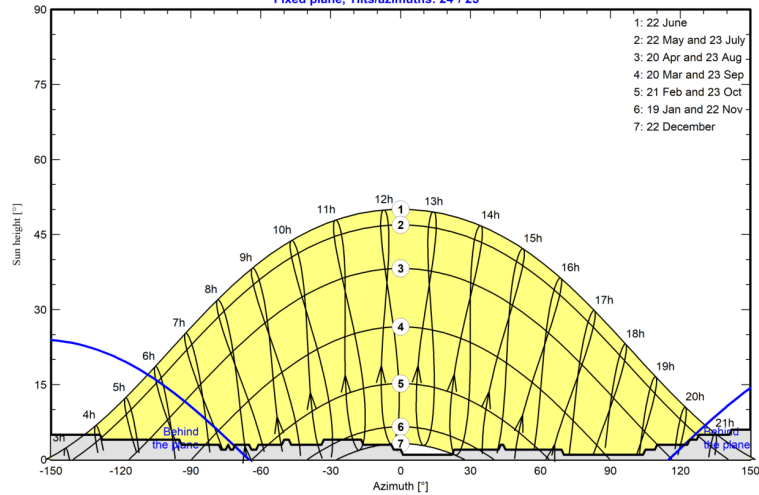
Average Height 3.4 ° Albedo Factor 0.90
 Diffuse Factor 0.99 Albedo Fraction 100 %

Horizon profile

Azimuth [°]	-180	-129	-128	-95	-94	-78	-77	-75	-74	-73	-72	-71	-65	-64
Height [°]	5.0	5.0	4.0	4.0	3.0	3.0	2.0	2.0	3.0	2.0	2.0	3.0	3.0	2.0
Azimuth [°]	-62	-61	-51	-50	-48	-47	-34	-33	-17	-16	-4	-3	0	1
Height [°]	2.0	3.0	3.0	4.0	4.0	3.0	3.0	4.0	4.0	3.0	3.0	2.0	2.0	1.0
Azimuth [°]	22	23	42	43	44	45	69	70	104	105	109	110	123	124
Height [°]	1.0	2.0	2.0	3.0	3.0	2.0	2.0	1.0	1.0	2.0	2.0	3.0	3.0	4.0
Azimuth [°]	127	128	141	142	156	157	165	166	175	176	179			
Height [°]	4.0	5.0	5.0	6.0	6.0	7.0	7.0	6.0	6.0	5.0	5.0			

Sun Paths (Height / Azimuth diagram)

Fixed plane, Tilts/azimuths: 24°/ 25°



10/06/23

PVsyst Student License for Ingrid Brøndbo (Norway)

Page 5/9

Figure E.14: PVsyst report TIP building page 5/9.



PVsyst V7.3.4
VCE, Simulation date:
10/06/23 23:43
with v7.3.4

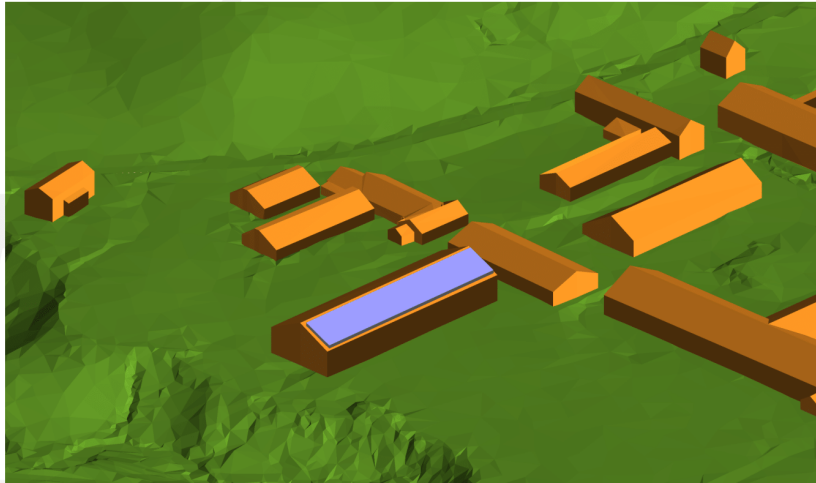
Project: Skjetlein_scenario1

Variant: TIP_bygg

Ingrid Brøndbo (Norway)

Near shadings parameter

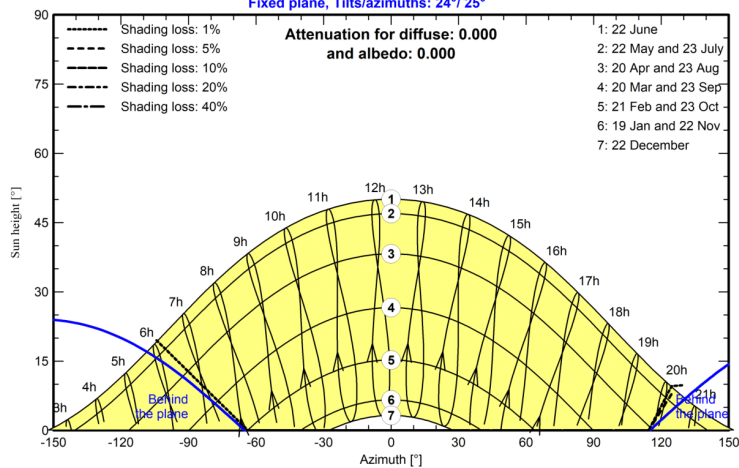
Perspective of the PV-field and surrounding shading scene



Iso-shadings diagram

Orientation #1

Fixed plane, Tilts/azimuths: 24°/ 25°



10/06/23

PVsyst Student License for Ingrid Brøndbo (Norway)

Page 6/9

Figure E.15: PVsyst report TIP building page 6/9.



Main results

System Production

Produced Energy 71649 kWh/year

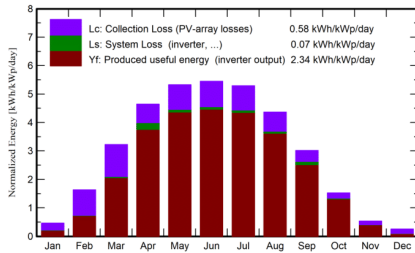
Specific production

853 kWh/kWp/year

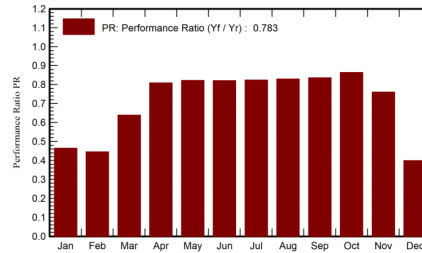
Perf. Ratio PR

78.32 %

Normalized productions (per installed kWp)



Performance Ratio PR



Balances and main results

	GlobHor kWh/m ²	DiffHor kWh/m ²	T_Amb °C	GlobInc kWh/m ²	GlobEff kWh/m ²	EArray kWh	E_Grid kWh	PR ratio
January	5.8	3.90	-1.06	14.3	7.5	587	558	0.464
February	22.9	11.74	-0.97	45.7	21.3	1745	1708	0.445
March	67.0	25.70	0.92	100.0	66.7	5476	5368	0.639
April	111.6	44.99	5.22	139.5	127.2	10080	9481	0.809
May	151.1	64.36	9.43	165.1	155.6	11625	11396	0.822
June	159.5	72.78	12.22	163.4	153.6	11499	11272	0.821
July	154.8	79.90	15.61	164.0	154.3	11583	11355	0.824
August	116.1	57.06	14.94	135.5	127.5	9630	9441	0.830
September	67.8	36.75	10.95	90.5	84.7	6645	6353	0.836
October	29.6	16.65	6.26	47.4	44.0	3508	3435	0.864
November	8.1	5.66	2.26	16.0	13.0	1044	1019	0.760
December	2.7	2.05	-0.24	7.8	3.6	270	261	0.399
Year	896.9	421.55	6.34	1089.0	959.1	73693	71649	0.783

Legends

GlobHor Global horizontal irradiation
DiffHor Horizontal diffuse irradiation
T_Amb Ambient Temperature
GlobInc Global incident in coll. plane
GlobEff Effective Global, corr. for IAM and shadings

EArray Effective energy at the output of the array
E_Grid Energy injected into grid
PR Performance Ratio

Figure E.16: PVsyst report TIP building page 7/9.



PVsyst V7.3.4
VCE, Simulation date:
10/06/23 23:43
with v7.3.4

Project: Skjetlein_scenario1

Variant: TIP_bygg

Ingrid Brøndbo (Norway)

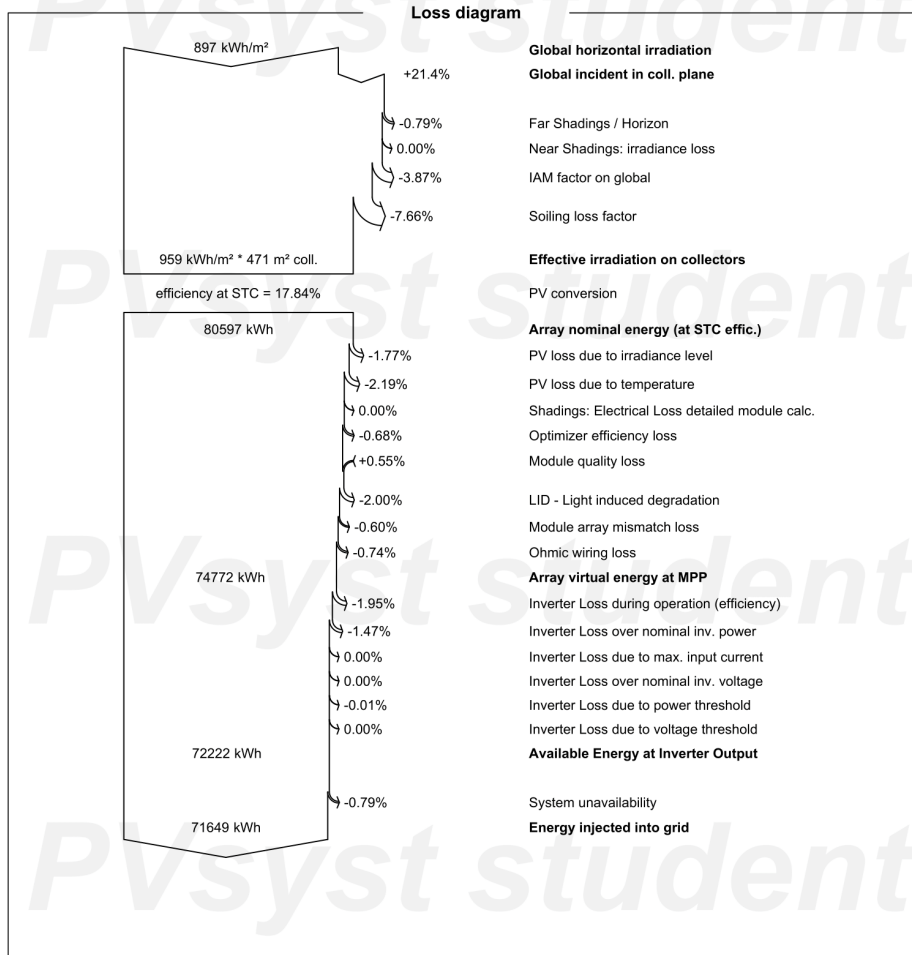


Figure E.17: PVsyst report TIP building page 8/9.

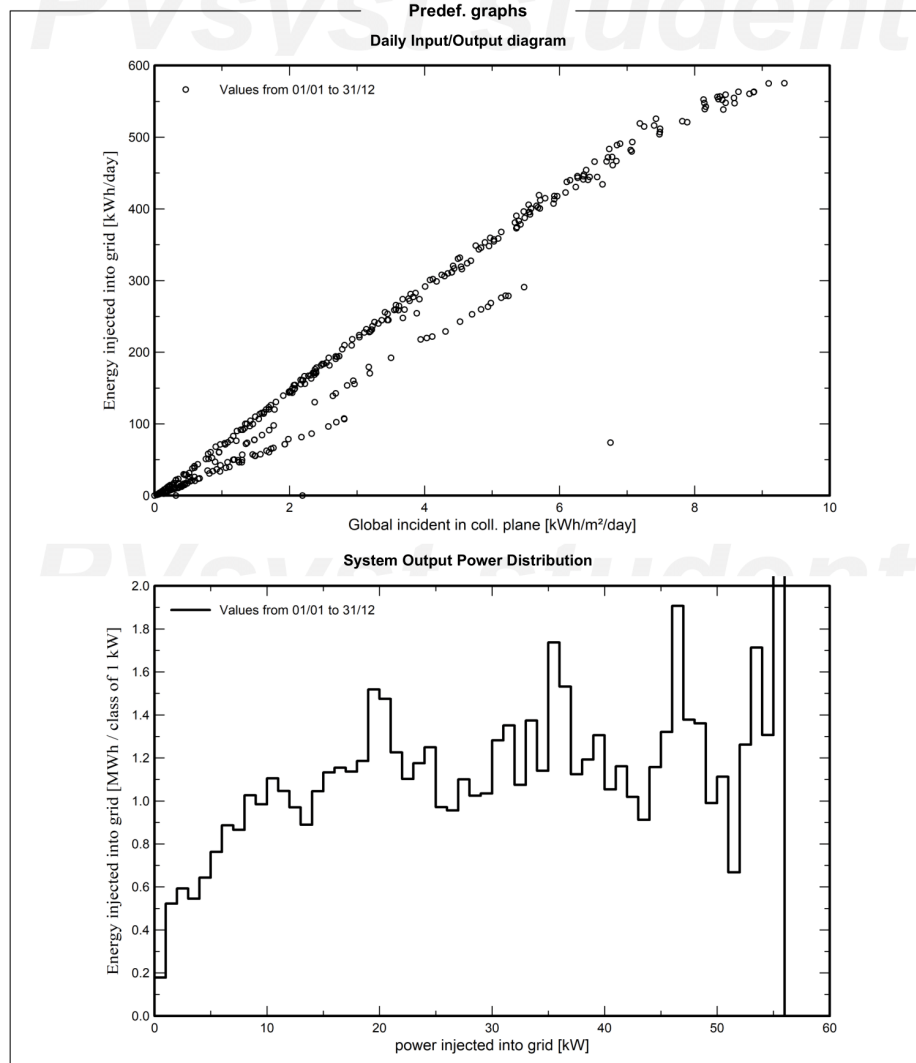


PVsyst V7.3.4
VCE, Simulation date:
10/06/23 23:43
with v7.3.4

Project: Skjetlein_scenario1

Variant: TIP_bygg

Ingrid Brøndbo (Norway)



10/06/23

PVsyst Student License for Ingrid Brøndbo (Norway)

Page 9/9

Figure E.18: PVsyst report TIP building page 9/9.

D3 - PVSyst Report Main Building



Version 7.3.4

PVsyst - Simulation report

Grid-Connected System

Project: Skjetlein_scenario1

Variant: Flatt_tak

Rows as domes east-west

System power: 109 kWp

Nypan - Norway

Author
Ingrid Brøndbo (Norway)

Figure E.19: PVSyst report main building page 1/9.



PVsyst V7.3.4

VCC, Simulation date:
10/06/23 20:08
with v7.3.4

Project: Skjetlein_scenario1

Variant: Flatt_tak

Ingrid Brøndbo (Norway)

Project summary

Geographical Site	Situation	Meteo data
Nypan	Latitude 63.34 °N	Nypan
Norway	Longitude 10.30 °E	Meteonorm 8.1 (1991-2013) - Synthetic
	Altitude 58 m	
	Time zone UTC+1	

Monthly albedo values

	Jan.	Feb.	Mar.	Apr.	May	June	July	Aug.	Sep.	Oct.	Nov.	Dec.
Albedo	0.70	0.70	0.40	0.20	0.20	0.20	0.20	0.20	0.20	0.20	0.40	0.70

System summary

Grid-Connected System	Rows as domes east-west	User's needs
PV Field Orientation	Near Shadings	Unlimited load (grid)
Fixed planes 2 orientations	Detailed electrical calculation	
Tilts/azimuths 13 / 114.4 °	acc. to module layout	
13 / -65.6 °		
System information	Inverters	
PV Array	Nb. of units	2 units
Nb. of modules 240 units	Pnom total	100 kWac
Pnom total 109 kWp	Pnom ratio	1.092

Results summary

Produced Energy	75190 kWh/year	Specific production	689 kWh/kWp/year	Perf. Ratio PR	77.40 %
-----------------	----------------	---------------------	------------------	----------------	---------

Table of contents

Project and results summary	2
General parameters, PV Array Characteristics, System losses	3
Horizon definition	5
Near shading definition - Iso-shadings diagram	6
Main results	8
Loss diagram	9
Predef. graphs	10
Single-line diagram	11

Figure E.20: PVsyst report main building page 2/9.



PVsyst V7.3.4
 VCC, Simulation date:
 10/06/23 20:08
 with v7.3.4

Project: Skjetlein_scenario1
 Variant: Flatt_tak

Ingrid Brøndbo (Norway)

General parameters

Grid-Connected System		Rows as domes east-west	
PV Field Orientation		Sheds configuration	Models used
Orientation		Nb. of sheds	Transposition Perez
Fixed planes	2 orientations	96 units	Diffuse Perez, Meteororm
Tilts/azimuths	13 / 114.4 °	Several orientations	Circumsolar separate
	13 / -65.6 °		
Horizon		Near Shadings	User's needs
Average Height	3.5 °	Detailed electrical calculation acc. to module layout	Unlimited load (grid)

PV Array Characteristics

PV module		Inverter	
Manufacturer	Generic	Manufacturer	Generic
Model	JAM72-S20-455-MR	Model	MAX 50KTL3 LV
(Original PVsyst database)		(Original PVsyst database)	
Unit Nom. Power	455 Wp	Unit Nom. Power	50.0 kWac
Number of PV modules	240 units	Number of inverters	2 units
Nominal (STC)	109 kWp	Total power	100 kWac
Modules	12 Strings x 20 In series	Operating voltage	200-1000 V
At operating cond. (50°C)		Pnom ratio (DC:AC)	1.09
Pmpp	100 kWp	Power sharing within this inverter	
U mpp	765 V		
I mpp	131 A		
Total PV power		Total inverter power	
Nominal (STC)	109 kWp	Total power	100 kWac
Total	240 modules	Number of inverters	2 units
Module area	533 m ²	Pnom ratio	1.09

Array losses

Array Soiling Losses											
Average loss Fraction	22.3 %										
Jan.	Feb.	Mar.	Apr.	May	June	July	Aug.	Sep.	Oct.	Nov.	Dec.
60.0%	75.0%	45.0%	8.0%	2.0%	2.0%	2.0%	2.0%	2.0%	2.0%	15.0%	53.0%
Thermal Loss factor		DC wiring losses		Series Diode Loss							
Module temperature according to irradiance		Global array res.		Voltage drop							
Uc (const)	27.0 W/m ² K	97 mΩ		0.7 V							
Uv (wind)	0.0 W/m ² K/m/s	Loss Fraction		Loss Fraction							
		1.5 % at STC		0.1 % at STC							
LID - Light Induced Degradation		Module Quality Loss		Module mismatch losses							
Loss Fraction		Loss Fraction		Loss Fraction							
2.0 %		-0.8 %		2.0 % at MPP							
Strings Mismatch loss											
Loss Fraction											
0.2 %											
IAM loss factor											
Incidence effect (IAM): User defined profile											
0°	30°	50°	65°	70°	75°	80°	85°	90°			
1.000	1.000	0.992	0.943	0.898	0.813	0.677	0.426	0.000			

Figure E.21: PVsyst report main building page 3/9.



PVsyst V7.3.4
VCC, Simulation date:
10/06/23 20:08
with v7.3.4

Project: Skjetlein_scenario1

Variant: Flatt_tak

Ingrid Brøndbo (Norway)

System losses

Unavailability of the system

Time fraction	2.0 %
	7.3 days,
	0 periods

10/06/23

PVsyst Student License for Ingrid Brøndbo (Norway)

Page 4/11

Figure E.22: PVsyst report main building page 4/9.



PVsyst V7.3.4
 VCC, Simulation date:
 10/06/23 20:08
 with v7.3.4

Project: Skjetlein_scenario1

Variant: Flatt_tak

Ingrid Brøndbo (Norway)

Horizon definition

Horizon from Meteornorm web service, lat=63,3426, lon=10,301

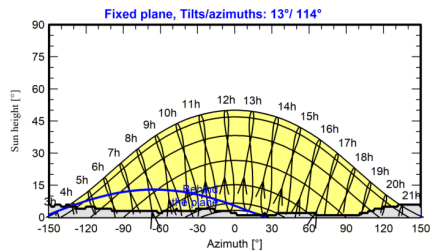
Average Height 3.5 ° Albedo Factor 0.84
 Diffuse Factor 0.99 Albedo Fraction 100 %

Horizon profile

Azimuth [°]	-180	-149	-148	-146	-145	-141	-140	-137	-136	-134	-133	-128	-127	-121
Height [°]	6.0	6.0	5.0	5.0	6.0	6.0	5.0	5.0	6.0	6.0	5.0	5.0	4.0	4.0
Azimuth [°]	-120	-113	-112	-100	-99	-63	-62	-59	-58	-48	-47	-46	-32	-31
Height [°]	5.0	5.0	4.0	4.0	3.0	3.0	2.0	2.0	3.0	3.0	4.0	3.0	3.0	4.0
Azimuth [°]	-17	-16	-4	-3	1	2	23	24	25	33	34	65	66	100
Height [°]	4.0	3.0	3.0	2.0	2.0	1.0	1.0	2.0	1.0	1.0	2.0	2.0	1.0	1.0
Azimuth [°]	101	107	108	112	113	119	120	131	132	149	150	175	176	179
Height [°]	2.0	2.0	3.0	3.0	4.0	4.0	5.0	5.0	6.0	6.0	5.0	5.0	6.0	6.0

Sun Paths (Height / Azimuth diagram)

Orientation #1



Orientation #2

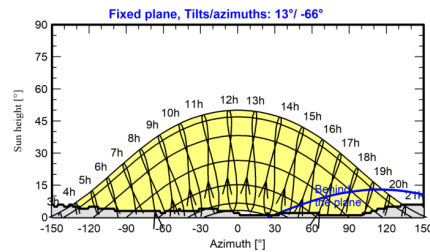


Figure E.23: PVsyst report main building page 5/9.



PVsyst V7.3.4
VCC, Simulation date:
10/06/23 20:08
with v7.3.4

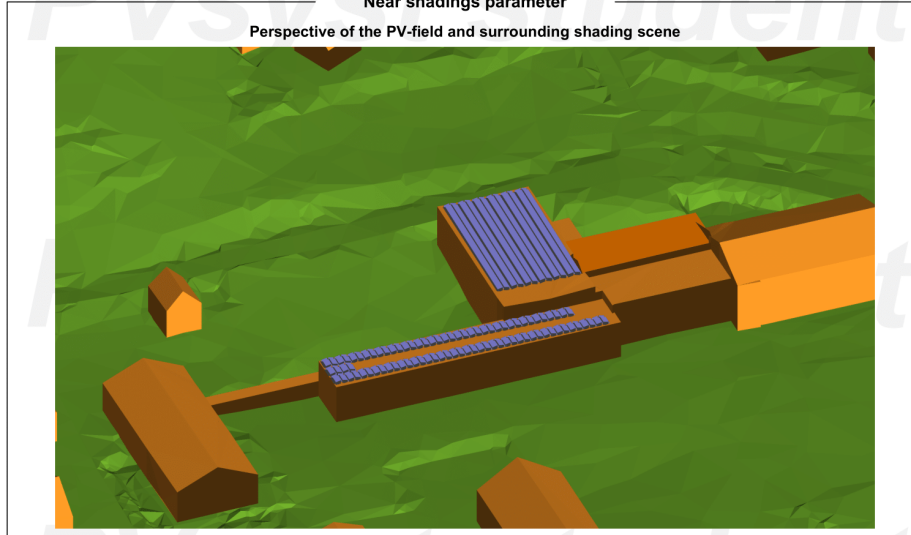
Project: Skjetlein_scenario1

Variant: Flatt_tak

Ingrid Brøndbo (Norway)

Near shadings parameter

Perspective of the PV-field and surrounding shading scene



10/06/23

PVsyst Student License for Ingrid Brøndbo (Norway)

Page 6/11

Figure E.24: PVsyst report main building page 6/9.

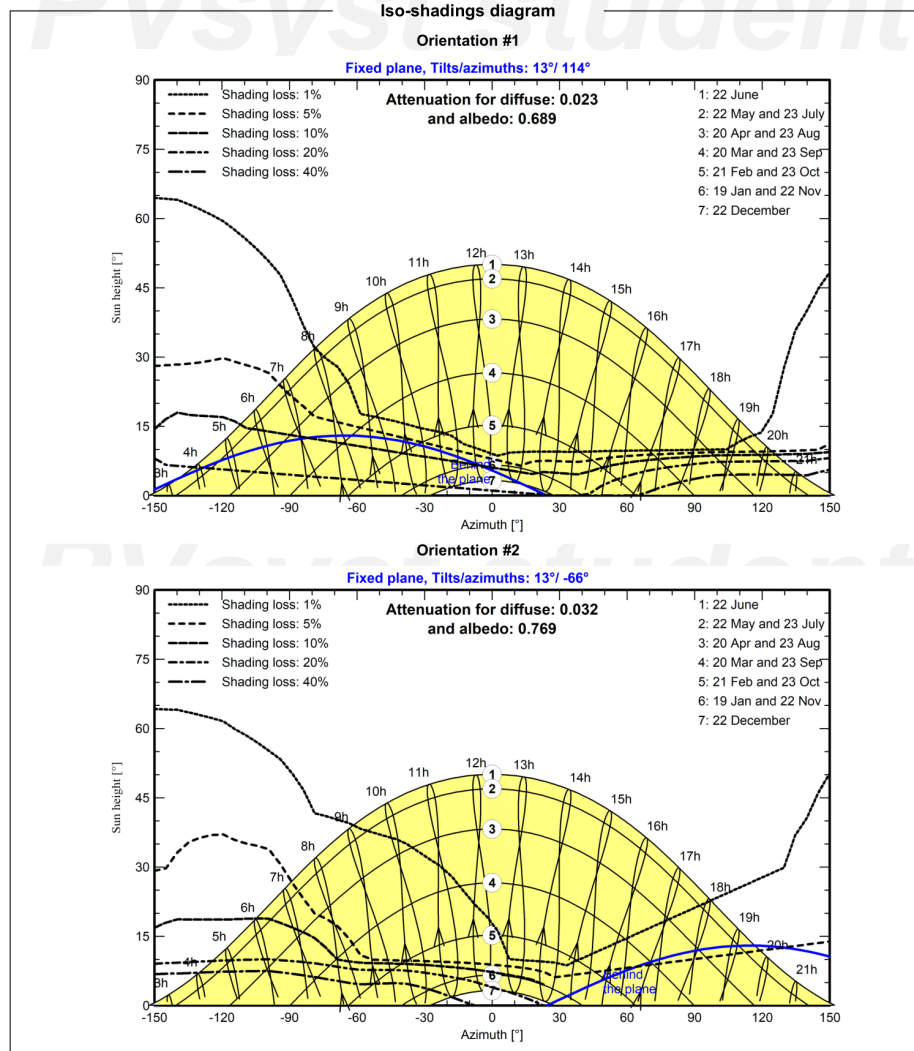


PVsyst V7.3.4
VOC, Simulation date:
10/06/23 20:08
with v7.3.4

Project: Skjetlein_scenario1

Variante: Flatt_tak

Ingrid Brøndbo (Norway)



10/06/23

PVsyst Student License for Ingrid Brøndbo (Norway)

Page 7/11

Figure E.25: PVsyst report main building page 7/9.



Main results

System Production

Produced Energy 75190 kWh/year

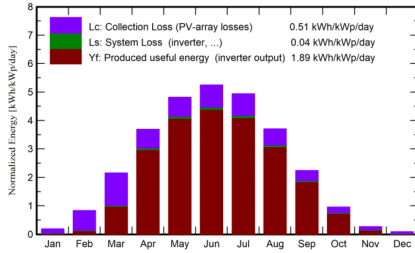
Specific production

689 kWh/kWp/year

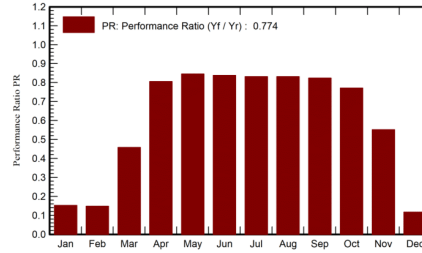
Perf. Ratio PR

77.40 %

Normalized productions (per installed kWp)



Performance Ratio PR



Balances and main results

	GlobHor kWh/m ²	DiffHor kWh/m ²	T_Amb °C	GlobInc kWh/m ²	GlobEff kWh/m ²	EArray kWh	E_Grid kWh	PR ratio
January	5.8	3.90	-1.06	5.9	1.8	155	98	0.152
February	22.9	11.74	-0.97	23.4	4.8	454	377	0.148
March	67.0	25.70	0.92	66.9	33.3	3469	3351	0.458
April	111.6	44.99	5.22	110.8	95.3	9931	9753	0.806
May	151.1	64.36	9.43	149.4	138.1	14044	13800	0.846
June	159.5	72.78	12.22	157.4	145.3	14670	14410	0.838
July	154.8	79.90	15.61	153.1	141.4	14146	13895	0.831
August	116.1	57.06	14.94	115.0	105.8	10635	10438	0.831
September	67.8	36.75	10.95	67.3	60.6	6189	6053	0.824
October	29.6	16.65	6.26	29.6	25.4	2593	2494	0.771
November	8.1	5.66	2.26	8.1	5.6	545	485	0.551
December	2.7	2.05	-0.24	2.8	0.9	74	35	0.117
Year	896.9	421.55	6.34	889.6	758.2	76906	75190	0.774

Legends

- GlobHor Global horizontal irradiation
- DiffHor Horizontal diffuse irradiation
- T_Amb Ambient Temperature
- GlobInc Global incident in coll. plane
- GlobEff Effective Global, corr. for IAM and shadings
- EArray Effective energy at the output of the array
- E_Grid Energy injected into grid
- PR Performance Ratio

Figure E.26: PVsyst report main building page 8/9.



PVsyst V7.3.4
VCC, Simulation date:
10/06/23 20:08
with v7.3.4

Project: Skjetlein_scenario1

Variant: Flatt_tak

Ingrid Brøndbo (Norway)

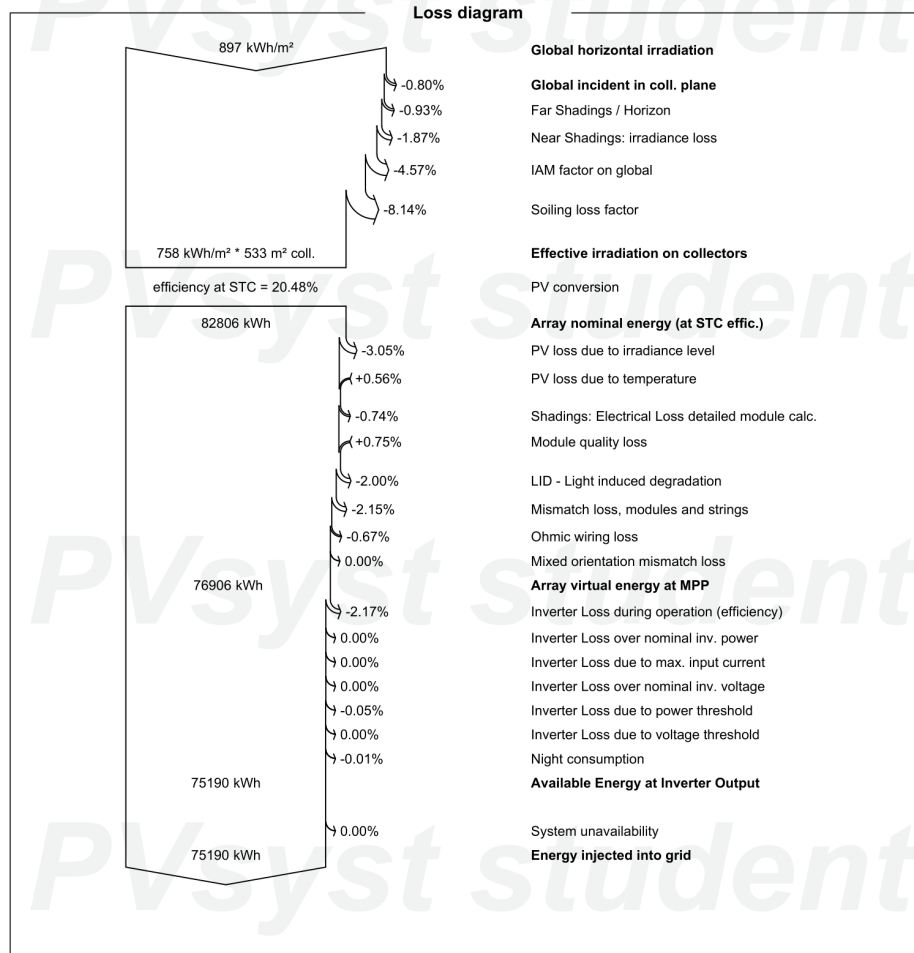


Figure E.27: PVsyst report main building page 9/9.

Appendix E - PVSyst Reports from APV Scenarios

E1 - PVSyst Report APV North E/W



Version 7.3.4

PVsyst - Simulation report

Grid-Connected System

Project: Skjetlein_scenario1

Variant: North_scenario_terrain_east-west

Ground system (tables) on a hill

System power: 711 kWp

Nypan - Norway

Author
Ingrid Brøndbo (Norway)

Figure F.1: PVSyst report APV North E/W page 1/10.



PVsyst V7.3.4

VCF, Simulation date:
11/06/23 11:01
with v7.3.4

Project: Skjetlein_scenario1
Variant: North_scenario_terrain_east-west

Ingrid Brøndbo (Norway)

Project summary

Geographical Site		Situation		Meteo data								
Nypan		Latitude 63.34 °N		Nypan								
Norway		Longitude 10.30 °E		Meteonorm 8.1 (1991-2013) - Synthetic								
		Altitude 58 m										
		Time zone UTC+1										
Monthly albedo values												
	Jan.	Feb.	Mar.	Apr.	May	June	July	Aug.	Sep.	Oct.	Nov.	Dec.
Albedo	0.70	0.70	0.40	0.20	0.20	0.20	0.20	0.20	0.20	0.20	0.40	0.70

System summary

Grid-Connected System		Ground system (tables) on a hill		User's needs	
PV Field Orientation		Near Shadings		Unlimited load (grid)	
Fixed plane		According to strings			
Tilt/Azimuth 90 / -90.2 °		Electrical effect 100 %			
System information					
PV Array					
Nb. of modules		1530 units		Inverters	
Pnom total		711 kWp		Nb. of units 6 units	
				Pnom total 600 kWac	
				Pnom ratio 1.186	

Results summary

Produced Energy	545652 kWh/year	Specific production	767 kWh/kWp/year	Perf. Ratio PR	112.39 %
-----------------	-----------------	---------------------	------------------	----------------	----------

Table of contents

Project and results summary	2
General parameters, PV Array Characteristics, System losses	3
Horizon definition	5
Near shading definition - Iso-shadings diagram	6
Main results	8
Loss diagram	9
Predef. graphs	10
Single-line diagram	11

Figure F.2: PVsyst report APV North E/W page 2/10.



PVsyst V7.3.4

VCF, Simulation date:
11/06/23 11:01
with v7.3.4

Project: Skjetlein_scenario1
Variant: North_scenario_terrain_east-west

Ingrid Brøndbo (Norway)

General parameters

Grid-Connected System		Ground system (tables) on a hill										
PV Field Orientation		Sheds configuration										
Orientation		Nb. of sheds	780 units									
Fixed plane		Sizes										
Tilt/Azimuth	90 / -90.2 °	Sheds spacing	13.0 m									
		Collector width	2.10 m									
		Ground Cov. Ratio (GCR)	16.2 %									
		Shading limit angle										
		Limit profile angle	9.2 °									
Horizon		Near Shadings										
Average Height	3.5 °	According to strings										
		Electrical effect	100 %									
Bifacial system		User's needs										
Model	2D Calculation unlimited sheds	Unlimited load (grid)										
Bifacial model geometry		Bifacial model definitions										
Sheds spacing	12.96 m	Ground albedo average	0.36									
Sheds width	2.14 m	Bifaciality factor	90 %									
Limit profile angle	9.2 °	Rear shading factor	5.0 %									
GCR	16.5 %	Rear mismatch loss	10.0 %									
Height above ground	0.80 m	Shed transparent fraction	0.0 %									
Monthly ground albedo values												
Jan.	Feb.	Mar.	Apr.	May	June	July	Aug.	Sep.	Oct.	Nov.	Dec.	Year
0.70	0.70	0.40	0.20	0.20	0.20	0.20	0.20	0.20	0.20	0.40	0.70	0.36

PV Array Characteristics

PV module		Inverter	
Manufacturer	Generic	Manufacturer	Generic
Model	SK8612HDGDC-465	Model	SUN2000-100KTL-INM0-415Vac
(Original PVsyst database)		(Original PVsyst database)	
Unit Nom. Power	465 Wp	Unit Nom. Power	100 kWac
Number of PV modules	1530 units	Number of inverters	6 units
Nominal (STC)	711 kWp	Total power	600 kWac
Modules	102 Strings x 15 In series	Operating voltage	200-1000 V
At operating cond. (50°C)		Max. power (=>35°C)	110 kWac
Pmpp	670 kWp	Pnom ratio (DC:AC)	1.19
U mpp	626 V	Power sharing within this inverter	
I mpp	1070 A		
Total PV power		Total inverter power	
Nominal (STC)	711 kWp	Total power	600 kWac
Total	1530 modules	Max. power	660 kWac
Module area	3326 m²	Number of inverters	6 units
		Pnom ratio	1.19

Figure F.3: PVSyst report APV North E/W page 3/10.



PVsyst V7.3.4

VCF, Simulation date:
11/06/23 11:01
with v7.3.4

Project: Skjetlein_scenario1
Variant: North_scenario_terrain_east-west

Ingrid Brøndbo (Norway)

Array losses

Array Soiling Losses

Average loss Fraction 2.3 %

Jan.	Feb.	Mar.	Apr.	May	June	July	Aug.	Sep.	Oct.	Nov.	Dec.
2.0%	3.0%	3.0%	3.0%	3.0%	2.0%	2.0%	2.0%	2.0%	2.0%	2.0%	2.0%

Thermal Loss factor

Module temperature according to irradiance
Uc (const) 29.0 W/m²K
Uv (wind) 0.0 W/m²K/m/s

DC wiring losses

Global array res. 9.4 mΩ
Loss Fraction 1.5 % at STC

Serie Diode Loss

Voltage drop 0.7 V
Loss Fraction 0.1 % at STC

LID - Light Induced Degradation

Loss Fraction 2.0 %

Module Quality Loss

Loss Fraction -0.3 %

Module mismatch losses

Loss Fraction 2.0 % at MPP

Strings Mismatch loss

Loss Fraction 0.2 %

IAM loss factor

Incidence effect (IAM): Fresnel, AR coating, n(glass)=1.526, n(AR)=1.290

0°	30°	50°	60°	70°	75°	80°	85°	90°
1.000	0.999	0.987	0.962	0.892	0.816	0.681	0.440	0.000

System losses

Unavailability of the system

Time fraction 0.5 %
1.8 days,
3 periods

Figure F.4: PVsyst report APV North E/W page 4/10.



Horizon definition

Horizon from Meteornorm web service, lat=63,3426, lon=10,301

Average Height	3.5 °	Albedo Factor	0.81
Diffuse Factor	0.91	Albedo Fraction	100 %

Horizon profile

Azimuth [°]	-180	-149	-148	-146	-145	-141	-140	-137	-136	-134	-133	-128	-127	-121
Height [°]	6.0	6.0	5.0	5.0	6.0	6.0	5.0	5.0	6.0	6.0	5.0	5.0	4.0	4.0
Azimuth [°]	-120	-113	-112	-100	-99	-63	-62	-59	-58	-48	-47	-46	-32	-31
Height [°]	5.0	5.0	4.0	4.0	3.0	3.0	2.0	2.0	3.0	3.0	4.0	3.0	3.0	4.0
Azimuth [°]	-17	-16	-4	-3	1	2	23	24	25	33	34	65	66	100
Height [°]	4.0	3.0	3.0	2.0	2.0	1.0	1.0	2.0	1.0	1.0	2.0	2.0	1.0	1.0
Azimuth [°]	101	107	108	112	113	119	120	131	132	149	150	175	176	179
Height [°]	2.0	2.0	3.0	3.0	4.0	4.0	5.0	5.0	6.0	6.0	5.0	5.0	6.0	6.0

Sun Paths (Height / Azimuth diagram)

Fixed plane, Tilts/azimuths: 90° / -90°

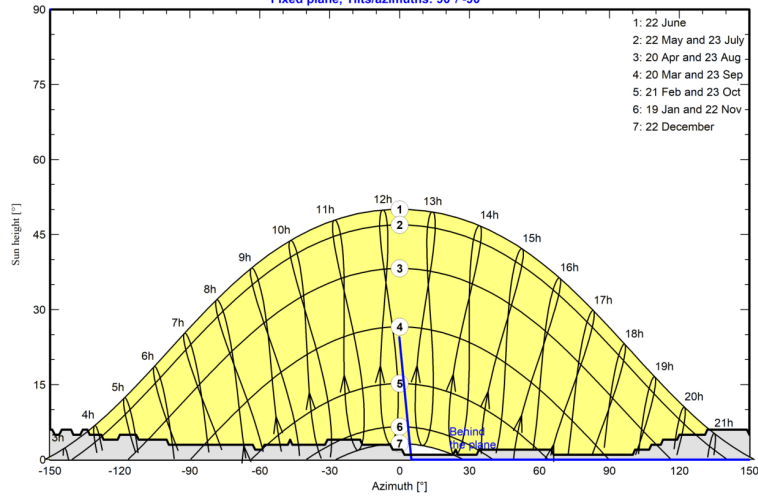
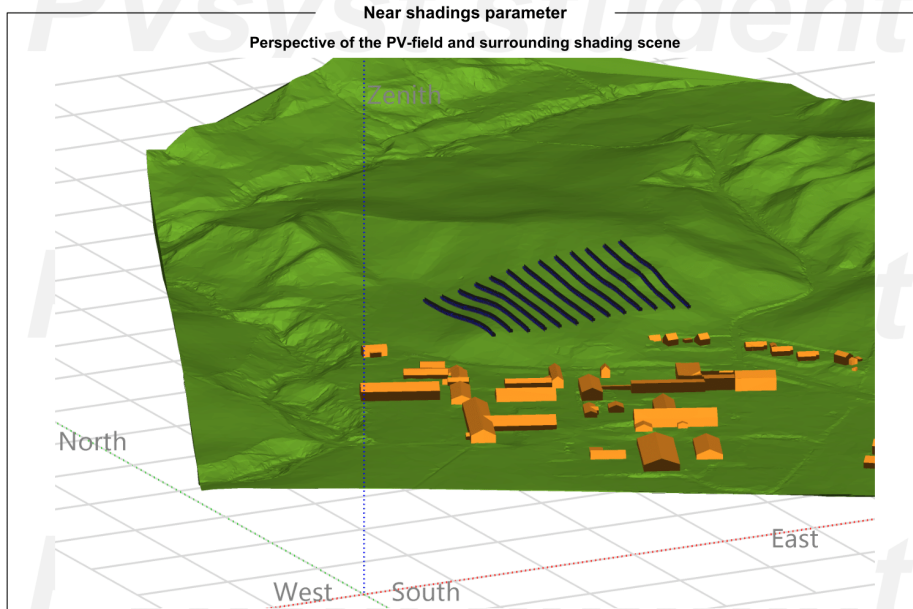


Figure F.5: PVsyst report APV North E/W page 5/10.



PVsyst V7.3.4
VCF, Simulation date:
11/06/23 11:01
with v7.3.4

Project: Skjetlein_scenario1
Variant: North_scenario_terrain_east-west
Ingrid Brøndbo (Norway)



11/06/23

PVsyst Student License for Ingrid Brøndbo (Norway)

Page 6/11

Figure F.6: PVSyst report APV North E/W page 6/10.



PVsyst V7.3.4
VCF, Simulation date:
11/06/23 11:01
with v7.3.4

Project: Skjetlein_scenario1
Variant: North_scenario_terrain_east-west
Ingrid Brøndbo (Norway)

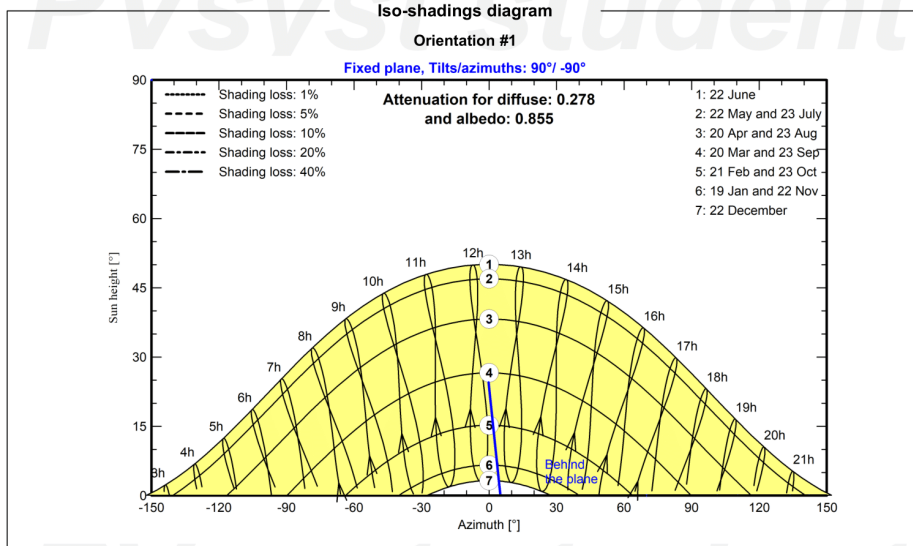


Figure F.7: PVsyst report APV North E/W page 7/10.



PVsyst V7.3.4

VCF, Simulation date:
 11/06/23 11:01
 with v7.3.4

Ingrid Brøndbo (Norway)

Main results

System Production

Produced Energy 545652 kWh/year

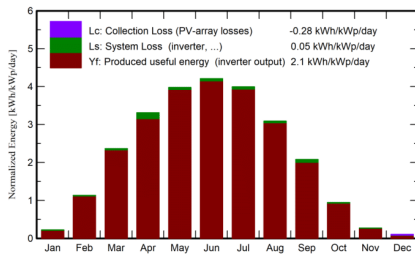
Specific production

767 kWh/kWp/year

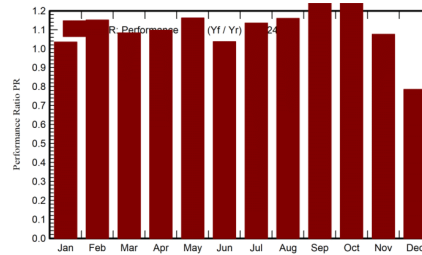
Perf. Ratio PR

112.39 %

Normalized productions (per installed kWp)



Performance Ratio PR



Balances and main results

	GlobHor kWh/m ²	DiffHor kWh/m ²	T_Amb °C	GlobInc kWh/m ²	GlobEff kWh/m ²	EArray kWh	E_Grid kWh	PR ratio
January	5.8	3.90	-1.06	6.3	3.67	4923	4669	1.035
February	22.9	11.74	-0.97	27.2	17.68	22562	22233	1.151
March	67.0	25.70	0.92	66.7	46.41	52153	51408	1.084
April	111.6	44.99	5.22	86.3	59.94	70735	67375	1.097
May	151.1	64.36	9.43	104.7	72.97	87827	86565	1.162
June	159.5	72.78	12.22	120.0	85.84	89911	88614	1.038
July	154.8	79.90	15.61	107.5	76.11	88100	86838	1.136
August	116.1	57.06	14.94	81.5	56.78	68214	67238	1.159
September	67.8	36.75	10.95	48.5	33.17	44452	42782	1.240
October	29.6	16.65	6.26	23.1	14.85	20839	20493	1.245
November	8.1	5.66	2.26	7.4	4.46	5803	5658	1.076
December	2.7	2.05	-0.24	3.2	1.42	1856	1779	0.785
Year	896.9	421.55	6.34	682.4	473.31	557375	545652	1.124

Legends

GlobHor Global horizontal irradiation
 DiffHor Horizontal diffuse irradiation
 T_Amb Ambient Temperature
 GlobInc Global incident in coll. plane
 GlobEff Effective Global, corr. for IAM and shadings

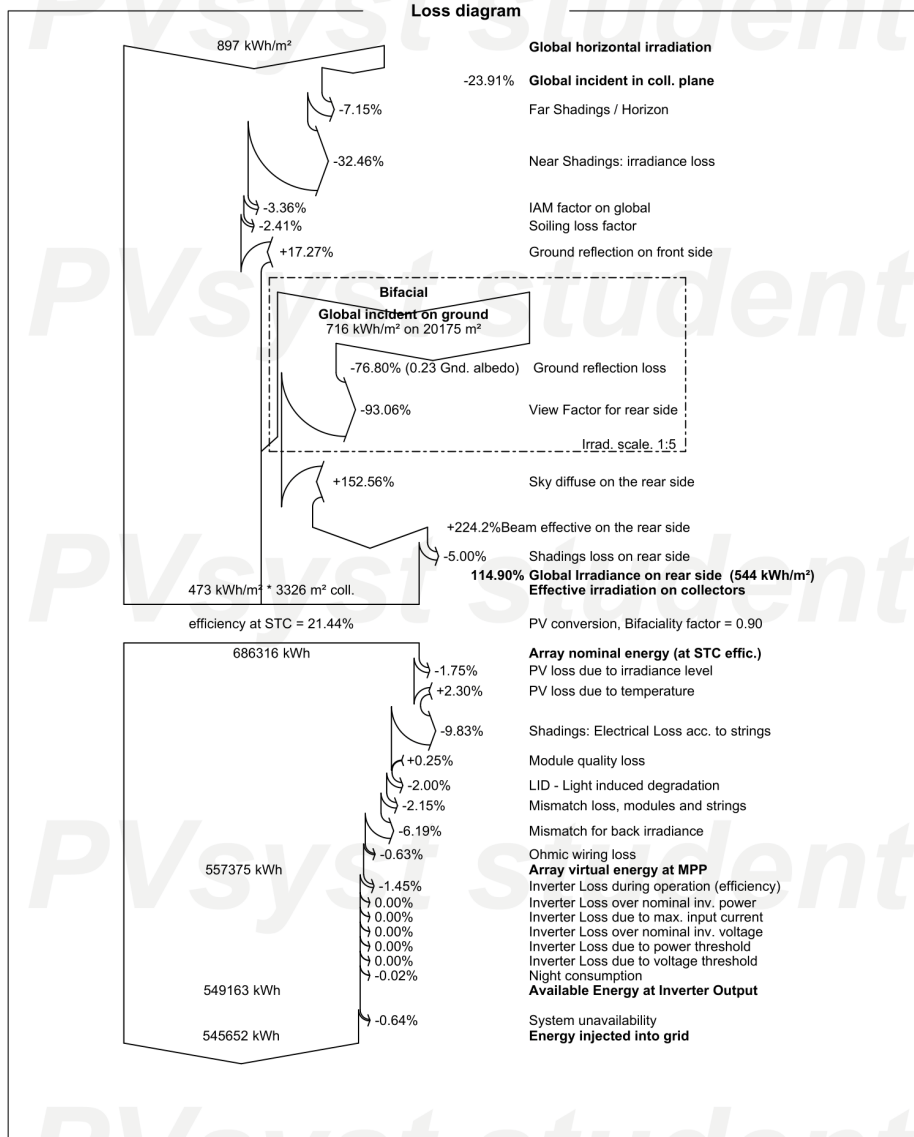
EArray Effective energy at the output of the array
 E_Grid Energy injected into grid
 PR Performance Ratio

Figure F.8: PVsyst report APV North E/W page 8/10.



PVsyst V7.3.4
VCF, Simulation date:
11/06/23 11:01
with v7.3.4

Project: Skjetlein_scenario1
Variant: North_scenario_terrain_east-west
Ingrid Brøndbo (Norway)



11/06/23

PVsyst Student License for Ingrid Brøndbo (Norway)

Page 9/11

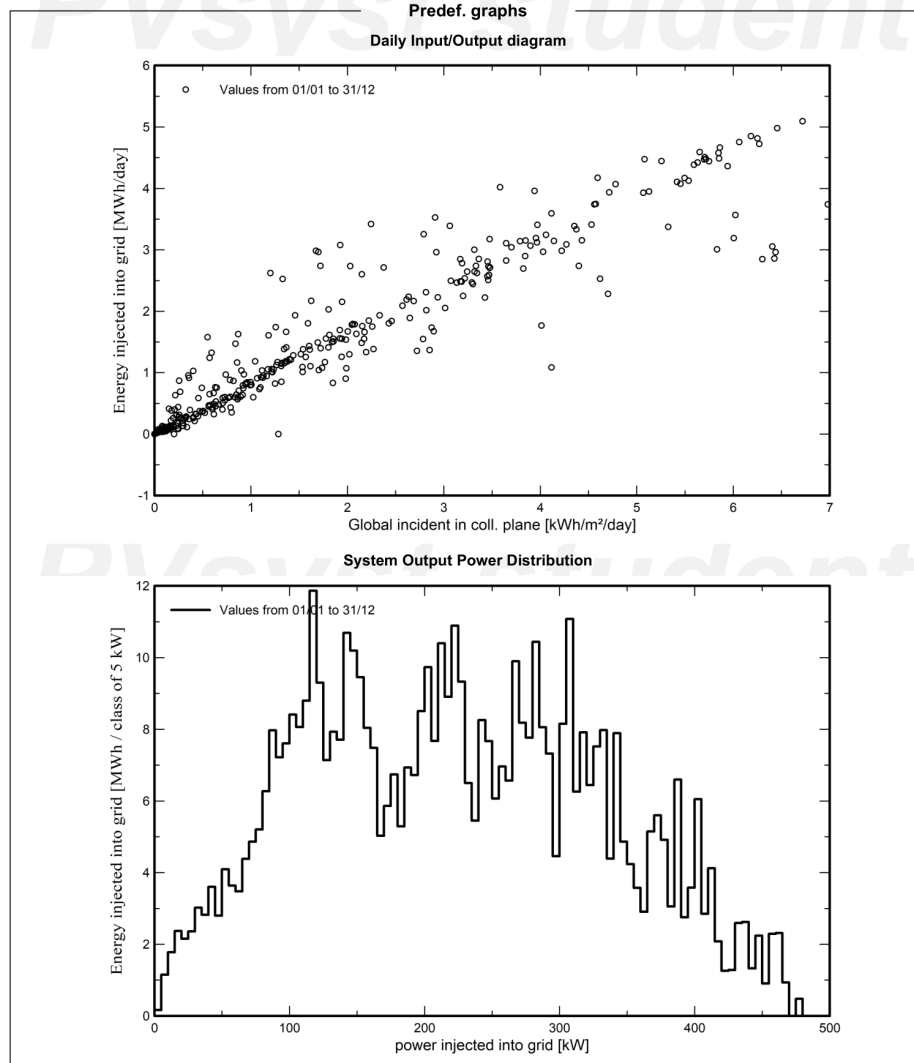
Figure F.9: PVsyst report APV North E/W page 9/10.



PVsyst V7.3.4
VCF, Simulation date:
11/06/23 11:01
with v7.3.4

Project: Skjetlein_scenario1
Variant: North_scenario_terrain_east-west

Ingrid Brøndbo (Norway)



11/06/23

PVsyst Student License for Ingrid Brøndbo (Norway)

Page 10/11

Figure F.10: PVsyst report APV North E/W page 10/10.



Version 7.3.4

PVsyst - Simulation report

Grid-Connected System

Project: Skjetlein_scenario1

Variant: North_scenario_terrain_south-north

Ground system (tables) on a hill

System power: 711 kWp

Nypan - Norway

Author
Ingrid Brøndbo (Norway)

Figure F.11: PVSyst report APV North S/N page 1/10.



PVsyst V7.3.4

VCG, Simulation date:
11/06/23 11:11
with v7.3.4

Project: Skjetlein_scenario1
Variant: North_scenario_terrain_south-north

Ingrid Brøndbo (Norway)

Project summary

Geographical Site	Situation	Meteo data
Nypan	Latitude 63.34 °N	Nypan
Norway	Longitude 10.30 °E	Meteonorm 8.1 (1991-2013) - Synthetic
	Altitude 58 m	
	Time zone UTC+1	

Monthly albedo values

	Jan.	Feb.	Mar.	Apr.	May	June	July	Aug.	Sep.	Oct.	Nov.	Dec.
Albedo	0.70	0.70	0.40	0.20	0.20	0.20	0.20	0.20	0.20	0.20	0.40	0.70

System summary

Grid-Connected System	Ground system (tables) on a hill	User's needs
PV Field Orientation	Near Shadings	Unlimited load (grid)
Fixed plane	According to strings	
Tilt/Azimuth 90 / 0 °	Electrical effect 100 %	

System information		Inverters	
PV Array		Nb. of units	6 units
Nb. of modules	1530 units	Pnom total	600 kWac
Pnom total	711 kWp	Pnom ratio	1.186

Results summary

Produced Energy	769502 kWh/year	Specific production	1082 kWh/kWp/year	Perf. Ratio PR	112.44 %
-----------------	-----------------	---------------------	-------------------	----------------	----------

Table of contents

Project and results summary	2
General parameters, PV Array Characteristics, System losses	3
Horizon definition	5
Near shading definition - Iso-shadings diagram	6
Main results	8
Loss diagram	9
Predef. graphs	10
Single-line diagram	11

Figure F.12: PVsyst report APV North S/N page 2/10.



PVsyst V7.3.4

VCG, Simulation date:
11/06/23 11:11
with v7.3.4

Project: Skjetlein_scenario1
Variant: North_scenario_terrain_south-north

Ingrid Brøndbo (Norway)

General parameters

Grid-Connected System		Ground system (tables) on a hill	
PV Field Orientation		Sheds configuration	
Orientation		Nb. of sheds	715 units
Fixed plane		Sizes	
Tilt/Azimuth	90 / 0 °	Sheds spacing	13.1 m
		Collector width	2.10 m
		Ground Cov. Ratio (GCR)	16.0 %
		Shading limit angle	
		Limit profile angle	9.1 °
Horizon		Near Shadings	
Average Height	3.5 °	According to strings	
		Electrical effect	100 %
		User's needs	
		Unlimited load (grid)	
Bifacial system			
Model	2D Calculation unlimited sheds		
Bifacial model geometry		Bifacial model definitions	
Sheds spacing	13.07 m	Ground albedo	0.25
Sheds width	2.14 m	Bifaciality factor	90 %
Limit profile angle	9.1 °	Rear shading factor	5.0 %
GCR	16.3 %	Rear mismatch loss	10.0 %
Height above ground	1.50 m	Shed transparent fraction	0.0 %

PV Array Characteristics

PV module		Inverter	
Manufacturer	Generic	Manufacturer	Generic
Model	SK8612HDGDC-465	Model	SUN2000-100KTL-INM0-415Vac
(Original PVsyst database)		(Original PVsyst database)	
Unit Nom. Power	465 Wp	Unit Nom. Power	100 kWac
Number of PV modules	1530 units	Number of inverters	6 units
Nominal (STC)	711 kWp	Total power	600 kWac
Modules	85 Strings x 18 In series	Operating voltage	200-1000 V
At operating cond. (50°C)		Max. power (=>35°C)	110 kWac
Pmpp	670 kWp	Pnom ratio (DC:AC)	1.19
U mpp	751 V	Power sharing within this inverter	
I mpp	892 A		
Total PV power		Total inverter power	
Nominal (STC)	711 kWp	Total power	600 kWac
Total	1530 modules	Max. power	660 kWac
Module area	3326 m²	Number of inverters	6 units
		Pnom ratio	1.19

Array losses

Array Soiling Losses	
Average loss Fraction	2.3 %
Jan.	2.0%
Feb.	3.0%
Mar.	3.0%
Apr.	3.0%
May	3.0%
June	2.0%
July	2.0%
Aug.	2.0%
Sep.	2.0%
Oct.	2.0%
Nov.	2.0%
Dec.	2.0%

Figure F.13: PVsyst report APV North S/N page 3/10.



PVsyst V7.3.4

VCG, Simulation date:
11/06/23 11:11
with v7.3.4

Project: Skjetlein_scenario1
Variant: North_scenario_terrain_south-north

Ingrid Brøndbo (Norway)

Array losses

Thermal Loss factor		DC wiring losses		Series Diode Loss				
Module temperature according to irradiance		Global array res.	14 mΩ	Voltage drop	0.7 V			
Uc (const)	29.0 W/m²K	Loss Fraction	1.5 % at STC	Loss Fraction	0.1 % at STC			
Uv (wind)	0.0 W/m²K/m/s							
LID - Light Induced Degradation		Module Quality Loss		Module mismatch losses				
Loss Fraction	2.0 %	Loss Fraction	-0.3 %	Loss Fraction	2.0 % at MPP			
Strings Mismatch loss								
Loss Fraction	0.1 %							
IAM loss factor								
Incidence effect (IAM): Fresnel, AR coating, n(glass)=1.526, n(AR)=1.290								
0°	30°	50°	60°	70°	75°	80°	85°	90°
1.000	0.999	0.987	0.962	0.892	0.816	0.681	0.440	0.000

System losses

Unavailability of the system	
Time fraction	0.5 %
	1.8 days,
	3 periods

Figure F.14: PVsyst report APV North S/N page 4/10.



PVsyst V7.3.4

VCG, Simulation date:
11/06/23 11:11
with v7.3.4

Project: Skjetlein_scenario1
Variant: North_scenario_terrain_south-north

Ingrid Brøndbo (Norway)

Horizon definition

Horizon from Meteornorm web service, lat=63,3426, lon=10,301

Average Height 3.5 ° Albedo Factor 0.89
Diffuse Factor 0.96 Albedo Fraction 100 %

Horizon profile

Azimuth [°]	-180	-149	-148	-146	-145	-141	-140	-137	-136	-134	-133	-128	-127	-121
Height [°]	6.0	6.0	5.0	5.0	6.0	6.0	5.0	5.0	6.0	6.0	5.0	5.0	4.0	4.0
Azimuth [°]	-120	-113	-112	-100	-99	-63	-62	-59	-58	-48	-47	-46	-32	-31
Height [°]	5.0	5.0	4.0	4.0	3.0	3.0	2.0	2.0	3.0	3.0	4.0	3.0	3.0	4.0
Azimuth [°]	-17	-16	-4	-3	1	2	23	24	25	33	34	65	66	100
Height [°]	4.0	3.0	3.0	2.0	2.0	1.0	1.0	2.0	1.0	1.0	2.0	2.0	1.0	1.0
Azimuth [°]	101	107	108	112	113	119	120	131	132	149	150	175	176	179
Height [°]	2.0	2.0	3.0	3.0	4.0	4.0	5.0	5.0	6.0	6.0	5.0	5.0	6.0	6.0

Sun Paths (Height / Azimuth diagram)

Fixed plane, Tilts/azimuths: 90°/ 0°

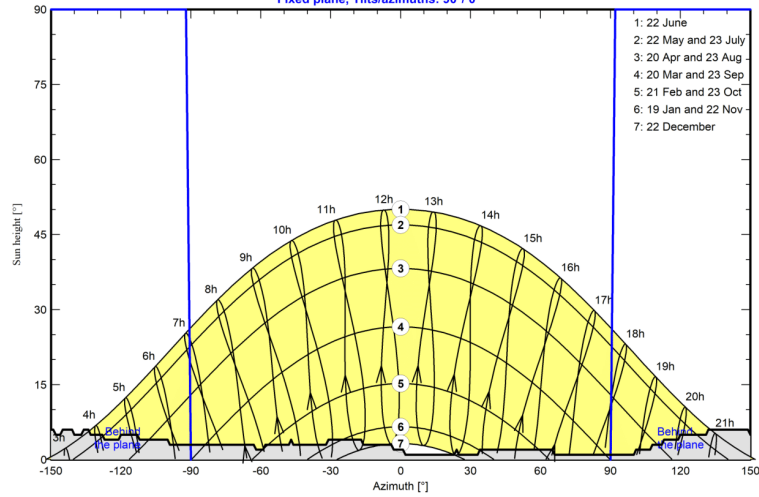


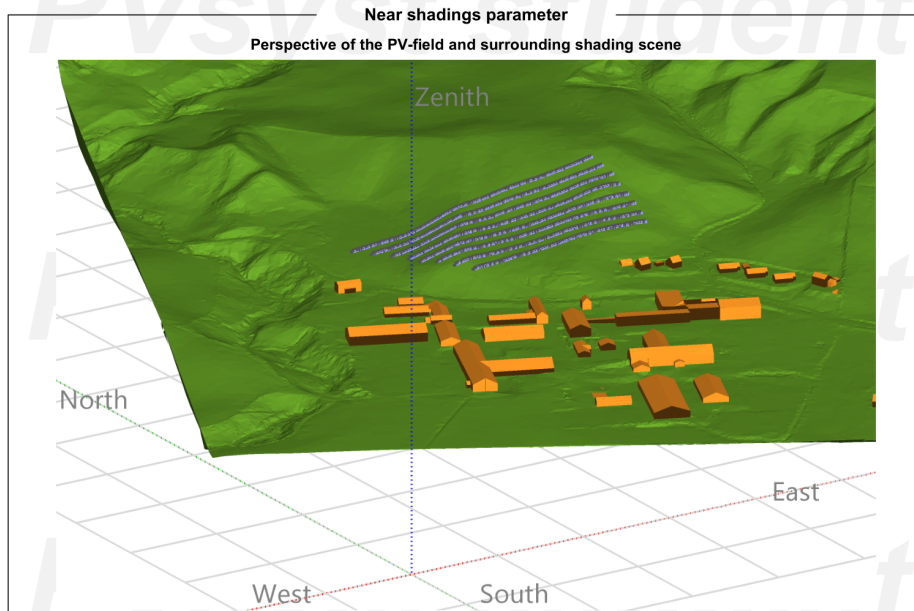
Figure F.15: PVsyst report APV North S/N page 5/10.



PVsyst V7.3.4
VCG, Simulation date:
11/06/23 11:11
with v7.3.4

Project: Skjetlein_scenario1
Variant: North_scenario_terrain_south-north

Ingrid Brøndbo (Norway)



11/06/23

PVsyst Student License for Ingrid Brøndbo (Norway)

Page 6/11

Figure F.16: PVsyst report APV North S/N page 6/10.



PVsyst V7.3.4
 VCG, Simulation date:
 11/06/23 11:11
 with v7.3.4

Project: Skjetlein_scenario1
 Variant: North_scenario_terrain_south-north
 Ingrid Brøndbo (Norway)

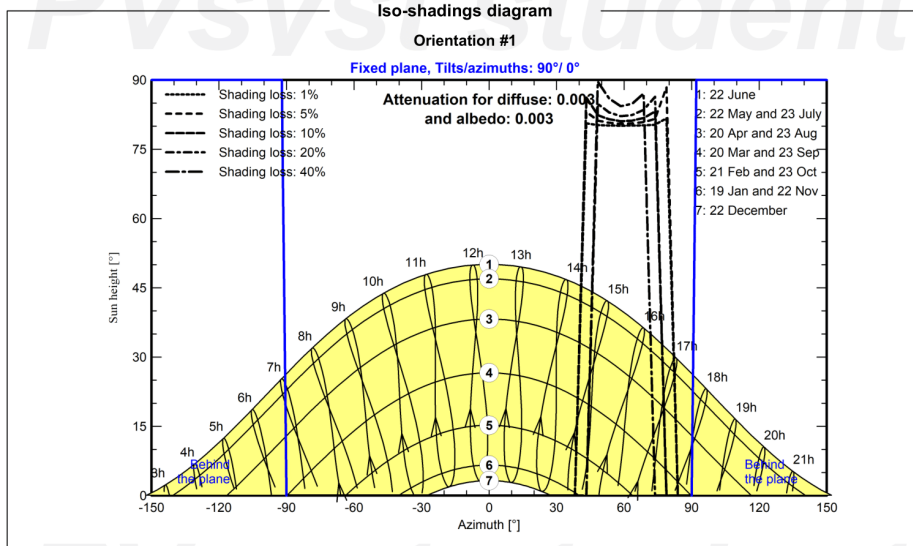


Figure F.17: PVsyst report APV North S/N page 7/10.



PVsyst V7.3.4

VCG, Simulation date:
 11/06/23 11:11
 with v7.3.4

Ingrid Brøndbo (Norway)

Main results

System Production

Produced Energy 769502 kWh/year

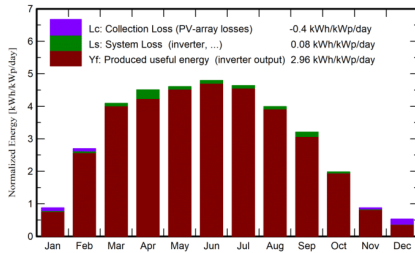
Specific production

1082 kWh/kWp/year

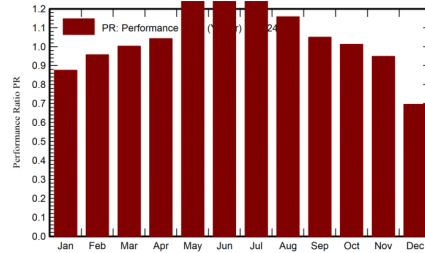
Perf. Ratio PR

112.44 %

Normalized productions (per installed kWp)



Performance Ratio PR



Balances and main results

	GlobHor kWh/m ²	DiffHor kWh/m ²	T_Amb °C	GlobInc kWh/m ²	GlobEff kWh/m ²	EArray kWh	E_Grid kWh	PR ratio
January	5.8	3.90	-1.06	27.1	24.2	17571	16914	0.876
February	22.9	11.74	-0.97	75.5	71.2	52291	51397	0.957
March	67.0	25.70	0.92	124.2	121.5	90294	88630	1.003
April	111.6	44.99	5.22	122.1	122.7	96132	90584	1.043
May	151.1	64.36	9.43	109.9	113.4	101628	99889	1.277
June	159.5	72.78	12.22	101.9	106.9	102278	100565	1.387
July	154.8	79.90	15.61	106.1	110.5	102327	100630	1.333
August	116.1	57.06	14.94	105.1	107.6	88077	86553	1.158
September	67.8	36.75	10.95	87.8	88.1	68412	65575	1.050
October	29.6	16.65	6.26	59.6	58.4	43726	42938	1.012
November	8.1	5.66	2.26	26.2	24.4	18025	17691	0.948
December	2.7	2.05	-0.24	16.4	11.4	8295	8137	0.695
Year	896.9	421.55	6.34	961.9	960.3	789055	769502	1.124

Legends

GlobHor Global horizontal irradiation
 DiffHor Horizontal diffuse irradiation
 T_Amb Ambient Temperature
 GlobInc Global incident in coll. plane
 GlobEff Effective Global, corr. for IAM and shadings

EArray Effective energy at the output of the array
 E_Grid Energy injected into grid
 PR Performance Ratio

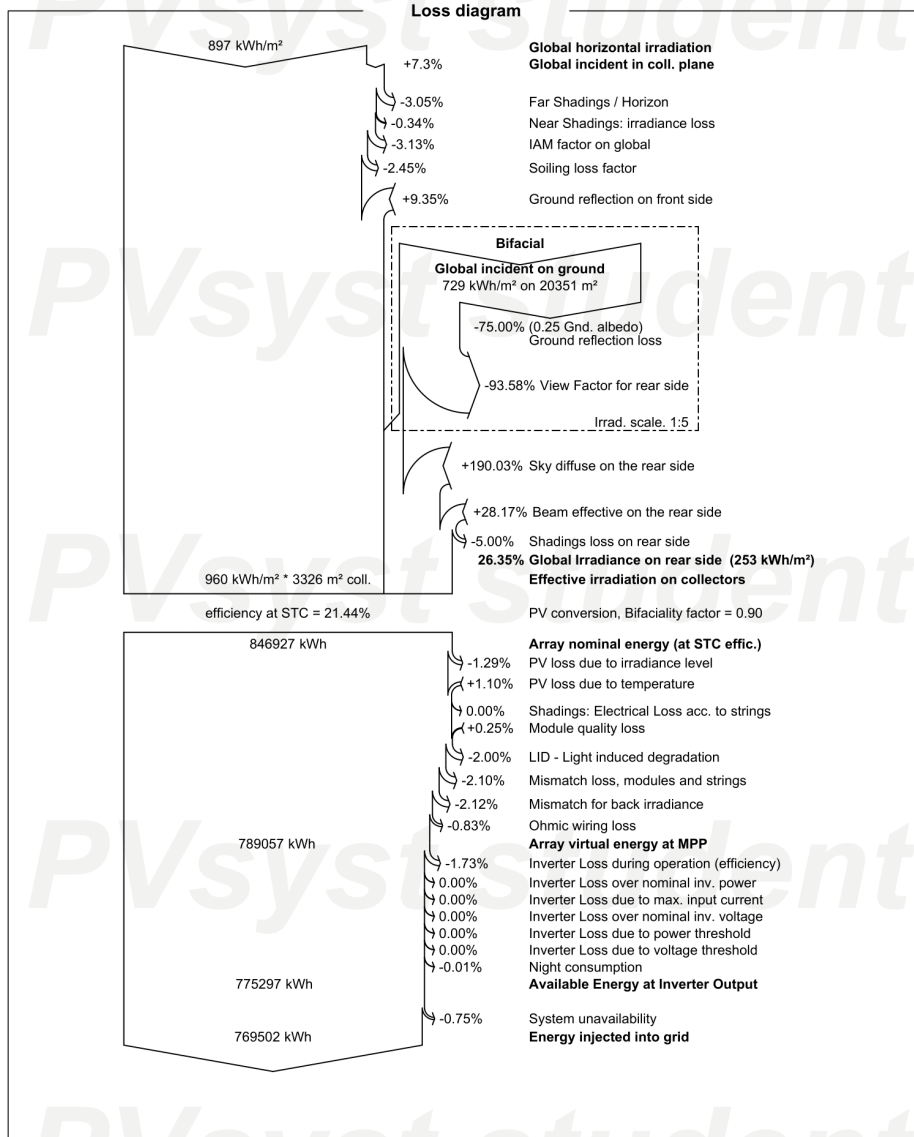
Figure F.18: PVsyst report APV North S/N page 8/10.



PVsyst V7.3.4
 VCG, Simulation date:
 11/06/23 11:11
 with v7.3.4

Project: Skjetlein_scenario1
 Variant: North_scenario_terrain_south-north

Ingrid Brøndbo (Norway)



11/06/23

PVsyst Student License for Ingrid Brøndbo (Norway)

Page 9/11

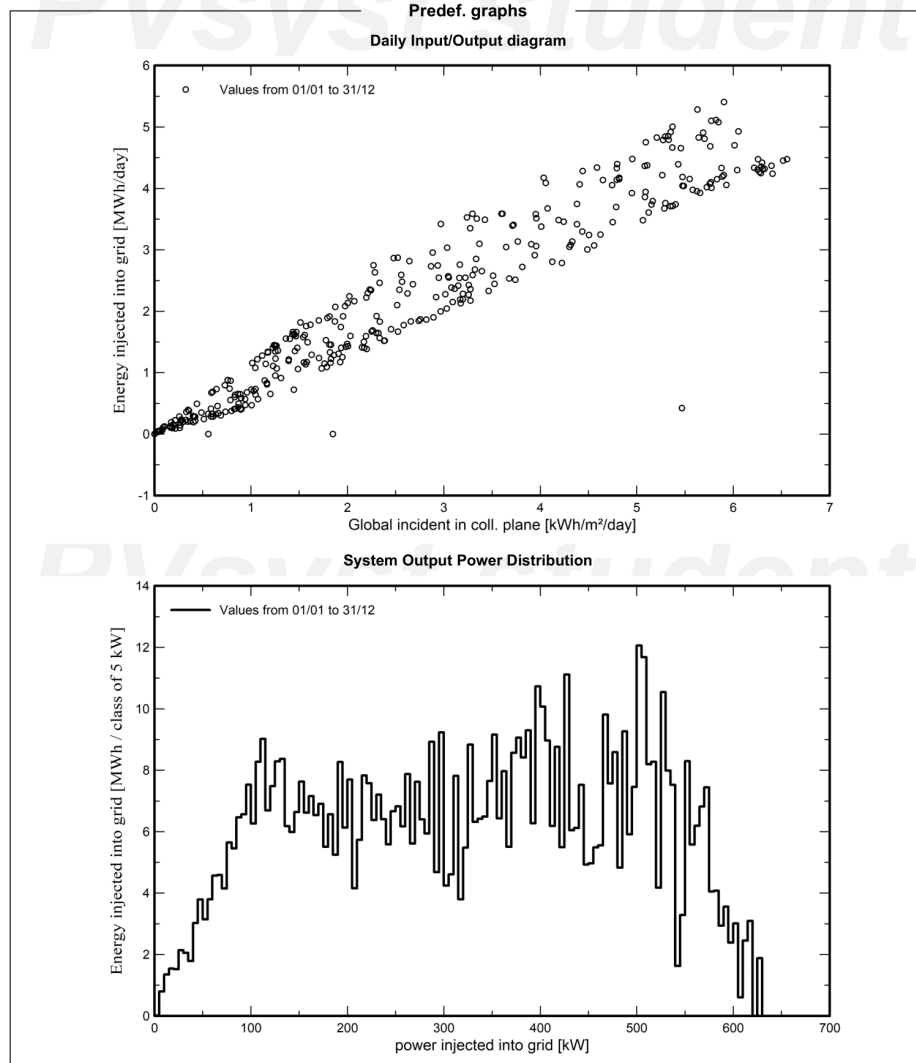
Figure F.19: PVsyst report APV North S/N page 9/10.



PVsyst V7.3.4
VCG, Simulation date:
11/06/23 11:11
with v7.3.4

Project: Skjetlein_scenario1
Variant: North_scenario_terrain_south-north

Ingrid Brøndbo (Norway)



11/06/23

PVsyst Student License for Ingrid Brøndbo (Norway)

Page 10/11

Figure F.20: PVsyst report APV North S/N page 10/10.



Version 7.3.4

PVsyst - Simulation report

Grid-Connected System

Project: Skjetlein_scenario1

Variant: South_scenario_terrain_east-west

Sheds, single array

System power: 1600 kWp

Nypan - Norway

PVsyst student

PVsyst student

PVsyst student

PVsyst student

PVsyst student

Author
Ingrid Brøndbo (Norway)

Figure F.21: PVSyst report APV South E/W page 1/10.



PVsyst V7.3.4

VCH, Simulation date:
11/06/23 10:31
with v7.3.4

Project: Skjetlein_scenario1
Variant: South_scenario_terrain_east-west

Ingrid Brøndbo (Norway)

Project summary

Geographical Site		Situation		Meteo data								
Nypan		Latitude 63.34 °N		Nypan								
Norway		Longitude 10.30 °E		Meteonorm 8.1 (1991-2013) - Synthetic								
		Altitude 58 m										
		Time zone UTC+1										
Monthly albedo values												
	Jan.	Feb.	Mar.	Apr.	May	June	July	Aug.	Sep.	Oct.	Nov.	Dec.
Albedo	0.70	0.70	0.40	0.20	0.20	0.20	0.20	0.20	0.20	0.20	0.40	0.70

System summary

Grid-Connected System		Sheds, single array		User's needs	
PV Field Orientation		Near Shadings		Unlimited load (grid)	
Fixed plane		According to strings			
Tilt/Azimuth 90 / -90 °		Electrical effect 100 %			
System information					
PV Array			Inverters		
Nb. of modules		3440 units		Nb. of units 13 units	
Pnom total		1600 kWp		Pnom total 1300 kWac	
				Pnom ratio 1.230	

Results summary

Produced Energy	1581302 kWh/year	Specific production	989 kWh/kWp/year	Perf. Ratio PR	144.66 %
-----------------	------------------	---------------------	------------------	----------------	----------

Table of contents

Project and results summary	2
General parameters, PV Array Characteristics, System losses	3
Horizon definition	5
Near shading definition - Iso-shadings diagram	6
Main results	8
Loss diagram	9
Predef. graphs	10
Single-line diagram	11

Figure F.22: PVsyst report APV South E/W page 2/10.



PVsyst V7.3.4

VCH, Simulation date:
11/06/23 10:31
with v7.3.4

Project: Skjetlein_scenario1
Variant: South_scenario_terrain_east-west

Ingrid Brøndbo (Norway)

General parameters

Grid-Connected System		Sheds, single array	
PV Field Orientation		Sheds configuration	
Orientation		Nb. of sheds	18 units
Fixed plane		Single array	
Tilt/Azimuth	90 / -90 °	Sizes	
		Sheds spacing	13.0 m
		Collector width	2.10 m
		Ground Cov. Ratio (GCR)	16.1 %
		Top inactive band	0.02 m
		Bottom inactive band	0.02 m
		Shading limit angle	
		Limit profile angle	9.2 °
Horizon		Near Shadings	
Average Height	3.5 °	According to strings	
		Electrical effect	100 %
		User's needs	Unlimited load (grid)
Bifacial system			
Model	2D Calculation		
	unlimited sheds		
Bifacial model geometry		Bifacial model definitions	
Sheds spacing	13.00 m	Ground albedo	0.25
Sheds width	2.14 m	Bifaciality factor	90 %
Limit profile angle	9.2 °	Rear shading factor	5.0 %
GCR	16.4 %	Rear mismatch loss	10.0 %
Height above ground	1.50 m	Shed transparent fraction	0.0 %

PV Array Characteristics

PV module		Inverter	
Manufacturer	Generic	Manufacturer	Generic
Model	SK8612HDGDC-465	Model	SUN2000-100KTL-INM0-415Vac
(Original PVsyst database)		(Original PVsyst database)	
Unit Nom. Power	465 Wp	Unit Nom. Power	100 kWac
Number of PV modules	3440 units	Number of inverters	13 units
Nominal (STC)	1600 kWp	Total power	1300 kWac
Modules	215 Strings x 16 In series	Operating voltage	200-1000 V
At operating cond. (50°C)		Max. power (=>35°C)	110 kWac
Pmpp	1506 kWp	Pnom ratio (DC:AC)	1.23
U mpp	668 V	Power sharing within this inverter	
I mpp	2256 A		
Total PV power		Total inverter power	
Nominal (STC)	1600 kWp	Total power	1300 kWac
Total	3440 modules	Max. power	1430 kWac
Module area	7477 m²	Number of inverters	13 units
		Pnom ratio	1.23

Figure F.23: PVsyst report APV South E/W page 3/10.



PVsyst V7.3.4

VCH, Simulation date:
11/06/23 10:31
with v7.3.4

Project: Skjetlein_scenario1
Variant: South_scenario_terrain_east-west

Ingrid Brøndbo (Norway)

Array losses

Array Soiling Losses

Average loss Fraction 2.3 %

Jan.	Feb.	Mar.	Apr.	May	June	July	Aug.	Sep.	Oct.	Nov.	Dec.
2.0%	3.0%	3.0%	3.0%	3.0%	2.0%	2.0%	2.0%	2.0%	2.0%	2.0%	2.0%

Thermal Loss factor

Module temperature according to irradiance
Uc (const) 29.0 W/m²K
Uv (wind) 0.0 W/m²K/m/s

DC wiring losses

Global array res. 4.8 mΩ
Loss Fraction 1.5 % at STC

Serie Diode Loss

Voltage drop 0.7 V
Loss Fraction 0.1 % at STC

LID - Light Induced Degradation

Loss Fraction 2.0 %

Module Quality Loss

Loss Fraction -0.3 %

Module mismatch losses

Loss Fraction 2.0 % at MPP

Strings Mismatch loss

Loss Fraction 0.2 %

IAM loss factor

Incidence effect (IAM): Fresnel, AR coating, n(glass)=1.526, n(AR)=1.290

0°	30°	50°	60°	70°	75°	80°	85°	90°
1.000	0.999	0.987	0.962	0.892	0.816	0.681	0.440	0.000

System losses

Unavailability of the system

Time fraction 0.5 %
1.8 days,
3 periods

Figure F.24: PVsyst report APV South E/W page 4/10.



PVsyst V7.3.4
 VCH, Simulation date:
 11/06/23 10:31
 with v7.3.4

Project: Skjetlein_scenario1
 Variant: South_scenario_terrain_east-west

Ingrid Brøndbo (Norway)

Horizon definition

Horizon from Meteornorm web service, lat=63,3426, lon=10,301

Average Height 3.5 ° Albedo Factor 0.81
 Diffuse Factor 0.91 Albedo Fraction 100 %

Horizon profile

Azimuth [°]	-180	-149	-148	-146	-145	-141	-140	-137	-136	-134	-133	-128	-127	-121
Height [°]	6.0	6.0	5.0	5.0	6.0	6.0	5.0	5.0	6.0	6.0	5.0	5.0	4.0	4.0
Azimuth [°]	-120	-113	-112	-100	-99	-63	-62	-59	-58	-48	-47	-46	-32	-31
Height [°]	5.0	5.0	4.0	4.0	3.0	3.0	2.0	2.0	3.0	3.0	4.0	3.0	3.0	4.0
Azimuth [°]	-17	-16	-4	-3	1	2	23	24	25	33	34	65	66	100
Height [°]	4.0	3.0	3.0	2.0	2.0	1.0	1.0	2.0	1.0	1.0	2.0	2.0	1.0	1.0
Azimuth [°]	101	107	108	112	113	119	120	131	132	149	150	175	176	179
Height [°]	2.0	2.0	3.0	3.0	4.0	4.0	5.0	5.0	6.0	6.0	5.0	5.0	6.0	6.0

Sun Paths (Height / Azimuth diagram)

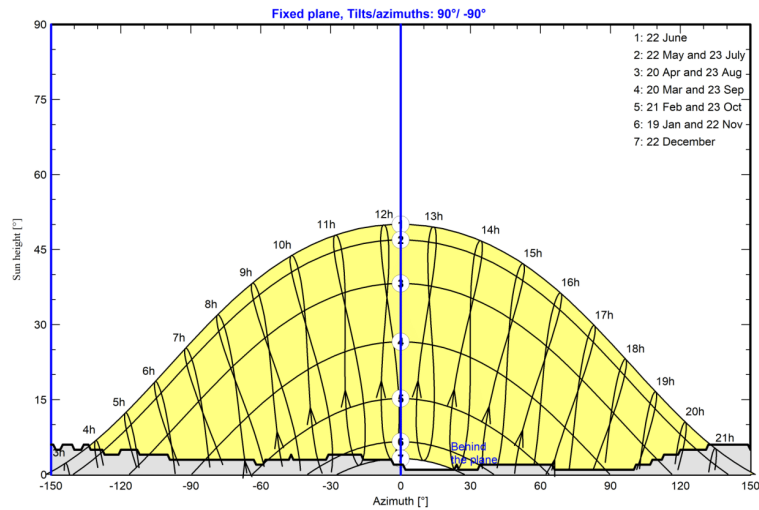
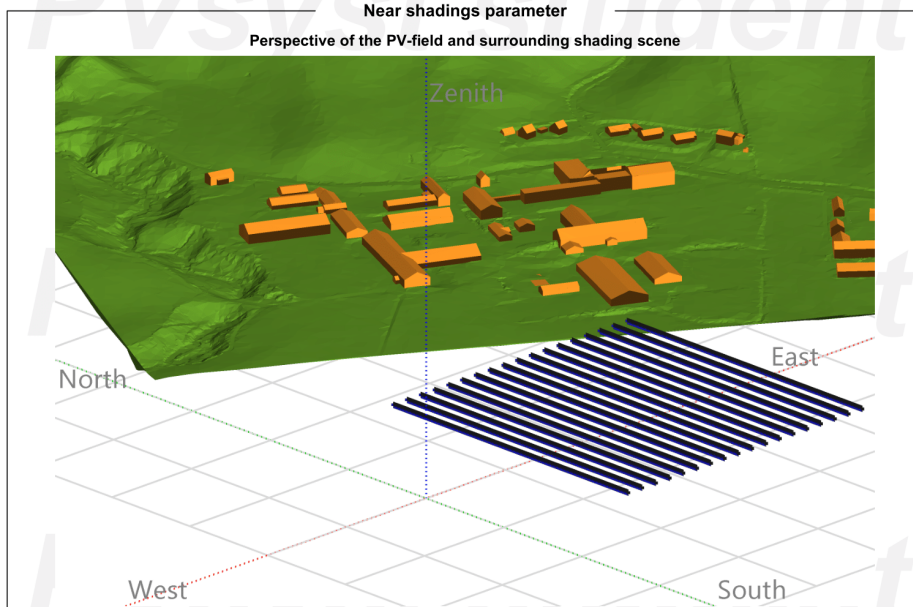


Figure F.25: PVsyst report APV South E/W page 5/10.



PVsyst V7.3.4
VCH, Simulation date:
11/06/23 10:31
with v7.3.4

Project: Skjetlein_scenario1
Variant: South_scenario_terrain_east-west
Ingrid Brøndbo (Norway)



11/06/23

PVsyst Student License for Ingrid Brøndbo (Norway)

Page 6/11

Figure F.26: PVsyst report APV South E/W page 6/10.



PVsyst V7.3.4
VCH, Simulation date:
11/06/23 10:31
with v7.3.4

Project: Skjetlein_scenario1
Variant: South_scenario_terrain_east-west
Ingrid Brøndbo (Norway)

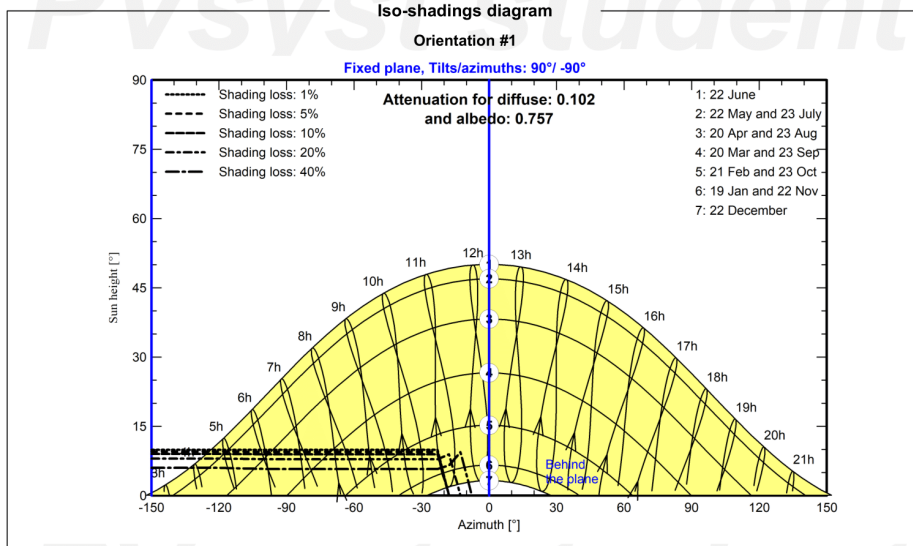


Figure F.27: PVsyst report APV South E/W page 7/10.



PVsyst V7.3.4

VCH, Simulation date:
 11/06/23 10:31
 with v7.3.4

Ingrid Brøndbo (Norway)

Main results

System Production

Produced Energy 1581302 kWh/year

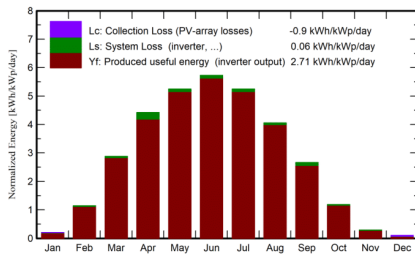
Specific production

989 kWh/kWp/year

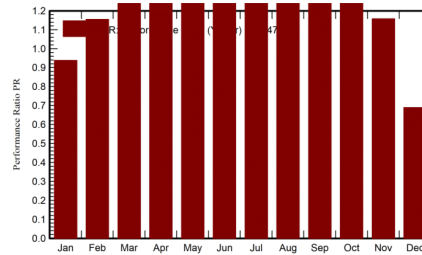
Perf. Ratio PR

144.66 %

Normalized productions (per installed kWp)



Performance Ratio PR



Balances and main results

	GlobHor kWh/m ²	DiffHor kWh/m ²	T_Amb °C	GlobInc kWh/m ²	GlobEff kWh/m ²	EArray kWh	E_Grid kWh	PR ratio
January	5.8	3.90	-1.06	6.4	3.4	10119	9569	0.938
February	22.9	11.74	-0.97	27.3	17.8	51173	50386	1.155
March	67.0	25.70	0.92	66.8	54.2	142853	140657	1.316
April	111.6	44.99	5.22	86.4	77.6	212185	201173	1.455
May	151.1	64.36	9.43	104.8	93.5	260205	256106	1.528
June	159.5	72.78	12.22	120.1	109.1	274948	270569	1.409
July	154.8	79.90	15.61	107.5	96.9	260175	256190	1.489
August	116.1	57.06	14.94	81.6	73.2	201429	198365	1.520
September	67.8	36.75	10.95	48.6	42.8	128073	123173	1.584
October	29.6	16.65	6.26	23.2	19.0	58773	57823	1.557
November	8.1	5.66	2.26	7.4	4.8	14085	13751	1.158
December	2.7	2.05	-0.24	3.2	1.3	3711	3540	0.690
Year	896.9	421.55	6.34	683.4	593.5	1617728	1581302	1.447

Legends

GlobHor Global horizontal irradiation
 DiffHor Horizontal diffuse irradiation
 T_Amb Ambient Temperature
 GlobInc Global incident in coll. plane
 GlobEff Effective Global, corr. for IAM and shadings

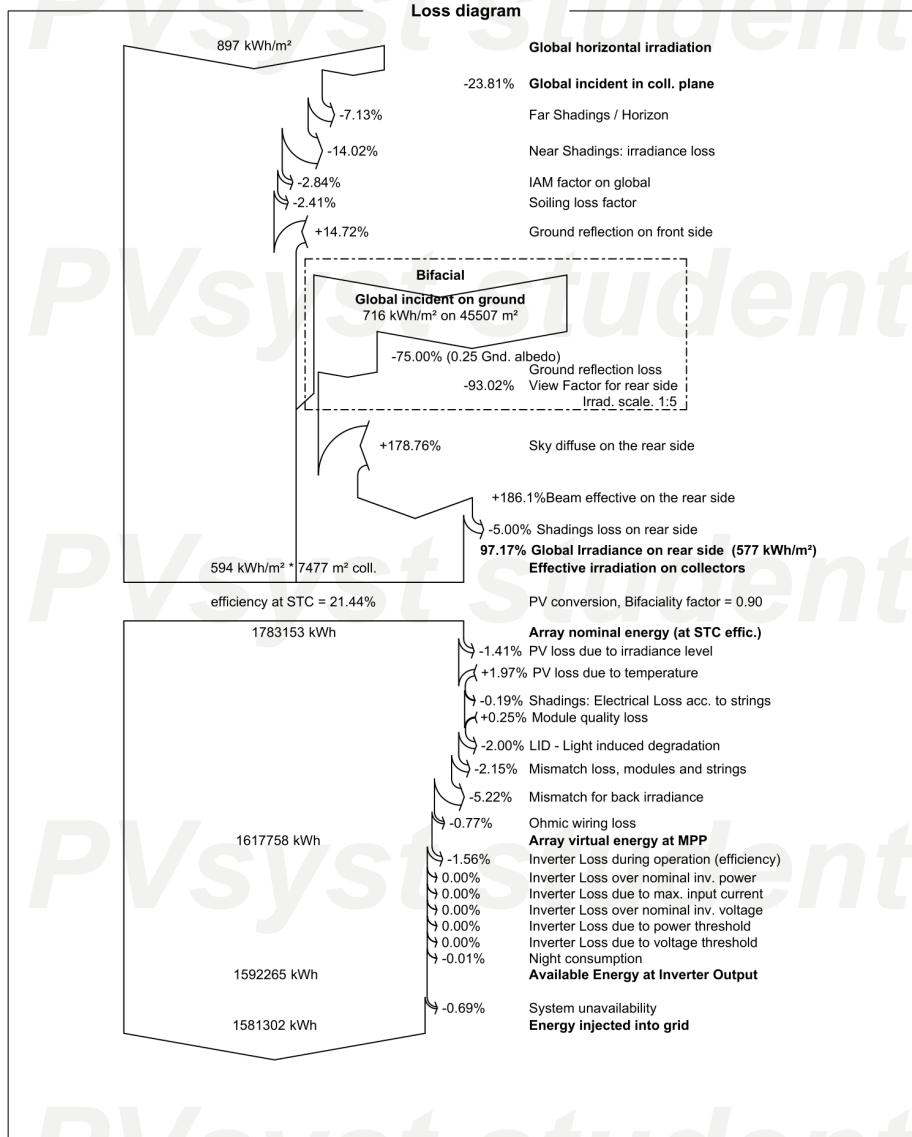
EArray Effective energy at the output of the array
 E_Grid Energy injected into grid
 PR Performance Ratio

Figure F.28: PVsyst report APV South E/W page 8/10.



PVsyst V7.3.4
VCH, Simulation date:
11/06/23 10:31
with v7.3.4

Project: Skjetlein_scenario1
Variant: South_scenario_terrain_east-west
Ingrid Brøndbo (Norway)



11/06/23

PVsyst Student License for Ingrid Brøndbo (Norway)

Page 9/11

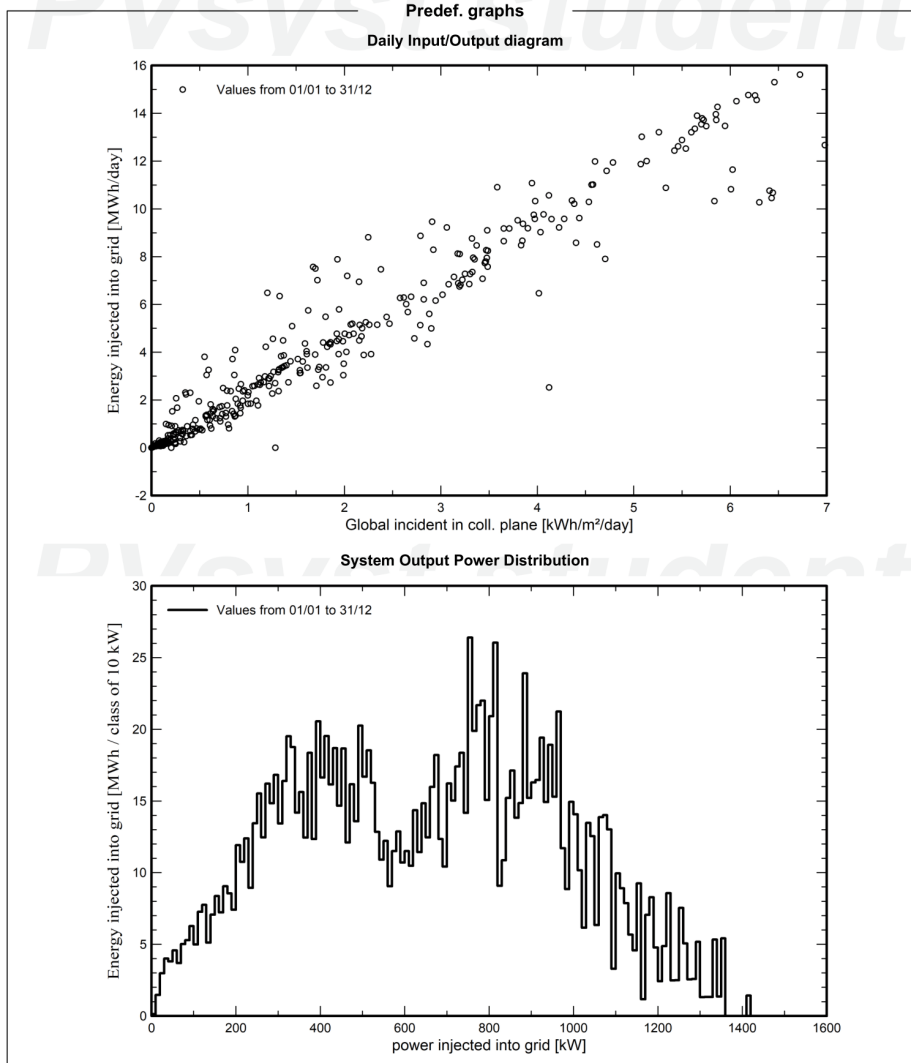
Figure F.29: PVsyst report APV South E/W page 9/10.



PVsyst V7.3.4
VCH, Simulation date:
11/06/23 10:31
with v7.3.4

Project: Skjetlein_scenario1
Variant: South_scenario_terrain_east-west

Ingrid Brøndbo (Norway)



11/06/23

PVsyst Student License for Ingrid Brøndbo (Norway)

Page 10/11

Figure F.30: PVsyst report APV South E/W page 10/10.



 **NTNU**

Norwegian University of
Science and Technology